Investigation of Gas Generation by Riverine Sediments: Production Dynamics and Effects of Sediment Properties

Xin Li

TU Delft

Investigation of Gas Generation by Riverine Sediments: Production Dynamics and Effects of Sediment Properties

By

Xin Li

in partial fulfilment of the requirements for the degree of

Master of Science
in Civil Engineering

at the Delft University of Technology,
to be defended publicly on Thursday, 18th April 2019

Supervisor:	Dr. Julia Gebert	TU Delft – Geo-engineering
Thesis committee:	Dr. Claire Chassagne	TU Delft – Hydraulic engineering
	Dr. Joep Storms	TU Delft – Applied geology
	Florian Zander	TU Delft – Geo-engineering

TU Delft

Acknowledgement

With this thesis I am completing the Master Program of Geo-Engineering in Faculty of Civil Engineering and Geosciences at Delft University of Technology. This project is part of project BIOMUD; without the valuable contributions of many people from different organizations I would never be able to realize the project.

I would like to primarily thank my two closest supervisors, Dr. Julia Gebert and Florian Zander, who have helped me every step of the project. They gave me continuous supports, plentiful insights with both theoretical and practical points, and precious opportunity to work in laboratory. Many thanks to Dr. Claire Chassagne and Dr. Joep Storms as my committee members who provided insightful guidance, suggestions and accurate comments that helped me to complete the master thesis.

I would also like to thank Hamburg Port Authority (HPA) who provided me with the rare opportunity to participate in the sampling collection work in Hamburg, Germany. During the three days' in-situ work I gained experience on sampling and learned a lot of knowledge from the staff.

Finally, I want to thank my family and friends for all the supports. Special thanks to my mother who always supported me and encouraged me throughout the stressful times during the past two years in Delft.

Xin Li
Delft, April 2019

Content

Abstract

Due to microbial activities, the anaerobic degradation of organic matter happens in the sediments and leads to considerable gas production. Especially for low flow areas gas production is more easily fostered. To prevent the potential problems caused by gas production from the riverine sediments, this study focuses on magnitude of gas formation and its relation with soil properties. Nine locations of known at Port of Hamburg were sampled; for each location the fresh sediment samples were collected at different depths and on different seasons. Samples were stored and transported to several institutes for various analyses, including analysis on sediment standard properties, and on gas production by incubation.

Being part of the BIOMUD project, this study analyzed data from several research institutes. A strong correlation was found between magnitude of gas production and some of the soil properties including content of TOC, TN, ratio of TOC/P, TOC/S, density fractionation, and content of various types of metal elements. A clear relationship was found between magnitude of short-term and long-term gas production, providing possibilities for estimation work on gas formation in the future. The modified Afvalzorg multi-phase model was applied in analyzing gas production on the timeline, which played a key role in describing and predicting gas production in the long-term. The total gas potential of the river sediments at the Port of Hamburg was then predicted as 105.3 mg C/g TOC on average, relating to 10.5% of the organic matter being degraded. By temperature experiment a Q_{10} value of 2.06 was determined for assessing the sensitivity of gas production to temperature. Gas composition inside the bottles was also measured after four months' incubation in the temperature experiment, with the results of CH_4/CO_2 ratio ranged from 0.92 to 1.86 for different temperature conditions. Parts of the results acquired from the experiments mentioned above were also compared with the results from previous studies made by other researches.

List of Figures

List of Tables

List of Abbreviations

BfG	German Federal Institute of Hydrology
CEC	Cation exchange capacity
CS	Consolidated sediment
DOC	Dissolved organic carbon
DOM	Dissolved organic matter
DW	Dry weight
EC	Electric conductivity
FM	Fluid mud
FW	Fresh weight
GC	Gas-chromatographic
GE	Gas Endeavour
HPA	Hamburg Port Authority
IfB	Institut für Bodenkunde (Institute for Soil Science)
KB	Köhlbrand site
KH	Köhlfleet mit Köhlfleethafen site
LFG	Landfill gas
LOI	Loss on ignition
PK	Parkhafen site
PS	Pre-consolidated sediment
RBS	River bed sediment
RT	Rethe site
RV	Reiherstieg Vorhafen site
SC	Strandhafen Chicagokai site
S.D.	Standard deviation
SH	Sandauhafen site
SPM	Suspended particulate matter
SW	Sedimentfang Wedel site
TEA	Terminal electron acceptors
TIC	Total inorganic carbon
TN	Total Nitrogen
TOC	Total organic carbon
VH	Vorhafen site
WC	Water content (or Water column)

1 Introduction

1.1 Background

In area of ports and waterways, it is sometimes observed that gases are released as bubbles from the sediments, into the water column, the water surface and eventually the atmosphere, as shown in Figure 1. The gases are mainly composed of methane (CH_4) and carbon dioxide (CO_2), coming from the microbial turnover of sediment organic matter in river. Gas generation is more easily fostered in low flow areas of spur fields, harbor basins, drinking water reservoirs, barrages or sluices where the hydro-morphological conditions are conducive to the settlement and consolidation of suspended organic matter (Gebert, 2018). Besides, elevated degradable organic matter content, low O_2 saturation of water column also contribute to the formation of gas. This phenomenon is regarded as part of the natural biogeochemical cycling of organic matter.

Figure 1. Gas bubbles at site Reiherstieg-Vorhafen (source: project BIOMUD 2018)

A series of potential problems can be caused by gas generation. Sediment physical properties are changed: density, viscosity and shear strength of sediment are reduced, which enhances the susceptibility of subaquatic embankments and constructions towards erosion. Also, sediment rheological properties are changed, which impacts the navigable depth. On the other hand, gas generation delays consolidation of sediment to be dredged, and the degradation of organic matter causes undesired subsidence in constructions made from sediments (Gebert, 2018). Furthermore, methane and carbon dioxide are both greenhouse gases which contribute to global warming. Methane emission from lakes contributes 6-16% to the atmospheric CH_4 budget (Blume et al., 2004). Therefore, the study on sediment organic matter degradation and gas generation is meaningful for both construction and maintenance of port area.

The BIOMUD project was thus established in order to investigate the turnover of suspended and settled organic matter in ports and waterways. It is funded by Hamburg Port Authority (HPA) and is a member of the MUDNET network. This thesis project being part of the BIOMUD project, mainly focuses on gas generation in the case of Elbe River, in area of Port of Hamburg.

1.2 Objectives

Given the above background, the main objective of the thesis is to assess gas generation dynamics and the influence of different sediment properties hereon. This is the prerequisite for building a sediment gas generation model for describing gas generation development with time, so that a prediction of gas generation can be given when only few days' measured data on gas generation are available. In order to achieve the main objective, more detailed objectives have to be considered:

(1) Assessment of the role of location, depth and season on gas generation;
(2) Identification of physical and chemical factors of influence relevant for gas generation and degradability in situ;
(3) Development and validation of a riverine sediment gas generation model;
(4) Quantification of size of degradable organic matter pool, and quantification of gas generation potential;
(5) Interpretation of the role of organic matter degradation on composition of gas generated and other experimental phenomena.

The thesis focuses on gas generation in the case of Elbe River, in the area of Port of Hamburg. Magnitude and rate of sediment gas generation in this area are investigated in order to find the production dynamics in relation to location and time, and how gas production is affected by sediment properties. Sediment samples were taken in different locations in the Port of Hamburg and sent to a commercial laboratory for analysis of standard physical and chemical properties and to the University of Hamburg for analysis of respiratory activity. At TU Delft, gas generation was measured by incubating the sediment samples under standardized conditions. Furthermore, the experimental data were organized and analyzed to allow for an explicit interpretation of gas generation dynamics, including the guiding parameters of influence.

1.3 Research questions

Given the background and objectives mentioned above, the following research questions were formulated:

(1) What is the spatial and temporal variability of gas generation within sediment profiles in the Port of Hamburg?
(2) How do the mass-normalized and TOC-normalized gas generations correlate with the abiotic sediment properties?
(3) How do the rate and magnitude of gas generation develop with time?
    a. What is the size of short-term and long-term pools of degradable organic carbon?
    b. What is the relationship between magnitude of short-term and long-term gas production?
(4) How does temperature affect the rate and magnitude of gas generation and how sensitive is it?

1.4 Thesis outline

The thesis mainly presents the investigation on magnitude and rate of gas generation along with the sediment properties in the Elbe River, Port of Hamburg, including laboratory work on research of temperature effects. The report contains six main chapters listed as below:

1. Introduction
2. Project overview: Case of Elbe River
3. Literature review
4. Experimental methods and available data
5. Results and discussion
6. Conclusions and recommendations

In Chapter 2, the background of the project in Port of Hamburg will be introduced. An overview will be provided including site information, sampling process, project requirements and dimensions of the investigation area.

In Chapter 3, the relevant literature for this study is summarized, including theory of organic matter degradation in riverine sediment; Influential factors on degradation rate, especially temperature; models and methods for analyzing gas generation on time series; and finally an overview of previous research on this topic.

In Chapter 4, experiment procedures and statistical methods used in the thesis are presented, as well as complete available data of the thesis project. Firstly, procedures of sampling and sample incubation are introduced. Secondly, procedures and available data of additional temperature experiment on gas production are given. Finally, statistical and mathematical methods used for data analyses in the thesis are introduced.

In Chapter 5, each research question is analyzed in detail on the basis of data. It mainly contains spatial and temporal variability analysis, correlation analysis, time series analysis and temperature effect analysis. Part of the results is compared with previous research here. In time series analysis, model and method for detecting and predicting gas potential will also be introduced.

Finally in Chapter 6, general conclusions and discussions are summarized, and also some recommendations for further research are given.

2 Project overview: Case of Elbe River

The investigation area of the project is located in the Port of Hamburg as shown in the map of Figure 2. The Elbe River flows through Port of Hamburg from southeast to west, and finally flows into the North Sea at Cuxhaven, 110 km (68 mi) northwest of Hamburg. The Elbe River has been navigable by commercial vessels since 1842 (source: Wikipedia), and provides important trade links for inland places. Therefore, Hamburg Port Authority funds the project, aiming to develop a standard measurement procedure to determine the navigable depth at which the safety and ease of ship traffic are ensured. It is hypothesized that organic matter degradation plays a role in defining sediment properties at the nautical bottom. The project is hence also profound for the maintenance of the depth of fairways and harbor basins in the Port of Hamburg.

Figure 2. Project location in Port of Hamburg (source: www.google.com/maps)

In order to investigate the extent of sediment organic matter degradation and gas generation in the Elbe River at Port of Hamburg, sediment samples were taken here for further laboratory studies. Due to the complexity of the question, a multi-year research program was scheduled. In the year 2018, the sampling campaigns for basic research were taken for the following periods in the Elbe River at Port of Hamburg:

- Campaign # 0 in week 17: 23.04. until 26.04.2018
- Campaign # 1 in week 22 / week 23: 01.06. until 08.06.2018
- Campaign # 2 in week 25 / week 26: 22.06. until 29.06.2018
- Campaign # 3 in week 31 / week 32: 03.08. until 10.08.2018
- Campaign # 4 in week 37 / week 38: 14.09. until 21.09.2018
- Campaign # 5 in week 44 / week 45: 03.11. until 10.11.2018

Samples from Campaign # 0 served to test sampling and analytical procedures, thus the data for analyzing in this thesis start from Campaign # 1. In each of the campaigns the samples were taken from nine selected areas in or around Port of Hamburg listed as below:

- Reiherstieg Vorhafen (RV)
- Sandauhafen (SH)

- Rethe (RT)
- Strandhafen Chicagokai (SC)
- Vorhafen (VH)
- Köhlbrand (KB)
- Parkhafen (PK)
- Köhlfleet mit Köhlfleethafen (KH)
- Sedimentfang Wedel (SW)

Figure 3 gives the detailed locations of these nine sampling spots and their corresponding distance to the source of Elbe River from 616 km to 643 km, upstream in the east and downstream in the west. In each of the sampling locations, three vertical cores were set at pre-defined positions; here location KB is taken for example, as shown in Figure 4. Among the points determined in advance, point 2 (in the middle of each sampling location) was normally used for sampling collection in the BIOMUD project; the other two points were used for other stakeholders' activities.

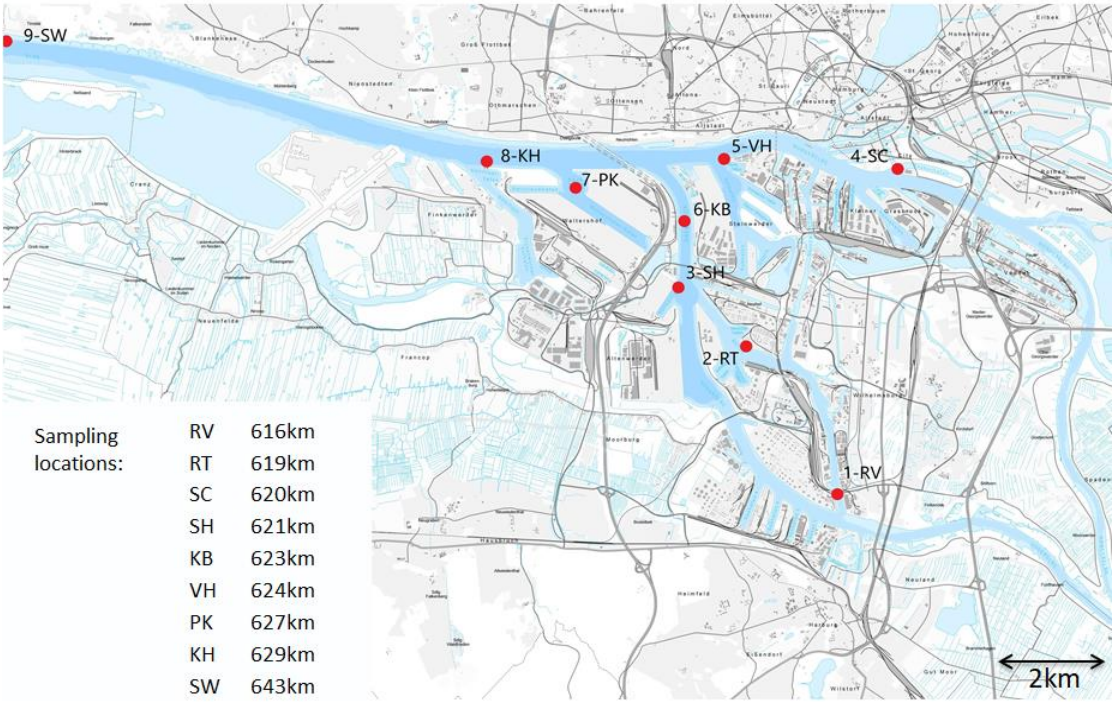

Figure 3. Sampling locations in the Elbe River (source: HPA)

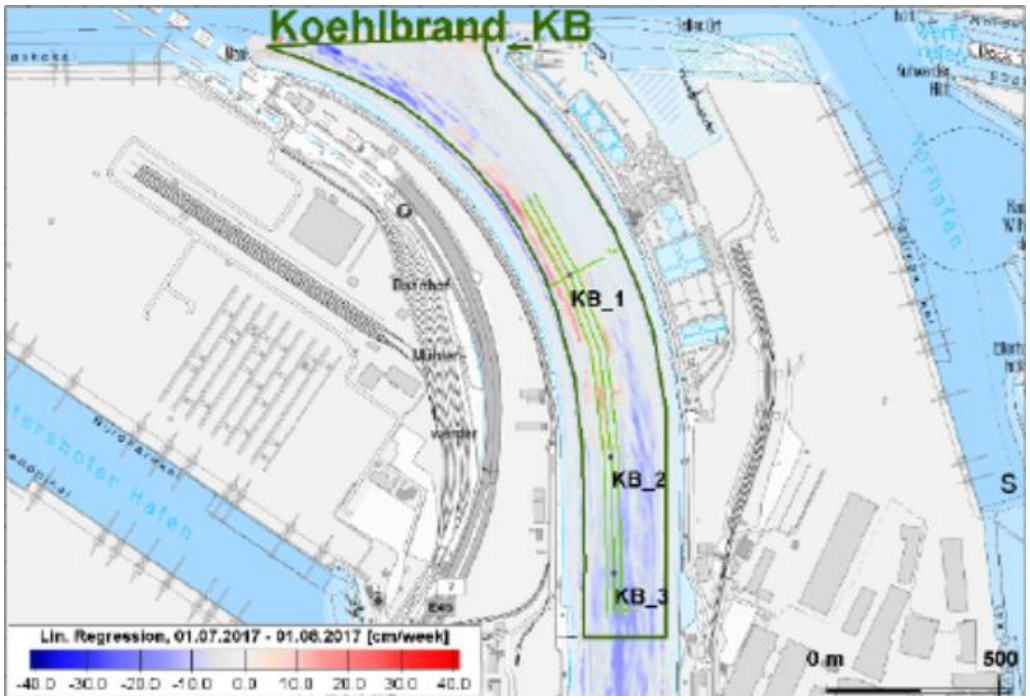

Figure 4. Three pre-defined points in one location KB (source: manual for measurements from HPA)

At each location, the sediment samples were collected using a one-meter vertical corer, and each one-meter core sample is divided into four parts, corresponding to four layers of different depth:

- Suspended Particulate Matter (SPM)
- Fluid Mud (FM)
- Pre-consolidated Sediment (PS)
- Consolidated Sediment (CS)

Figure 5 gives a conceptual model of these layers within the water-sediment-riverbed system. Note that the layer Water Column (WC) and River Bed Sediment (RBS) are not included in the samples taken as they contain negligible organic matter and thus can be regarded as no contribution to gas generation.

After penetrating the sediments at certain location to a sufficient depth, the core sampling device was lifted up with collected samples. Then the one-meter long sample in the corer was divided and put in several sample containers. Normally the top part of the sample belongs to SPM layer, with suspended particles in water; then the FM layer, with quite high water content and fluidity; PS and CS layer come after, with a relatively dense status. Samples of different layers appear differently already to the naked eye and also show different fluidity characteristics, so it is easy to divide them immediately after collecting them from the river. In some cases, intermediary samples from transitionary layers were formed when clear categorization was not possible. Therefore, several new layers were defined manually that contained sediment features of both adjacent layers, as SPM/FM layer, FM/PS layer and PS/CS layer, which will be used later in analysis of the thesis.

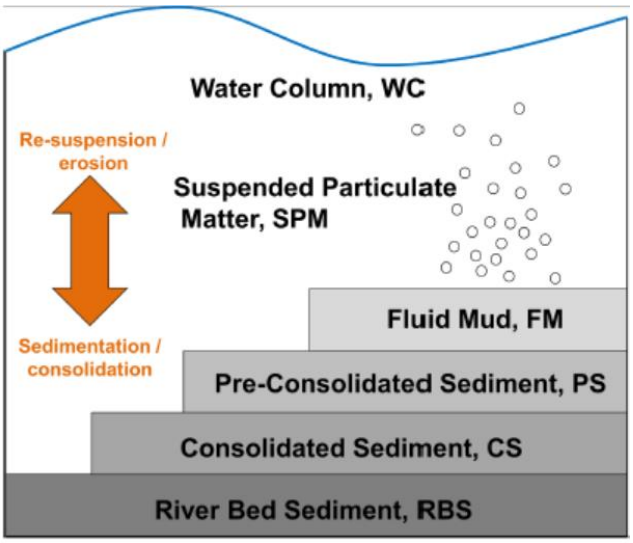

Figure 5. Conceptual model of layers within the water-sediment-riverbed system

After sampling work the samples were sent to several scientific research organizations including University of Hamburg, Delft University of Technology, and Hamburg Port Authority as well as a commercial laboratory for analyses and experiments. Basic properties of sediment samples are measured such as water content (WC), total organic carbon content (TOC), total inorganic carbon content (TIC), total nitrogen content (TN), particle size distribution; Standard chemical properties were also measured such as the content of macro-elements P, S, Fe, Ca and so on, but also the content of heavy metals both in extractions and filtrates of pore water. On the other hand, parts of the samples were incubated in the laboratory at certain conditions and were measured on gas generation situations, both in the short-term (21 days) and long-term (several hundred days). The thesis mainly focuses on the gas generation part and how gas generation is influenced by sediment properties.

3 Literature review

3.1 Organic matter degradation in river sediment

3.1.1 Composition and properties of organic matter

As mentioned in the background part, the gases produced in the Port of Hamburg come from the microbial turnover of organic matter in river sediments. Therefore, this chapter gives an overview over sediment organic matter and its composition and properties.

Sources of sediment organic matter mainly include living organisms (edaphon, consisting of the soil flora and fauna) and organic matter in soils. The living organisms in the water are important source consisting organic matter in sediments. They include a wide variety of micro-organisms such as bacteria, viruses, fungi, protozoa and algae, as well as plant roots, insects, earthworms, and larger animals such as moles, mice and rabbits that spend part of their life in the soil. The living portion represents about 5% of the total sediment organic matter. Among the components, algae make up a large part of the suspended organic matter that eventually settles in the sediment. Earthworms and insects help break down crop residues and manures by ingesting them and mixing them with the minerals in the soil, and in the process recycling energy and plant nutrients. Sticky substances on the skin of earthworms and those produced by fungi and bacteria help bind particles together. Earthworm casts are also more strongly aggregated than the surrounding soil as a result of the mixing of organic matter and soil mineral material, as well as the intestinal mucus of the worm (Bot et al., 2005). Thus, the living part of the soil is responsible for keeping air and water available, providing plant nutrients, breaking down pollutants and maintaining the soil structure.

Eroded topsoils are also an important source of sediment organic matter. In most topsoils, the mass of the soil organic matter only amounts to a few percent, but has an important influence on all soil functions and plays a central role in the global carbon cycle (Blume et al., 2016). The chemical composition of the organic matter in soils is heterogeneous, because it consists of plant and animal residues at different stages of degradation. Soil organic matter comprises all of the dead plant and animal residues and their organic transformation products found on and in the mineral soil. It also includes substances introduced by human activities, e.g. synthetic organic substances (e.g. pesticides, organic wastes) (Blume et al., 2016).

The carbon content of soil organic matter varies within individual substance classes, with polysaccharides containing about 40% C, and lipids about 70% C. The average C content is usually around 50%. In addition to the nonmetals C, H, O, N, S and P, the organic matter in soils also contains metals. These occur either in an exchangeable form (especially Ca, Mg), or are in the form of complexes, where they are generally firmly bound (e.g. Cu, Mn, Zn, Al and Fe). Particularly, N, S and P are found as important constituents of sedimentary organic matter besides carbon. While most of the C is liberated as CO_2 and CH_4 over the course of decomposition, N is initially mainly stored in the microbial biomass, more than 95% of which is stabilized in

organic matter on the long term. The C/N ratio of the organic matter therefore becomes increasingly narrow during the course of degradation and associated soil organic matter formation, which means the smaller the C/N ratio, the less readily degradable organic carbon remains in sediments. The majority of the N is found in the form of peptide groups, a smaller portion in the form of free amino groups. Wet chemical analyses demonstrate that amino acids and amino sugars, together accounting for about 30-70% of the total organic N, represent the majority of the molecular units containing N. S is also always a component of soil organic matter. The C/S ratio is of about 200 in grassland and forest soils, and about 130 in cultivated soils. Up to 90% of the S is bound in organic form, about 30-75% of which as sulfate ester. Another important binding form that is found is C-bound sulfur at various oxidation levels. According to Prietzel et al. (2007), the distribution of the S binding forms depends on the land use and the O_2 availability in the soil. The proportion of reduced organic S binding forms increases in the sequence: Arable land < forest soil < moor. What's more, P is also found in soils with more than 60% in organic form. Although a portion of the organically bound P could not yet be identified, more than 50% of the total P in soils has been found to be in the form of phosphate esters (Blume et al., 2016).

The mentioned two sources together constitute the organic matter in sediments. Generally, a wide range of structural motifs and functional groups are contained in sedimentary organic matter, representing a range of degradabilities (de Leeuw et al., 1993). At the most fundamental level, it is recognized that certain biopolymers (e.g. proteins and nucleic acids) are most labile under a wide range of conditions, owing to a combination of relatively weak bonds between monomers or the particularly important nutrient requirements (e.g. P and N) that such compounds provide. In comparison, diverse compounds like carbohydrates, including cellulose, are relatively labile; whereas others, including aliphatic ester-linked macromolecules such as cutin and suberin and the highly aromatic lignin, tend to be less degradable. Refractory biomacromolecules are of the least degradability (Arndt et al., 2013). Figure 6 gives concentrations of sedimentary organic matter compounds and their contributions on degradability in relation with the sediment depth in the marine system. The different organic matter compounds are characterized by different degradabilities. Degradability of sedimentary organic matter appears to be directly impacted by its continual alteration during transport, burial and diagenesis, all of which appear to impart decreasing degradability on the residual organic matter.

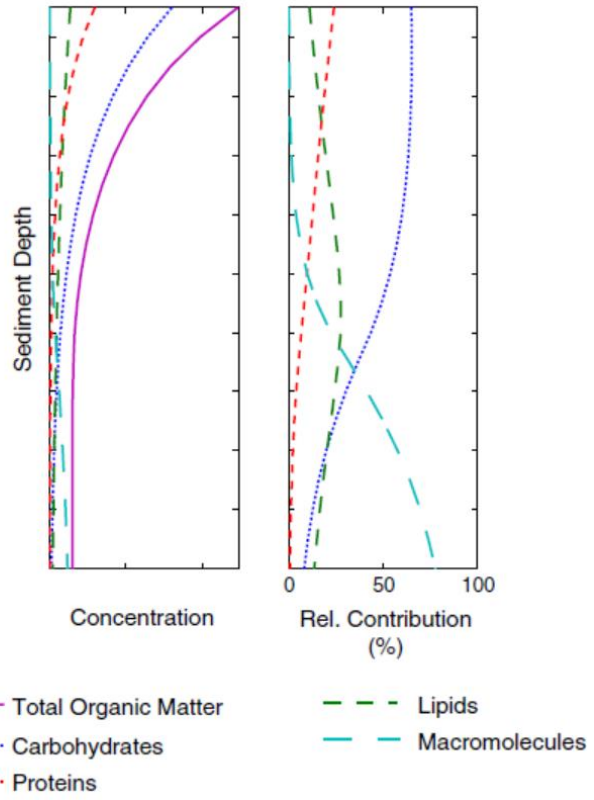

Figure 6. Characteristic depth profiles of organic matter and organic matter compounds in the marine sediments (Arndt et al., 2013).

The properties of organic matter determine the sediments' characteristics in many ways. Here the properties including the adsorption capacity, water storage capacity and effects on soil structural stability are mainly introduced. The adsorption capacity of organic matter is significant for the binding of many nutrients that are present as cations in the soil. During the course of the humification process, the cation exchange capacity (CEC) increases through oxidation and the formation of carboxyl groups. In general, a sufficient organic matter supply is particularly important for maintaining the CEC in clay-poor soils, or soils where the clay fraction mainly consists of clay minerals with low CEC. Additionally, organic matter also has a great significance for the binding of inorganic and organic pollutants in soils, which prevents direct harm to organisms, and it also reduces or retards their translocation to deeper soil layers or to the groundwater. Furthermore, organic matter has a high water storage capacity: it can store about 3-5 times its own weight in water. Through the aggregating effect, organic matter also has an indirect effect on the pore size distribution and water balance. Finally, organic matter is found to have a positive effect on the structural stability of soils. It favors the formation of a stable aggregate structure. The binding of organic matter onto the surfaces of (hydr)oxides and clay minerals leads to the development of very stable microaggregates (<250µm), which serve as building blocks for the less stable macroaggregates (>250µm). The development of macroaggregates is particularly characteristic for clayey soils and requires the continuous input of organic residues. This promotes microbial activity and thus the production of microbial polysaccharides, which are mainly responsible for the stabilization of macroaggregates (Blume et al., 2016).

3.1.2 Aerobic and Anaerobic degradation

Bio-degradation is the process by which organic matter is broken down into smaller compounds by the enzymes produced by living microbial organisms. Degradation processes vary greatly; organic matter can be degraded aerobically, with oxygen, or anaerobically, without oxygen.

In an aerobic system, the microbial organisms can access free, gaseous oxygen directly from the surrounding atmosphere. Aerobic organisms have the ability to mineralize organic matter completely via the tricarboxylic acid cycle. The end products of an aerobic process are primarily carbon dioxide and water which are the stable, oxidized forms of carbon and hydrogen. In such a system the majority of the energy in the starting material is released as heat by their oxidization into carbon dioxide and water. While in an anaerobic system, organic matter is mineralized in an anaerobic food chain. The initial breakdown occurs through extracellular and membrane-bound hydrolytic enzymes produced by certain microorganisms. The hydrolytic products are then consumed by fermenting and acetogenic bacteria that produce compounds such as acetate and hydrogen. The terminal step in this anaerobic food chain involves the utilization of these latter compounds by microorganisms that reduce sulfate and oxidized manganese/iron or produce methane (Arndt et al., 2013). The anaerobic degradation process thus can be summarized as three steps: hydrolysis, acetogenesis, and methanogenesis. Decomposition is slower and usually incomplete in such a system; the majority of the chemical energy contained within the starting material is released by methanogenic bacteria as methane (Ding et al., 2003).

In the case of Elbe River in this thesis, anaerobic environment was observed for the deep river sediments. As mentioned, methane production is proved to be the terminal step in the degradation of organic matter in most anoxic lake sediments (Liu et al., 2017). Various substrates can be consumed during anaerobic respiration for CH_4 formation. Equations for methanogenic pathways under anaerobic conditions are included in Table 1. It is generally assumed CH_4 production in peatlands or lake sediments is dominated by the acetoclastic and hydrogenotrophic methanogenic pathways (Zalman et al., 2018). In the acetoclastic pathway, acetate is split to form CO_2 and CH_4, while in the hydrogenotrophic pathway, CO_2 is reduced to CH_4 using H_2 as an electron donor. Three successive phases can be distinguished concerning methane production, marked by Kengen et al. (1995) in results of measurements on soil samples (at 15°C) from a drained peat soil in Holland. In the first phase (±20 days) the substrate (acetate and H_2) was used by the reduction of alternative electron acceptors. A low methane emission and a relatively high CO_2 production were measured. CO_2 was probably mainly produced by alternative electron acceptor reduction. The second phase (±10 days) started after all alternative electron acceptors had been reduced. In this phase a strong increase of the methane production rate up to a sediment-characteristic maximum was observed and the growth of methanogenic biomass seemed to be the limiting factor for methane production. An accumulation of acetate was found followed by an exponential increase of methane production. The third phase was characterized by substrate limitation of methane production, while no accumulation of acetate occurred anymore. In this final phase the rate of methane production decreased and reached a more long-term level (Hulzen, 1997).

Table 1. Processing of methanogenic substrates under anaerobic conditions. Δ G values from Whitman et al., (2006) under standard conditions

Substrate:	Equation:	Δ G (kJ mol^{-1} of CH_4)
Methanol	$4CH_3OH \rightarrow 3CH_4 + CO_2 + 2H_2O$	−104.9
Monomethylamine	$4CH_3\text{-}NH_2 + 2H_2O + 4H^+ \rightarrow 3CH_4 + CO_2 + 4NH_4^+$	−75.0
Dimethylsulfide	$2(CH_3)_2\text{-}S + 2H_2O \rightarrow 3CH_4 + CO_2 + 2H_2S$	−73.8
H_2	$4H_2 + CO_2 \rightarrow CH_4 + 2H_2O$	−135.6
Acetate	$CH_3COOH \rightarrow CH_4 + CO_2$	−31.0
Methanol reduction coupled to H_2 oxidation	$CH_3OH + 4H_2 + CO_2 + 2H^+ \rightarrow 2CH_4 + 3H_2O$	—

The degradation rates of soil organic matter under both aerobic and anaerobic conditions were investigated in various researches. Laboratory experiments have demonstrated that fresh, marine-derived organic matter is initially mineralized at the same rate under aerobic and anaerobic conditions (e.g. Westrich et al., 1984; Henrichs, 2005). However, this is only true for planktonic biomass, polysaccharides and proteins, and is not valid for lignins, lipids, chloropigments and other carbon-rich polymers (e.g. Henrichs, 1992). Oxygen might influence organic carbon burial if microbial degradation of sedimentary organic matter is oxygen-dependent and if bioturbation, which normally does not occur in anoxic systems, affects carbon degradation. When the most labile organic compounds have been consumed, the rate of organic matter degradation in anoxic settings decreases much more rapidly than when oxygen is present. It has thus been hypothesized that the enzymes catalyzing the respiration of phenolic and other terrestrial-derived organic compounds, such as lignin, cellulose and tannins, are more active in the presence of oxygen (e.g. Freeman et al., 2001). Under aerobic conditions, organic matter degradation rates remain high because of the very high oxidative potential and the resulting weak sensitivity towards the depletion of energy-rich organic compounds. However, in anaerobic environments deprived of energy rich-organics and powerful terminal electron acceptors (TEAs), the degradation rate becomes thermodynamically limited.

3.1.3 Influential factors

Rates of greenhouse gas emissions from tropical peatlands are regulated through the interaction of a range of biotic and abiotic environmental variables including water table height, temperature, nutrient availability, oxygen availability, and pH (Girkin et al., 2018). By reference, rates of organic matter degradation and gas production in riverine sediments are more or less influenced by similar factors. Thus the influential factors on organic matter degradation in the case of Elbe River are summarized as: oxygen availability, temperature, pH, deposition rates, and macrobenthic activity.

The influence of oxygen on degradation of organic matter is introduced in the last chapter by

comparing degradation under anaerobic and aerobic conditions. The temperature effects on gas production will be analyzed in detail in the following chapter 3.2. For the factor of pH, laboratory experiments have demonstrated that pH value affects rates of organic matter degradation by testing the responses of CH_4 metabolism in slurries of peat samples to different pH values using citric acid-phosphate (Dunfield et al., 1993). The optimum pH values at which maximum activities were observed were up to about two units above the native pH. In some cases the activity declined very markedly both above and below the optimum pH. The deviation of observed pH optima from the native pH values of the peat, especially in the more acid samples, suggest that the methanogens and methanotrophs are only partially adapted to the acidic conditions. The marked sensitivity of CH_4 production to low pH values may be due to an effect on the methanogens itself but it could also result from the effect of acidity on H_2 production in the peat.

For the factor of deposition rate, the observed correlation between average organic matter degradability and sediment accumulation rate (Canfield, 1994) has led to the hypothesis that deposition rate exerts an important influence on organic matter degradation rates. This relationship can be explained by the rapid burial of freshly deposited material below the biologically active, mixed sediment layer, at depths where organic matter degradation proceeds at a slower pace. However, the relationship might also be partly explained by the correlation between organic carbon flux and total flux in the examined slope and deep ocean environments. Furthermore, Emerson et al. (1985) have argued that since the half-lives of labile organic compounds are generally one or two orders of magnitude shorter than typical residence times in the mixed layer, deposition rate should only exert a small effect on degradation rates. Therefore, deposition rate only exerts a significant effect on organic matter degradation rates if the bulk material is refractory enough to escape degradation in the upper, mixed layer.

Macrobenthic activity also exerts an important influence on organic matter degradation on different spatial and temporal scales. In aerobic sediments, benthic invertebrates such as polychaetes, holothurians and bivalves extensively rework the upper centimeters of the sediment column, modifying their physical and chemical properties. A large fraction of the deposited organic matter may be decomposed within these shallow sediment horizons. The impact of macrobenthic activity on organic matter degradation results from particle transport through feeding and burrowing activities, bioturbation, and the ventilation of these burrows through exchange with the overlying water, bioirrigation. The magnitude of this impact depends on various factors such as sediment characteristics, supply of organic matter, as well as functional group, abundance and size of benthic macrofauna (van Duyl et al., 1992). Studies indicate that macrobenthic activity generally stimulates the degradation of refractory organic compounds that are not directly assimilable by most deposit-feeders (Findlay et al., 1982; Kristensen et al., 2001). Its impact on fresh, labile organic matter is more complex.

3.2 Temperature effects on gas production

Gas production results from the interaction of various biological and physical processes in the soil (Hogan, 1993; Schimel et al., 1993) where degradation of organic matter takes place. In the soil one crucial factor for the microbial production of gas, especially methane, is the temperature.

Deep lake or river sediments have more or less constant low-temperature conditions compared with marshes and peats which are influenced more strongly by seasonal temperature changes. Nevertheless, Methanogenesis has repeatedly been proved to occur at a wide range of temperatures from 2°C to 70°C (Nozhevnikova et al., 1997, 2003), and it is found that river sediments represent a unique natural reservoir of different kinds of anaerobic microorganisms. The optima temperature range for methanogenesis in lake sediments is found between 35°C and 42°C (Zeikus et al., 1976), which is considered to be higher than the maximum temperature observed in situ. However, in freshwater marsh soil a low optima temperature of methanogenesis is found at 10°C (Wagner et al., 1997). Within a certain range microbial activity is regarded to increase with temperature (Hofle, 1979).

A significant concept, Q_{10} value, is introduced here for describing temperature sensitivity of methane production. The Q_{10} value is a temperature coefficient that measures the rate of change of a biological or chemical system as a consequence of increasing a temperature change of 10°C, described as below:

$$Q_{10} = \left(\frac{R_2}{R_1}\right)^{\left(\frac{10}{T_2 - T_1}\right)} \quad (1)$$

Where R_1 and R_2 are the rates of methane production at temperatures T_1 and T_2, respectively. In which T is the temperature in °C or Kelvins. The Q_{10} value of different systems can vary in a large extent, which will be listed and compared later in the thesis. An R_0 value is the extrapolated production rate at 0°C ($R_0 = R/Q_{10}^{T/10}$).

Substrate also plays a key role in methanogenic activities, as well as the temperature. The substrates including acetate, formate and hydrogen are produced during degradation process of organic matter by relevant bacteria involved in the anaerobic foodchain (Wagner et al., 1997). Under low-temperature conditions, as shown in equation (2), acetate has been proved to be a major methane substrate based on different experimental evidence (Kuivila et al., 1989; Kotsyurbenko et al., 1993); while at high-temperature environment, methane is mainly formed from bicarbonate. When the hydrogen-carbon dioxide mixture (H_2/CO_2) is used as a substrate at high temperature of 70°C, it is directly converted to methane (Nozhevnikova et al., 2007), as shown in equation (3). At low temperature conditions (5°C and 15°C), H_2/CO_2 is converted into methane by two steps: first acetate is formed, followed by methane production from acetate.

$$CH_3COO^- + H_2O \rightarrow CH_4 + HCO_3^- \quad (2)$$

$$CO_2 + 4H_2 \rightarrow CH_4 + 2H_2O \quad (3)$$

Since homoacetogenesis is enhanced at low temperatures (Conrad et al., 1989; Nozhevnikova et al., 1994), it is not surprising that CH_4 production has been found to be dominated by aceticlastic methanogenesis in most lake sediments, since these sediments usually exhibit low temperatures (4-10°C) (Glissmann et al., 2004).

Various experiments were carried out for investigating the temperature dependence of methane production in the sediments. Here three representative experiments are introduced, described in thesis from Wagner, Nozhevnikova and Lupascu, respectively.

(1) Experiment of Wagner et al., 1997

In Wagner's experiment optima temperature for methane production in a typical soil of marshland was investigated. Undisturbed soil cores and homogenized soil material taken from the Elbe River marshland near Hamburg were used in this experiment.

For undisturbed soil cores, three cores were incubated under anaerobic conditions at 5°C, 10°C, 15°C and 20°C to determine methane production rates; while for homogenized soil material, the samples were incubated at 5°C, 10°C, 15°C, 22°C, 28°C, and 32°C. Gas chromatograph (GC) equipped with a Porapak-Q stainless steel column connected to a flame ionization detector was used for measuring the methane concentration in the experiment.

Table 2. Rates of methane production in undisturbed soil cores at different temperatures (Wagner et al., 1997)

	5°C	10°C	15°C	20°C	20°C after exchanging headspace atmosphere
CH_4 production rate 'initial phase' (nmol h^{-1} (g d.w.)$^{-1}$)	0.08 ± 0.01	0.31 ± 0.03	0.19 ± 0.02	0.58 ± 0.06	no initial phase
CH_4 production rate 'final phase' (nmol h^{-1} (g d.w.)$^{-1}$)	2.55 ± 0.06	19.89 ± 0.92	14.70 ± 0.35	23.54 ± 1.85	7.01 ± 0.63
CH_4 (%)	47	53	55	56	29
Gas volume (ml)	360	1250	928	1573	560

Means ± standard error, $n = 3$.

Table 3. Rates of methane production of homogenized soil samples at different temperatures (Wagner et al., 1997)

Temperature (°C)	CH_4 production rate (nmol h^{-1} g^{-1} f.w.)
5	3.08 ± 0.25
10	10.51 ± 0.96
15	6.48 ± 0.77
22	27.20 ± 3.14
28	30.84 ± 4.56
32	42.71 ± 4.84

The samples were supplied with 0.1 g organic matter (air-dried and ground roots of *Phragmites australis*). Means ± standard error, $n = 14$.

For both undisturbed soil cores and homogenized soil material, the results of methane production at different temperatures indicated the existence of a low optima temperature of methanogenesis for the investigated marshland soil, as shown in Table 2 and Table 3. The undisturbed soil cores showed higher variances of methane production rates at different temperatures, when compared with the homogenized soil material. Nevertheless, the results of both are confirmed to show an optimum temperature at 10°C for methane production by statistical analysis.

The soil cores experiment at different temperatures showed nearly the same progress of methane production: the first phase (initial phase) showed a lower methane production rate than the second phase (final phase). The latter phase was characterized as an abrupt increase in methane production. At the end of experiment the headspace of all cores was filled with concentrations of about 50% methane. At 5°C the fewest amount of methane was produced; at

10°C more methane was produced than at 15°C and the most methane was produced at 20°C. the results of homogenized soil material experiment were similar. One temperature optima at 10°C exists for methane production at low temperature conditions.

The results presented show that the increase of methane production with temperature is not linear in the typical soil of marshland. Two temperature optima in methane production at 10°C and in the mesophilic temperature range could be observed. Thus conclusions were made that in the investigated freshwater marsh soil, there exists two different methanogenic communities, indicated by the two temperature optima.

(2) Experiment of Nozhevnikova et al., 2007

In Nozhevnikova's experiment methanogenesis was investigated from the main methane substrates H_2/CO_2 and acetate using deep lake sediments from Lake Baldegg, Switzerland at different temperatures in a range from 2°C to 70°C. The goal was to assess the input of methanogenesis derived from H_2/CO_2 and acetate in sediment slurries and to investigate the influence of increasing initial H_2/CO_2 and acetate concentrations on methane production.

The samples were kept in the cold room at 6°C in a glove box under a nitrogen atmosphere after collected from Lake Baldegg. After slurry preparation, in order to enrich psychrophilic (5°C), mesophilic (30°C), and thermophilic (50°C) microbial communities, 1 L bottles were maintained at 5°C and 15°C for 3 months, 1.5 months at 30°C, and 1 month at 50°C. To study acetotrophic methanogenesis, acetate was added from sterile stock solutions up to the final concentrations needed; to study methanogenesis from hydrogen and carbon dioxide, the N_2 gas phase was replaced by H_2/CO_2. The sediment samples were incubated statically at different temperatures from 2°C to 70°C. All experiments were conducted in triplicate. The methane produced was measured by a gas chromatograph (GC) usually every 2-5 days during the first month of incubation and one to two times a month in long-term experiments. Then the rates of methane and acetate production were calculated by analyzing linear parts of the production curves.

Table 4. The total rates of methanogenesis and inputs(%) in sediment slurries enriched at different temperatures (Nozhevnikova et al., 2007)

Enrichment and incubation temperature (°C)	Rate of methanogenesis measured by* (μM h^{-1})			Input (%) to total methane production from†	
	GC	^{14}C-bicarbonate	^{14}C-acetate	^{14}C-bicarbonate	^{14}C-acetate
5	0.32 ± 0.021	0.015 ± 0.003	0.35 ± 0.07	2–8	93–99
15	1.15 ± 0.082	0.16 ± 0.02	1.22 ± 0.2	8–13	87–96
30	3.75 ± 0.24	0.95 ± 0.11	3.2 ± 0.4	22–30	74–86
50	5.80 ± 0.55	5.65 ± 0.7	0.03 ± 0.005	92–99	1–6

*Data of one experiment with five replicates.
†Data of five independent experiments. The sum of hydrogenotrophic plus acetotrophic methanogenesis was assumed to be 100%.

The rates of endogenous methane production in nonamended sediment slurries of Lake Baldegg enriched at different temperatures were measured using either ^{14}C-labeled acetate or ^{14}C-labeled bicarbonate. The results are given in Table 4: the methane production rates were the highest in the thermophilic (50°C) enrichments and the lowest in the psychrophilic (5°C) ones. This is

expectable as within a certain range microbial activity increases with temperature (Hofle, 1979). On the other hand, the part of methane produced from acetate was the highest in psychrophilic (5°C) enrichment and the lowest in the thermophilic (50°C) one. It ranged from about 95% at 5°C to <5% at 50°C. Conclusion are drawn preliminarily that at low temperature methane is mainly formed from acetate while at high temperature methane is mainly formed from bicarbonate.

Further experiments were conducted in this study to investigate methanogenesis and acetogenesis in sediment slurries amended with substrates of H_2/CO_2. The experiment was performed with slurries of fresh sediment samples that were incubated at eleven temperatures between 2°C and 50°C. Acetate was found to form for methanogenesis at 15°C and below during the first month of incubation. The accumulated acetate at low temperature was not utilized even after 1 year of incubation. Acetate was also formed at a higher temperature but it was subsequently consumed and methane was produced.

The results obtained in this work confirmed the influence of temperature on the pathway of methanogenesis. Acetate and bicarbonate play key roles in methanogenesis at low/high temperatures, respectively. H_2/CO_2 mixture is converted to acetate for methane production at low temperature while it is directly consumed for methanogenesis at high temperature.

(3) Experiment of Lupascu et al., 2012

In Lupascu's experiment temperature sensitivity of methanogenesis was investigated for the permafrost active layer of three contrasting peatlands located in a low Arctic discontinuous permafrost environment in northern Sweden. The variation in the controls of the methane concentration and production, including the potential effect of temperature increase on methane production rates, was assessed in the paper.

Two cores (A and B) were collected at three minerotrophic sites (Sedge mire, Sphagnum mire, and Ombrotrophic bog) and subsampled at six depths. The subsampling interval depended on the core length, which was between 22 cm to 50 cm. Right after collection and preparation of samples, laboratory analyses were carried out including elemental compositions analyses, pore water chemistry analyses, dissolved methane concentration and subsequent methane production rate incubations. For the incubation part, core subsamples were placed in 35 mL serum vials and flushed with oxygen-free nitrogen. Vials was stored in the dark at 4°C for a few days first, and transported to the relevant laboratory. Samples were subsequently incubated at 4°C, 14°C and 24°C. The headspace gas was sampled by syringe after 1, 2, and 3 days respectively for the three different temperatures. Methane concentrations were determined by gas chromatography (GC).

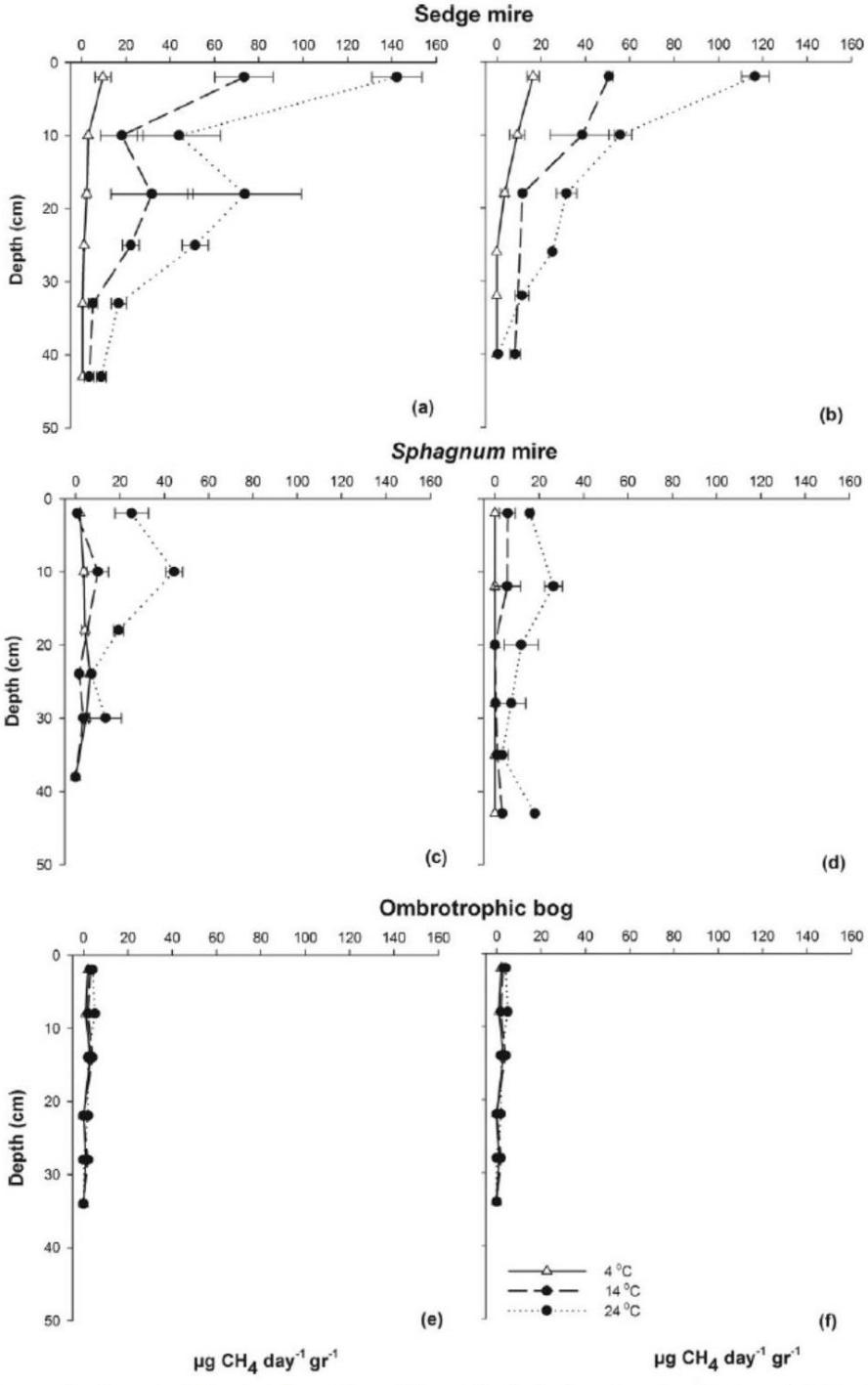

Figure 7. Methane production rates in incubated peat from Sedge mire, Sphagnum mire and Ombrotrophic bog [(a)(c)(e) August, (b)(d)(f) September]. Error bars represent the standard deviation of analyses in triplicate (Lupascu et al., 2012)

The results of anaerobic incubation of subsamples demonstrated that methane production rates vary with temperature, peatland type and soil depth. As shown in Figure 7, rates of methane production in the sedge site showed highest temperature sensitivity among three sites. However, with the increasing soil depth for all sampling months, the rates of methane production were less affected by the difference in temperature at this site. By comparison, the Sphagnum site and Ombrotrophic bog displayed much smaller variations in rate with depth and also with different temperatures. In order to better understand the methane production trends described, R_0 and

Q_{10} values were calculated, as shown in Table 5. In general, Q_{10} values in the sedge site are within the same range for the two sampling months: 2.4 to 3.5 and 1.9 to 2.8, in August and September, respectively. In the Sphagnum site Q_{10} values are found higher: 3.2 to 5.8 and 2.5 to 4.2, in August and September, respectively. The highest methane production potentials and extrapolated production rates at 0°C (R_0) always occurs in surface peat and declined with depth. It indicates the accumulation of above-ground litter inputs, in addition to inputs of fresh organic matter from root turnover.

Table 5. Main biological coefficients for the Sedge and Sphagnum mire in August and September (the number in parentheses indicate the standard deviation) (Lupascu et al., 2012)

Sedge site							
August							
Depth (cm)	**2**	**10**	**18**	**25**	**33**	**43**	***Mean***
R_o (μg CH_4 d gr^{-1})	17.7 (11.2)	3.9 (1.7)	6.3 (4.1)	4.3 (3.1)	0.8 (0.3)	0.7 (0.3)	5.6 (6.3)
Q10 (4–24 °C)	2.4 (0.7)	2.8 (0.5)	2.8 (0.8)	2.8 (0.9)	3.5 (0.6)	2.9 (0.6)	2.9 (0.4)
R^2	0.95	0.99	0.97	0.97	0.99	0.99	0.98 (0.02)
Ea (Activation Energy)	70.0	81.0	82.2	82.6	100.3	84.7	83.5 (9.8)
September							
Depth (cm)	**2**	**10**	**18**	***Mean***			
R_o (μg CH_4 d gr^{-1})	13.8 (2.3)	12.8 (7.5)	2.7 (0.3)	9.8 (6.2)			
Q10 (4–24 °C)	2.4 (0.2)	1.9 (0.5)	2.8 (0.2)	2.4 (0.5)			
R^2	1.00	0.90	1.00	0.96 (0.06)			
Ea (Activation Energy)	71.2	50.0	81.9	67.7 (16.2)			
***Sphagnum* site**							
August							
Depth (cm)	**2**	**12**	**35**	**43**	***Mean***		
R_o (μg CH_4 d gr^{-1})	0.9 (0.7)	0.5 (0.2)	0.2 (0.1)	0.3 (0.1)	0.5 (0.3)		
Q10 (4–24 °C)	3.3 (1.1)	5.1 (1.0)	3.2 (1.1)	5.8 (1.0)	4.4 (1.3)		
R^2	0.98	1.00	0.97	1.00	0.99 (0.01)		
Ea (Activation Energy)	95.5	129.8	93.2	140.1	114.6 (23.9)		
September							
Depth (cm)	**10**	**30**	***Mean***				
R^0 (μg CH_4 d gr^{-1})	1.4 (0.4)	1.7 (1.8)	1.5 (0.2)				
Q10 (4–24 °C)	4.2 (0.5)	5.4 (1.1)	4.8 (0.6)				
R^2	1.00	0.82	0.91 (0.09)				
Ea (Activation Energy)	114.5	68.0	91.3 (23.2)				

The results in this experiment indicate that temperature has a variable and direct influence on methane production rates at different sites, according to different Q_{10} values. In other words, it also reflects differences in temperature sensitivity of microbial processes that generate methane-precursors in the anaerobic chain of decay.

3.3 Models for describing gas production

Quantification of gas production (mainly CH_4 and CO_2) from sediments, or landfills, is important to evaluate measures for control of greenhouse gas emissions. All methods regarding to describing and estimating amount of gas production are based on models. Six different models for estimation of gas production in landfills are introduced by Scharff et al. (2006), including appliance in practical cases. The results of estimation on gas production in the same case can be of a huge difference using different models, which indicates the uncertainty in accuracy of these models. Through comparison and discussion one of the models was chosen and modified to be applied in the case of Elbe River.

The proposed six models to describe and calculate gas emissions in landfills are:

- First order model (TNO) (Oonk and Boom, 1995);
- Multi-phase model (Afvalzorg, developed in 1996);
- LandGEM (US-EPA) (US-EPA, 2001);
- GasSim (Enviroment Agency UK and Golder Associates) (Gregory et al., 2003);
- EPER model France (ADEME) (Budka, 2003);
- EPER model Germany (Umwelt Bundesamt) (Hermann, 2005).

The models mentioned above employ different dissimilation factors, degradation rate constants, types of waste categories and fractions in the calculation. Three landfill sites including Nauerna landfill, Braambergen landfill and Wieringermeer landfill were explored by Scharff et al. (2006) on methane production to compare six different models. The highest estimates obtained with the models are five to seven times higher than the lowest estimates. This huge variation in results cannot be considered to be acceptable. Among these models LandGEM model, GasSim model, the French EPER model and the German EPER model were proved to have more or less limitations or extreme results.

The most common type of models use single-phase or multi-phase first-order kinetics that describe the decay of biodegradable organic matter and the production of gas, such as the first order TNO model and the Afvalzorg multi-phase model. In these two models landfill gas (LFG) formation at a certain site is assumed to decay exponentially with time. As in practical situations landfill waste or riverine sediments usually contain different fractions of organic matter that degrade at different rates, multi-phase model is considered to be more reasonable in dealing with sophisticated gas production calculation compared with single-phase first order model.

In the Afvalzorg multi-phase model, eight waste categories and three fractions are taken into account and distinguished. For each fraction gas production is calculated separately. The waste fractions and rate constants used in the Afvalzorg multi-phase model are described in Table 6. The multi-phase model is a first-order model and can be described mathematically by:

$$\alpha_t = \varsigma \sum_{i=1}^{3} cAC_{0,i} k_{1,i} e^{-k_{1,i} t} \qquad (4)$$

Where

α_t	landfill gas production at a given time [m^3LFG • y^{-1}]
ς	dissimilation factor [-]
i	waste fraction number
c	conversion factor [m^3LFG • $kgOM^{-1}_{degraded}$]
A	amount of waste in place [Mg]
$C_{0\,i}$	amount of organic matter in waste of fraction i [kgOM • Mg $waste^{-1}$]
$k_{1\,i}$	degradation rate constant of fraction i [y^{-1}]
t	time elapsed since depositing [y]

Table 6. Afvalzorg multi-phase model constant values per waste fraction (Scharff et al., 2006)

Landfill	Dissimilation factor ς	Rapidly degradable k_1	Moderately degradable k_2	Slowly degradable k_3
Nauerna	0.7	0.187	0.099	0.030
Braambergen	0.8	0.231	0.116	0.030
Wieringermeer	0.7	0.187	0.099	0.030

The Afvalzorg multi-phase model calculates the landfill gas production based on organic matter content. Only rapidly, moderately and slowly degradable organic matter has been taken into consideration. The total organic matter content is higher than the sum of these three categories due to the presence of organic matter that is not considered biodegradable under anaerobic conditions.

In conclusion, for the estimation on gas production of riverine sediments in the case of Elbe River, the Afvalzorg multi-phase model is regarded as the most proper one for calculation. Although this model was applied for estimation on landfill gas formation in the literature, it is still valuable when analyzing gas production in other types of soil. It is a straightforward and robust model for estimation when little information is known about the soil material. It considers different pools of organic matter that degrade at different rates, which is just the case in the thesis project.

4 Experimental methods and available data

In this chapter, complete available data of the thesis project from the experiments are presented, as well as the experimental methods and statistical methods used for analysis. Firstly, procedures of sampling and sample incubation are introduced including devices used and material properties to be analyzed. These material properties are necessary for analyzing correlations between gas generation and sediment properties, as well as for interpretation of the experimental results. Secondly, procedures and available data of additional temperature experiment on gas production are given. Finally, statistical and mathematical methods used for data analyses in the thesis are introduced.

4.1 Sampling procedure and sample incubation

Fresh riverbed sediments were sampled from nine locations in the Elbe River, Port of Hamburg as discussed before using a sediment corer of 0.9 m depth. Per location, up to six cores were retrieved. Basic location and layer information of samples in Campaign #1 are summarized here in Table 7 as an example. The complete information of samples of all campaigns are listed in Appendix A. In brief, the cores were divided into layers SPM, FM, PS and CS and transitionary layers on board by visual inspection. Material from the same layers of the parallel cores was united, homogenized and some subsamples were analyzed for solids physical and chemical properties as well as pore water composition (parameters see Table 8) by a commercial laboratory; others were transferred to the laboratories of the University of Hamburg and TU Delft for analysis of respiration, gas generation, density fractions, microbial biomass and community analyses and other parameters. Rheological analyses were carried out on samples not previously homogenized in the Department of Hydraulic Engineering at TU Delft. The rest of the samples were stored at low temperature for further experiments. Various analyses work on sediment standard properties commenced right after sampling extraction work. Table 8 gives selected sediment property parameters and methods of standard solids and pore water analyses.

Table 7. Basic location and layer information of sampled sediments by example of Campaign #1

Sample No. (HPA)	Location	River km	Layer	Layer thickness cm	Sampling Date
1073	RT	619	SPM	15	05.06.2018
1074			FM	10	
1075			PS	20	
1076			CS	40	
1077	RV	616	SPM	10	05.06.2018
1078			FM	15	
1079			PS	10	
1080			CS	50	
1081	SH	621	SPM	20	05.06.2018
1082			FM	5	
1083			PS	25	
1084			CS	50	
1085	SC	620	SPM	8	06.06.2018
1086			FM	15	
1087			PS	15	
1088			CS	50	

Sample No. (HPA)	Location	River km	Layer	Layer thickness cm	Sampling Date
1090	KB	623	SPM	20	06.06.2018
1091			FM	10	
1092			PS	55	
1093			CS	15	
1095	VH	624	PS/CS	15	06.06.2018
1096			FM	10	
1097			PS	35	
1098			PS/CS	20	
1100			SPM	5	
1101	PK	627	SPM	20	07.06.2018
1102			PS	40	
1103			PS/CS	25	
1104	SW	643	SPM/FM	25	07.06.2018
1105			PS	15	
1106			CS	30	
1107	KH	629	SPM	25	07.06.2018
1108			FM	8	
1109			PS	17	
1110			CS	20	

Table 8. Sediment property parameters and methods of standard solids and pore water analyses

	Parameter	Method
Solids	Dry matter	ISO 11465/EN 14346
	Water content (WC)	Calculated from dry matter
	Particle size distribution Fraction > 2mm Fraction 1000-2000µm Fraction 600-1000µm Fraction 200-600µm Fraction 100-200 µm Fraction 63-100µm Fraction 20-63µm Fraction < 20µm Fraction < 100µm Fraction < 63 µm	Ultrasound sieving as by BfG
	Total nitrogen (TN)	EN 16168:2012-11
	Total organic carbon (TOC)	ISO 10694:1996-08
	Oxygen consumption after 3h	TV-W/I 1994
	Loss on ignition (LOI) 550°C	DIN 38414-S3/EN 15169
	P, S, Fe, Ca, Li, Al, Mn, Vn, Cu, Mg, Na, K	ISO 11885-E22:2009-07
In Fraction <20 µm	Total organic carbon (TOC)	ISO 10694:1996-08
	Loss on ignition (LOI) 550°C	DIN 38414-S3/EN 15169
	As, Pb, Cd, Cr, Cu, Ni, Zn	ISO 11885-E22:2009-07
	Hg	ISO 16772:2005-06
Pore water	pH value	ISO 10523-C5:2012-04

Parameter	Method
Electric conductivity (EC) at 25°C	EN 27888-C8:1993-11
Fe^{2+}, Mn^{2+}, Na^{+}, Ca^{2+}, Mg^{2+}	ISO 11885-E22:2009-09
NO_2^-, NO_3^-	ISO 13395-D28:1996-12
NH_4^+	ISO 11732-E23:2005-05
PO_4^{3-}	ISO 6878-D11:2004-09
Cl^-, SO_4^{2-}	ISO 10304-1-D20:2009-07
SiO_2	DIN 38405-D21:1990-10
Dissolved organic carbon (DOC)	EN 1484-H3:1997-08
Total nitrogen (TN)	EN 12260-H34:2003-12

Fresh sediment samples were incubated to measure carbon released by aerobic and anaerobic decomposition of organic matter. Institut für Bodenkunde (Institute for Soil Science, IfB) mainly did the aerobic part and TU Delft took charge of the anaerobic part. For the anaerobic incubation, sediment materials were placed in triplicate into 500 ml glass bottles which were closed with a gastight robber stopper secured with a ring cap. The bottles' headspace were flushed with 100% N_2 using an inlet and an outlet tube connected to the bottle headspace with a needle pushed through the stopper in order to create an anaerobic environment. After flushing, pressure in the bottle was equal to atmospheric pressure (no overpressure). Then the bottles together with the samples in were placed in 36°C-thermostatic equipment (water bath or oven) in the dark for incubation.

Figure 8. Devices of Gas Endeavour (left, source: www.bioprocesscontrol.com) and pressure gauge (right, photo taken in the laboratory of TU Delft)

Gas production of these samples under anaerobic incubation was monitored mainly by two measuring devices: Gas Endeavour (GE, bioprocesscontrol) and a pressure gauge, as shown in Figure 8. The Gas Endeavour is a fully automatic analytical device designed for the real-time monitoring of generating gas flows, allowing users to measure low gas volume change at high accuracy. The bottles with samples in were connected to the device and the corresponding

software of GE automatically recorded the volume increase in the system at any time. In that way the magnitude of gas production at a certain time can be calculated. The pressure gauge is another option for monitoring gas production in the bottles. It was connected to the bottle headspace using a needle pushed through the rubber stopper. Pressure inside the bottle was measured at regular intervals using a pressure gauge, thus an increase in pressure was recorded and then the magnitude of gas production were calculated using Ideal Gas Law and Boyle's Law. The complete calculated results of gas production of all samples are listed in Appendix B.

Furthermore, the evolution of gas composition inside bottles over time was analyzed by gas-chromatographic analysis of the headspace. As mentioned before the gases generated are mainly composed of methane (CH_4) and carbon dioxide (CO_2). Total generation of CH_4 and CO_2 was calculated from the gas concentration, headspace volume, incubation temperature, and pressure inside the bottle using Ideal Gas Law. The amount of produced CO_2 was corrected for the share dissolved in water for every single sample, according to Henry's constant (listed in Sander, 2015). The total amount of generated gas equals the sum of CO_2 and CH_4 produced.

4.2 Temperature experiment on gas production

Additionally, in order to find how temperature affects the rate and magnitude of gas generation and therefore to be able to predict gas generation based on the seasonal variation of temperature in the Elbe river, a controlled experiment in which sediment samples were incubated at different temperatures was carried out. The start date of the experiment is 8th October, 2018 and the end date is 6th February, 2019, hence lasting for about four months. Six levels of temperature were set for incubation: 5, 10, 20, 28, 36 and 42°C. Sample 4401 (location: PK, layer: PS/CS) was chosen for the whole temperature experiment. The moisture content of sample 4401 was determined by oven-drying method: part of samples were weighed and then dried in the 105°C-oven; water content thus was calculated using the weight loss during drying process, as shown in Table 9, which is determined to be 213.78% on average of the results.

Table 9. Water content calculation of experiment sample

Sample No. (HPA)	Vessel No.	Vessel, empty g	Vessel + moist sample g	Vessel + dry sample g	Water content %
4401	2T	57.91	105.79	73.13	214.59
4401	4A	76.95	143.33	98.16	212.97

Sample materials were placed in triplicate into 250 ml glass bottles. Around 160 g moist samples were weighed and placed in each bottle using a funnel, as shown in Figure 9. Detailed weight of each sample and information of each bottle are measured or calculated which are listed in Table 10. The dry weight of each sample and headspace volume in each bottle are necessary for calculation of gas production. As the experiment belongs to anaerobic incubation the bottles' headspace were flushed with 100% N_2 as well. Then the bottles together with the samples in were placed in thermostatic equipment (refrigerator, water bath or oven) at six different temperature levels in the dark for incubation. Figure 9 also shows the incubation of three parallels at 42°C-oven, as an example.

Figure 9. Sample set procedure using a funnel (left) and incubation of parallels at 42°C (right)

Table 10. Gravimetric and volumetric base data of incubated samples and vessels in the temperature test

Sample No. (HPA)	Temperature °C	Parallels	Moist sample g	Dry sample g	Volume soil + water ml	Headspace volume ml
4401	5	A	165.37	52.70	132.55	160.0
		B	166.34	53.01	133.33	159.2
		C	165.96	52.89	133.03	159.5
	10	A	166.25	52.98	133.26	159.3
		B	162.78	51.88	130.48	162.1
		C	167.07	53.25	133.92	158.7
	20	A	165.4	52.71	132.58	160.0
		B	169.59	54.05	135.94	156.6
		C	161.35	51.42	129.33	163.2
	28	A	164.47	52.42	131.83	160.7
		B	162.36	51.74	130.14	162.4
		C	162.68	51.85	130.40	162.2
	36	A	161.57	51.49	129.51	163.1
		B	165.55	52.76	132.70	159.9
		C	167.21	53.29	134.03	158.5
	42	A	164.69	52.49	132.01	160.6
		B	161.83	51.58	129.72	162.9
		C	163.26	52.03	130.86	161.7

The gas production of the samples was monitored by measuring the increase of pressure in the bottle headspace using a pressure gauge, in the same way as described in chapter 4.1. The measurement frequency was every 3-7 days during the first month of incubation, depending on the temperature (more frequently for those at higher temperature), and one to two times a month in the long-term. The temperature was checked by a thermometer at every measurement to ensure a constant temperature in the incubation environment. Therefore, the change in pressure was known for each bottle thus the magnitude of gas production could be calculated using Ideal Gas Law and Boyle's Law. The raw data of the recorded pressure of all samples is given in Appendix C.

In addition, gas-chromatographic (GC) analysis of the headspace was carried out twice for monitoring the gas composition change inside bottles over time. The first GC measurement was on 4th December, 2018, at the mid-time of the whole experiment; the second was on 6th February, 2019, at the end of the whole experiment on temperature. The GC device directly gave the composition of gas inside the bottle in the way of percentage, including generated CO_2 and CH_4, flushed N_2 at the start of the experiment and little O_2 mixed due to measurement. The amount of produced CO_2 was corrected for the share dissolved in water, based on the CO_2 concentration and the pressure measured in the bottle headspace as well as the solubility of CO_2 in water as given by Henry's constant (listed in Sander, 2015). The Henry's constant used in calculation of dissolved gas in this experiment are listed in Appendix D.

4.3 Statistical methods for data analyses

Various mathematical tools were used in data analyses, mainly including Matlab, Excel, and OriginPro. In this chapter the calculation methods for magnitude of gas production, estimation of total gas potential and cross-correlation are briefly introduced.

Firstly, the magnitude of gas production was calculated using Excel and OriginPro. As mentioned, gas production of samples under anaerobic incubation was measured by two methods: Gas Endeavour and a pressure gauge. GE provides continuous data points while pressure measurement can only give data with time intervals. Therefore, the calculation of gas production measured by GE could be easy: by reading the raw data automatically recorded by GE, the magnitude of gas production at any time node was acquired. While for the calculation of gas production measured by the pressure gauge, the Ideal Gas Law and Boyle's Law were applied for transforming the pressure increased inside the bottles to the amount of gas produced.

For reasons of comparability, the time nodes of 21 days (chosen to reflect the GB_{21}-value regulated in the German Landfill Ordinance; DepV, 2009) and 100 days were defined to describe the magnitude of gas production. For pressure measurement a time interval existed so that data at 21 days and 100 days could not always be directly acquired. In that case, available data points were input into OriginPro to create a fitting curve, from which the gas production after 21 days and 100 days can be directly read subsequently. The unit of magnitude of gas production was normalized to per gram total organic carbon (TOC), in order to analyze differences in the degradability of the organic matter between sites. Also the volume of gas production is described

by weight of TOC here as CH_4 and CO_2 can both be normalized to one molar carbon. After managing the unit needed, three parallels of data on gas production after 21 days and 100 days were acquired for each sample. A Grubb's check (Grubbs, 1969) was then conducted at 99% significance level among the three parallels for each sample to detect outlying observations in parallels and thus get rid of the extreme results. The check could be performed in Excel.

Secondly, estimation of total gas potential was realized using OriginPro or Matlab. As discussed already a multi-phase model as described by Afvalzorg (www.afvalzorg.nl) was considered most applicable to fit the data set in the thesis. Some small changes were made on the model's equation for better application to the investigated case, under the circumstance of keeping the idea of the model unchanged. The modified model can be described mathematically by:

$$y = A_1 * e^{(-x/t_1)} + A_2 * e^{(-x/t_2)} + y_0 \quad (5)$$

Where

x	Time spent for incubation of sample [day]
y	Amount of gas production at given time x [mg C/g TOC]
y_0	Total gas potential [mg C/g TOC]
t	Time constant for each phase [day]
A	Amplitude of the model [-]

The model is based on the assumption that at least two temporal phases exist in the course of gas formation, which will be discussed in detail in the following chapter. Compared to the equation (4) of the Afvalzorg multi-phase model, here the time constant *t* is the reciprocal of degradation rate constant *k*, which is also related to the half-life of the organic carbon in each pool; Amplitude *A* is corresponding to the multiplication of the dissimilation factor ς, conversion factor *c* and some other constant values used in the Afvalzorg multi-phase model. Amplitude *A* together with time constant *t* give the slope at $x = 0$ as $-A/t$ for each single phase by a calculation of first-order derivation of equation (5).

After input of data points calculated from GE or pressure measurement into the model, OriginLab will process immediately and provide the parameters mentioned in the equation (5), as well as a fitting curve describing development of gas production with time. From the parameters or the curve, the predicted result of total gas potential for each sample could be acquired. Note that this method is only fitted for samples that have been incubated for a long term (at least 200 days) and the model is still under testing phase. Errors might occur for short-term incubated samples when estimating the total potential.

Furthermore, cross-correlation tables were created in Excel for analyzing relations between gas generation and sediment properties. In detail, Pearson's coefficient r was calculated between gas production and every single sediment property. A Pearson correlation coefficient is a number between -1 and 1 that indicates the extent to which two variables are linearly related. The closer the coefficient is to -1 or 1, the stronger the correlation is between two variables. Given a pair of random variables (*X*, *Y*), Pearson's coefficient r could be calculated by:

$$r = \frac{\mathrm{cov}(X, Y)}{\sigma_X \sigma_Y} \tag{6}$$

Where

cov	Covariance
σ_X, σ_Y	Standard deviation of *X*, *Y*

Statistical significance of Pearson's coefficient r is accepted for a probability of error $p < 0.01$ for a two-sided test in the thesis project. According to the table provided in Appendix F, the value of r that checks significance of correlation is determined by the number of available samples. The number of available samples in each layer and the corresponding significant r are listed in Table 11.

Table 11. Significant Pearson's coefficient r for each layer, according to the table in Appendix F

Layer	Number of available samples	Significant value of r
SPM	20	0.537
FM	20	0.537
PS	25	0.487
PS/CS	10	0.708
CS	20	0.537

The total number of available samples is less than the number of samples collected at the Port of Hamburg. That is because for some certain properties the information was missing for part of the samples. After determining the significant value r of each layer, the correlation tables was created in Excel by calculating Pearson's coefficient r between gas production and every single sediment property. The results in the tables were then compared to the significant r in each layer to judge if the gas production is statistically correlated to each sediment property and how strong the correlation is.

5 Results and discussion

In this chapter, various analysis works are conducted based on the data acquired from several laboratories. If no otherwise specified, the data used in analysis are all under anaerobic incubation. Firstly an overview on data of sediment properties and calculation results on magnitude of gas production are presented. The spatial and temporal variability on gas production in the Port of Hamburg are then analyzed to get an overview of gas production situation at site. The correlation analysis is carried out subsequently to provide knowledge on relations between gas production and its sediment properties; difference between gas production under anaerobic and aerobic incubation is also compared. Then the time series analyses including short-term and long-term gas formation, as well as application in the gas generation model are presented. Finally the results of temperature experiment are analyzed including comparison with previous research.

5.1 Physical and chemical properties of sediments

According to various norms in Table 8, analysis of sediment standard properties were carried out in laboratory. For the statistical analyses conducted in this thesis, a reduced set of parameters was selected that was hypothesized to be of relevance for gas generation. Table 12 shows the corresponding data of the samples in Campaign #1 as an example. Table 13 gives an overview on properties of samples from all five campaigns including average, median and bold values.

Table 12. Data of selected sediment properties of selected samples from Campaign #1, as an example

Sample No. (HPA)	Note	TOC	TN	WC	P	S	Fe	Ca	pH	EC	NO_3^-	PO_4^{3-}	SO_4^{2-}
		(HPA) %DW			mg/kg DW					25°C µS/cm	mg/l		
1075	RT,PS	4.5	0.57	402.5	1690	5230	39800	47800	7.46	1656	1.6	0.069	13
1076	RT,CS	4.8	0.62	161.1	1750	5290	38500	55000	7.30	2680	1	0.11	3.8
1079	RV,PS	7.1	0.91	498.8	1820	4470	26300	133000	7.39	2000	0.5	0.11	8.6
1080	RV,CS	5.5	0.67	287.6	2150	4090	30400	77100	7.05	2570	0.5	0.14	34
1083	SH,PS	4.0	0.48	346.4	1520	4580	37100	41900	7.75	1572	1.3	0.38	73
1084	SH,CS	3.8	0.47	259.7	1420	4050	31300	49500	7.27	2380	0.5	0.12	9.3
1088	SC,CS	4.7	0.60	298.4	1580	4900	36000	54300	7.32	2070	0.5	0.097	38
1091	KB,FM	3.2	0.34	267.6	1170	3790	29500	36300	7.73	1449	2.1	0.24	160
1092	KB,PS	3.6	0.42	275.9	1310	4430	32200	42800	7.46	1877	0.5	0.11	5
1096	VH,FM	3.8	0.45	553.6	1440	4730	36200	38600	7.73	1439	0.5	0.34	150
1097	VH,PS	3.9	0.47	331.0	1480	4710	36600	40100	7.48	1786	0.5	0.15	21
1102	PK,PS	3.9	0.47	346.4	1580	4890	38100	39900	7.46	1828	0.5	0.14	93
1105	SW,PS	2.3	0.25	145.1	960	3110	23600	35800	7.59	1564	1	0.24	87
1109	KH,PS	3.9	0.47	365.1	1550	4960	38900	43000	7.42	1711	13	0.11	92
1110	KH,CS	3.8	0.47	249.7	1560	4520	33900	43500	7.36	2240	0.5	0.11	5

Table 13. Overview on data of selected sediment properties of all samples in five campaigns. Max. = maximum, Min. = minimum, S.D. = standard deviation, DW = dry weight

	TOC	TN	WC	P	S	Fe	Ca	pH	EC	NO_3^-	PO_4^{3-}	SO_4^{2-}
	(HPA) %DW			mg/kg DW					25°C µS/cm	mg/l		
Average	3.85	0.47	2388.2	1461	4890	33910	46496	7.52	1921	4.59	0.13	83.8
Medium	3.76	0.45	316.7	1480	4560	35400	41700	7.53	1704	3.50	0.11	92.5
Max.	7.60	1.00	99900.0	2470	21800	42500	133000	8.13	22902	36.0	0.38	180.0
Min.	0.64	0.04	88.0	630	1950	17100	29300	6.68	13	0.25	0.02	2.9
S.D.	1.26	0.19	10225.8	345	2297	5918	16636	0.24	1748	4.35	0.08	57.8

Note that only parts of important properties are listed here as an example in the above tables. Other properties should not be ignored in analysis. From the overview table it is indicated that the sediment in Port of Hamburg can differ strongly regarding physical and chemical parameters. The high SO_4^{2-} concentrations observed in FM layer indicate marine influence of the high-fluid-layer while the high NO_3^- concentrations of the samples indicate a more oxidized status of the sediment. PH value falls in the range of 6.68 - 8.13 which reflects a diversified environment in Port of Hamburg but most of the sediments stay in alkaline environment. Sediment TOC and TN values are in a relatively narrow span. However, some limitations in measurement can cause mistakes in data as well. For example, the extremely high water content of a certain sample shown as 99900 %DW is regarded as a wrong data and influences a lot on the average value of water content. In this case, the medium value is more reliable for reference.

When compared with sediment properties found from other researches as listed in Table 14, the data of the properties in our study are more or less of the same range. The TOC, TN and Fe content are a bit higher than that in other studies. Further analysis on these data and their relations to gas generation are followed in Chapter 5.4.

Table 14. Physical and chemical properties of sediments in other researches

Place	Soil type	Depth cm	TOC % DW	TN % DW	TIC % DW	WC % DW	pH	Fe mg/kg DW	SO_4^{2-} mg/l	Source
Lake in Tibetan plateau, China	Lake sediments	0-9	2.3	0.3			7.2	9717		Liu et al., 2017
		10-19	1.8	0.3			7.8	6813		
		20-29	1.9	0.3			7.3	4803		
		30-39	1.5	0.3			7.1	4188		
		40-50	2.4	0.4			7.5	279		
Landfill in Hamburg, Germany	Dredged sediments	140-280	3.51	0.37	0.92	50.4	7.4			Gebert et al., 2019
		430-460	2.11	0.21	0.53	32.7	7.3			
		540-680	2.66	0.28	0.65	41.0	7.5			
		710-790	2.49	0.22	0.19	29.7	7.3			
		790-880	2.95	0.26	0.24	36.3	7.2			
		920-1040	3.92	0.39	0.65	50.4	7.4			
		1080-1130	3.83	0.40	0.81	51.8	7.5			

Place	Soil type	Depth cm	TOC % DW	TN % DW	TIC % DW	WC % DW	pH	Fe mg/kg DW	SO_4^{2-} mg/l	Source
		1160-1260	3.44	0.35	0.54	45.7	7.5			
		1290-1450	1.35	0.13	0.40	23.2	7.8			
		1500-1590	1.42	0.12	0.18	13.4	7.9			
		1710-1780	3.09	0.25	0.20	30.7	7.5			
Lower Elbe	River sediments	-	2.7	0.26	1.48		7.8		505	Gebert et al., 2006
Tidal Elbe			3.9	0.4	0.62		7.3		40	
Weser			4.4	0.49	0.65		7.0		40	
Lower Spree			1.3	0.1	0.12		7.1		27	
Spree			3.6	0.21	0.37		7.5		46	
Lower Ems			2.8	0.28	1.47		7.4		9	
Lower Rhine			3.5	0.34	0.51		7.4		25	
Upper Rhine			3.0	0.34	5.89		7.3		13	
Warnow			14	1.16	1.32		7.2		267	
Zhenjiang, China	Rice paddy soil	-	1.04	0.07			7.7	7271		Yao et al., 1999
Changchun, China			1.68	0.14			6.0	7952		
Bugallon, Philippine			1.97	0.16			5.9	7416		
Luisiana, Philippine			1.65	0.16			5.1	23539		
Pavia, Italy			0.81	0.07			6.1	4926		
Vercelli, Italy			1.55	0.14			6.0	10884		

5.2 Gas formation under aerobic and anaerobic conditions

According to incubation procedures introduced before, data of magnitude of gas released were acquired for both aerobic and anaerobic incubation. For reasons of comparability here the time nodes of 21 days (chosen to reflect the GB_{21}-value regulated in the German Landfill Ordinance; DepV, 2009) and 100 days were defined to describe the magnitude of gas production. Gas formation of sediment samples after 21 days and 100 days were calculated from raw data recorded in laboratory, as presented in Table 15. Here, only calculations of samples in Campaign #1 are listed as an example. The complete calculated results of gas released of all samples are listed in Appendix B. The unit of magnitude of gas production was normalized to per gram total organic carbon (TOC) as explained already. Aerobic incubation was carried out at 20°C while anaerobic incubation was at 36°C. To compare anaerobic and aerobic degradation of organic matter, results under aerobic incubation were normalized to 36°C.

Table 15. Aerobic and anaerobic release of gas after 21 days and 100 days in Campaign #1, incubation at 36°C. Each data represents the average of three parallels

Sample No. (HPA)	Location	Layer	Aerobic respiration, 36°C		Anaerobic respiration, 36°C	
			21 days	100 days	21 days	100 days
			mg C/g TOC			
1073	RT	SPM	154.4	568.1	63.27	115.28
1074	RT	FM	174.3	637.6	53.33	96.30
1075	RT	PS	153.3	629.6	44.75	73.60
1076	RT	CS	147.1	727.7	53.26	91.44
1077	RV	SPM	248.2	1064.2	113.40	171.54
1078	RV	FM	268.4	778.9	103.39	173.76
1079	RV	PS	268.9	1157.0	90.37	168.46
1080	RV	CS	112.0	389.7	33.51	82.68
1081	SH	SPM	160.3	665.2	48.82	100.79
1082	SH	FM	163.3	700.2	48.60	74.31
1083	SH	PS	175.8	664.9	34.92	77.53
1084	SH	CS	173.1	621.9	41.13	84.46
1085	SC	SPM	177.4	705.9	16.47	43.18
1086	SC	FM	241.0	762.7	44.40	102.42
1087	SC	PS	174.7	750.8	54.80	92.92
1088	SC	CS	179.7	700.1	79.67	129.36
1090	KB	SPM	107.0	431.8	20.35	60.57
1091	KB	FM	124.7		20.68	60.10
1092	KB	PS	128.5	554.2	42.07	78.89
1093	KB	CS	67.2	311.7	29.99	67.92
1095	VH	PS/CS	104.6	526.4	36.94	69.54
1096	VH	FM	126.3	506.7	37.19	82.75
1097	VH	PS	147.6	601.8	36.91	65.76
1098	VH	PS/CS	117.0	547.1	39.48	84.56
1100	VH	SPM	194.4	602.9	13.32	33.20
1101	PK	SPM	60.1	229.4	12.94	43.20
1102	PK	PS	148.0	570.4	30.85	62.26
1103	PK	PS/CS	123.9	604.8	36.21	82.14
1104	SW	SPM/FM	82.2	403.2	7.17	35.72
1105	SW	PS	82.4	435.8	16.10	42.77
1106	SW	CS	59.6	344.0	17.79	46.94
1107	KH	SPM	71.7	278.5	8.16	21.86
1108	KH	FM	146.1	541.0	21.71	63.82
1109	KH	PS	136.9	593.4	29.20	62.58
1110	KH	CS	124.0	567.9	31.10	71.59

For the Campaigns #4 and #5 the incubation time was less than 100 days by the time of finalizing the thesis, thus the 100-day value could not be recorded in the table in Appendix B. From the magnitude of carbon released under aerobic and anaerobic incubation in the table, it is preliminarily concluded that organic matter degradation happens faster and easier with oxygen than without oxygen, which is as expected according to the theory of anaerobic and aerobic

respiration in literature study. In addition, an overview on aerobic and anaerobic release of carbon of all samples collected at the Port of Hamburg including average, median and bold values is presented in Table 16.

Table 16. Overview on aerobic and anaerobic release of carbon after 21 days and 100 days, incubation at 36°C, all samples

	Aerobic respiration, 36°C		**Anaerobic respiration, 36°C**	
	21-day	**100-day**	**21-day**	**100-day**
	mg C/g TOC			
Average	115.35	559.93	35.71	74.07
Medium	112.28	521.95	29.77	64.99
Max.	351.21	2952.58	153.17	229.13
Min.	13.64	118.72	4.05	17.57
S.D.	67.20	306.09	25.30	38.98

The average gas production rate under anaerobic incubation in this thesis project (incubated at 36°C) is calculated as 227.1 nmol h^{-1} g dw^{-1} when using the 21-day gas production amount for calculation and 98.9 nmol h^{-1} g dw^{-1} when using the 100-day gas production amount for calculation. It makes sense as gas production rate decreases in the long-term. The unit is normalized to nmol h^{-1} g dw^{-1} for convenience on comparison with the gas production rates in other researches, as shown in Table 17. Note that for each case the soil type, depth and incubation conditions are different, which affect the magnitude of gas production rate. In general, the 21-day gas production rate (227.1 nmol h^{-1} g dw^{-1}, incubated at 36°C) for the sum of CH_4 and CO_2 in our project is within the range found for other soils in previous researches.

Table 17. Anaerobic gas production rates for different types of soils in other researches

Place	**Soil type**	**Depth cm**	**Incubation**		**Gas prod. rate nmol h^{-1} g dw^{-1}**		**Source**
			Temp.	**Time**	**CH_4**	**CO_2**	
Peatlands at Minnesota, USA	Peat	10	25°C	100h	219.6	-	Williams et al., 1984
		25			213.2	-	
		40			200.7	-	
		90			40.8	-	
		120			6.2	-	
		210			2.0	-	
Bog Lake Fen, Minnesota, USA	Peat	25	18°C	15d	152.8	291.7	Zalman et al., 2018
S1 Bog, Minnesota, USA				11d	140.2	246.2	
Zim Bog, Minnesota, USA				22d	85.2	231.1	
Lake in Tibetan plateau, China	Lake sediments	0-9	10°C	80d	5.08	1.42	Liu et al., 2017
		10-19			0.58	0.54	
		20-29			0.07	0.50	
		30-39			0.01	0.63	
		40-50			0.01	0.63	
Wetland in Bocas del Toro, Panama	Peat	-	28°C	40d	14.2	71.0	Girkin et al., 2018

Place	Soil type	Depth cm	Incubation		Gas prod. rate nmol h^{-1} g dw^{-1}		Source
			Temp.	Time	CH_4	CO_2	
Bog in Southern Ontario, Canada	Peat	0-10	30°C	9d	2.50	-	Dunfield et al., 1993
Hudson Bay Lowland, Canada	Peat	0-10			3.75	-	
		10-20			3.33	-	
Landfill in Hamburg, Germany	Dredged sediments	140-280	36°C	757d	12.5		Gebert et al., 2019
		430-460			6.4		
		540-680			8.7		
		710-790			7.4		
		790-880			5.3		
		920-1040			13.1		
		1080-1130			18.6		
		1160-1260			12.9		
		1290-1450			5.1		
		1500-1590			3.1		
		1710-1780			4.7		
Marshes in Sapelo Island, USA	Salt marsh sediment	3-5	23°C	28h	1.3		Jones et al., 1980
Elbe River near Hamburg, Germany	Marsh sediment	60-70	20°C	6d	24		Wagner et al., 1997
Lake Biwa, Japan	Lake sediment	0-10	7°C	5d	0.40		Dan et al., 2004
Several waterways, Germany	River sediment	-	22°C	500d	5-30		Gebert et al., 2006
Zhenjiang, China	Rice paddy soil	-	30°C	36d	9.6	246.3	Yao et al., 1999
Changchun, China		-		47d	12.5	171.3	
Bugallon, Philippine		-		6d	52.1	343.8	
Luisiana, Philippine		-		16d	16.7	212.5	
Pavia, Italy		-		6d	41.3	153.3	
Vercelli, Italy		-		18d	21.3	237.9	
Elbe River near Hamburg, Germany	River sediment	0-100	36°C	21d	227.1		This study
				100d	98.9		

5.3 Spatial and temporal variability of gas production

As the sediment samples taken from the Elbe River came from different locations (RV, SH, RT, SC, VH, KB, PK, KH, SW) aligned along the river approximately 20 kilometers, different layers (SPM, FM, PS, CS), and different campaigns (Campaign #1, #2, #3, #4, #5 from June to November in 2018), variability of gas production was assumed to exist in all aspects. In order to get an overview of gas production situation at site for the thesis project, the spatial and temporal variability on gas production in the Port of Hamburg were analyzed.

A research question is asked for the variability analysis:

- What is the spatial and temporal variability of gas generation within sediment profiles in the Port of Hamburg?

5.3.1 Spatial variability

Spatial variability mainly focus on differences of sediment gas production resulted from different layers and locations. There are a couple of things to note in this part of analysis, though. Firstly, all analyses on variability were based on data of anaerobic gas production after 21 days only, as for short-term 21 days we have the most sufficient available data points. Secondly, as mentioned before, in some sediment samples the material could be mixed up with two adjacent layers, thus several transitionary layers were defined manually that contains sediment features of both adjacent layers, as SPM/FM layer, FM/PS layer and PS/CS layer. Nevertheless, only a few available samples belong to SPM/FM and FM/PS layer which leads to troubles in analysis, so these samples (No. 1104, 2221, 2238, 3210, 3229, 5206, 5210, 5226 and 5234, see Appendix A) are included in certain layers based on property similarities. Therefore, finally five layers are determined for variability analysis as well as other analysis later, as SPM, FM, PS, PS/CS and CS layer.

The results of variability of gas production with sampling locations for all five campaigns are presented below in Figure 10. As variability also exists in different depths and seasons, sediments from different layers and campaigns are separated and marked. The five graphs correspond to five distinguished layers and different colors stand for different campaigns. The x-axis represents different locations from RV (616 km) to SW (643 km) and the y-axis represents the 21-day gas production amount. Obviously, despite of differences in layers and campaigns, gas production rate shows a trend that it decreases from east (upstream) to west (downstream) in the Elbe River. It demonstrates a relatively higher readily degradable organic carbon content in the upstream areas. However, SPM and FM layers show larger variability of gas production along the river among the five layers, especially the SPM layer, varying from 153.2 mg C/g TOC at site RV (616 km) to 5.9 mg C/g TOC at site SW (643 km). On the contrary, gas production in the PS/CS layer and CS layer keeps in a stable level with relatively less variability along the river. This can be explained by the age of sediment materials in different layers. In the PS/CS and CS layer, most of the sediments are of the oldest materials, which means the share of readily degradable organic carbon has already been mostly depleted despite of the difference in locations in the stream. While in SPM and FM layer the sediment materials are relatively fresh, which contain sufficient content of degradable organic matter and are more easily influenced by the streams due to their high flow-ability.

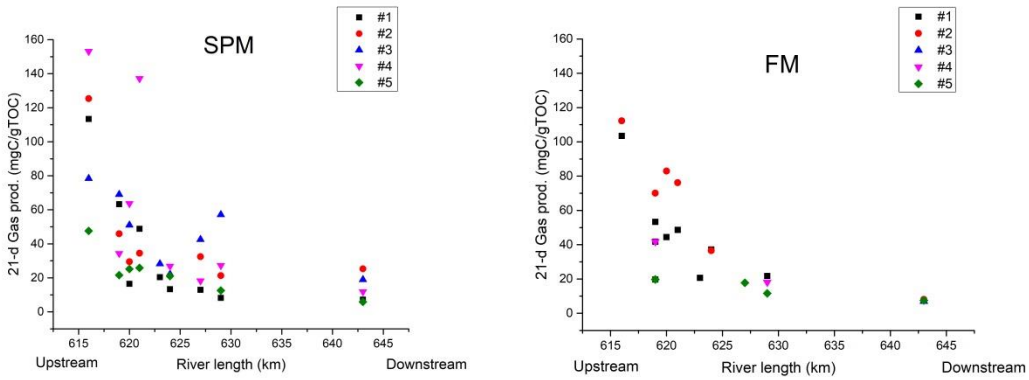

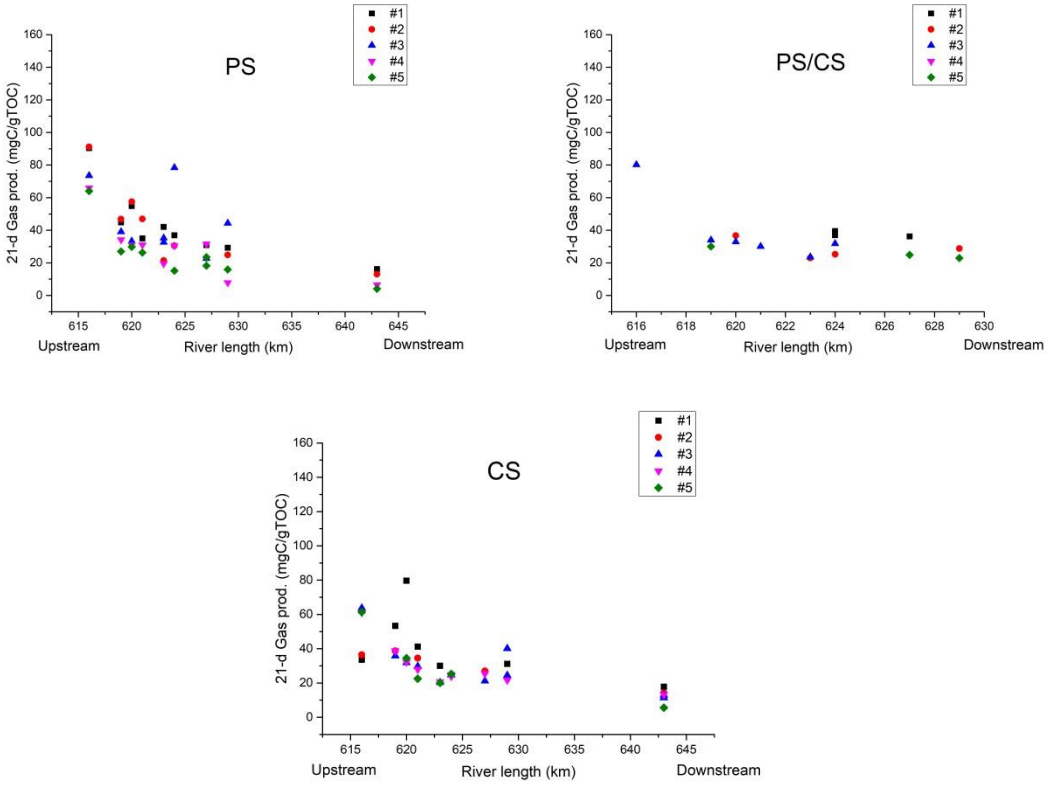

Figure 10. Relationship between gas production after 21 days and sampling locations, for each layer

Furthermore, the variability of gas production with depth was also analyzed. Here, samples from Campaign #2 at location RV, RT, SC, SH and VH site were used for comparison as this campaign delivered the most complete data set for all the layers. Generally, the top part of the sample cores belongs to SPM layer, with suspended particles in water; then below the water-solid interface in the cores, FM layer takes around 10 cm; the next 20 cm belongs to PS layer; finally about 40 cm at the bottom belongs to PS/CS or CS layer. Sometimes the thickness can be different for the mentioned layers but in average it is as described. Figure 11 gives the curves describing variability of gas production with depth. Obviously, besides samples at RV (616km) site, all samples in campaign #2 possess a highest 21-day gas production in FM layer. Those layers with higher degree of consolidation such as PS/CS and CS layer produce less gas compared with other layers. For SPM layer, the results are with uncertainties that in some locations (SC, VH) it produces the least gas while in other locations (RV) it produces the most gas. The suspended materials in water are of high flow-ability and influenced much by the river flow rates. In this layer organic matter input is much affected by the flows that bring down substances from the upstream or from the North Sea with the flood tide. Therefore the variability of gas production in the SPM layer can be large among different sites. The FM layer produces gas at a relatively stable and high level among all the layers which indicates a high readily degradable organic carbon content in this layer. Also, the graph of variability on gas production with depth again proves a higher gas production in the upstream when we look into the curve of different colors in the vertical direction.

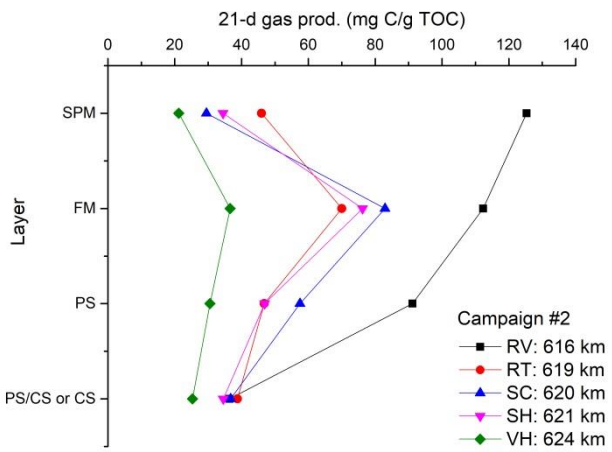

Figure 11. Relationship between gas production after 21 days and depth (layers), for RV, RT, SC, SH, VH in Campaign #2

5.3.2 Temporal variability

Because gas production in sediments is influenced by temperature as introduced in literature study, variability can also exist among different seasons. As mentioned before that sediment samples in five campaigns were collected from June to November, the influence of seasonal difference on gas production cannot be ignored. As gas generation is controlled by the availability of degradable organic matter, seasonal variability also reflects the seasonal change in availability of degradable organic matter. Generally speaking, in SPM, FM layers organic matter input is expected to be influenced much by the flood tide or river flows in different seasons while in PS and CS layers it is less affected.

Here samples in the SPM, PS, PS/CS and the CS layer at sites RV, RT, SC, VH and KH were used for comparison as they delivered the most complete data set for all the campaigns. As shown in Figure 12, the relationship between magnitude of gas production and sampling time is hard to summarize in one sentence. The variability of gas production with season is quite different at each location, and also in each layer. Generally, in the CS layer, the amount of gas production in different months is stable at all sites, which indicates the degradable organic matter pool to be of comparable stability in this highly consolidated layer. While in SPM layer the variability of gas production rate can be quite large among different months, especially at upstream site RV (616 km). Gas production rate reaches its maximum in August at sites RT (619 km) and KH (629 km), and in September at sites RV (616 km), SC (620 km) and VH (624 km), for the SPM layer. For the PS layer, at sites VH (624 km) and KH (629 km) the most gas was produced in August while other locations show a relatively stable gas production rate among all five campaigns. The gas production rate in the last campaign (November) keeps at a low level in most cases, which indicates a low readily degradable organic carbon content in this very last campaign. The temporary variability analysis can be sophisticated as some uncontrollable factors exist on the timeline such as human dredging activities.

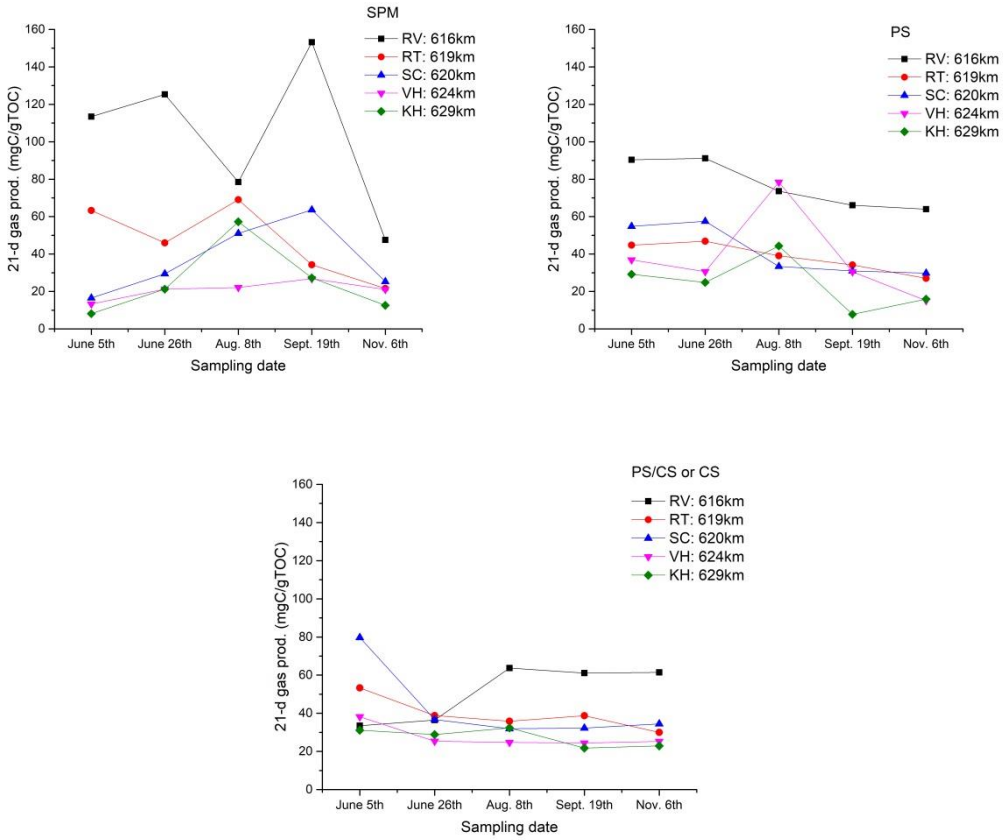

Figure 12. Relationship between gas production after 21 days and sampling time, for RV, RT, SC, VH, KH in SPM, PS, PS/CS and CS layer

5.4 Correlation between gas production and sediment properties

Linear regression analysis was carried out to detect possible interrelations between magnitude of gas production and sediment properties. This kind of analysis helps to better understand guiding parameters that have an influence on gas production and how strong the effects of these parameters are.

A research question is asked for the correlation analysis:

- How do the mass-normalized and TOC-normalized gas generations correlate with the abiotic sediment properties?

For answering the research question, complete correlation tables are made for separated layers as shown in Appendix E. Here, a part of the sediment properties and experimental results on gas production in the PS layer are selected to build such a cross-correlating table as an example for presenting (Table 18). Statistical significance of Pearson's coefficient r was accepted for a probability of error $p < 0.01$ for a two-sided test in the thesis case. According to the table provided in Appendix F, the value of r that checks significance of correlation is determined by the number of available samples (25 in the PS layer). Therefore, in this example the limit was set as $r = 0.487$ for the PS layer. This means a positive correlation was statistically significant when the

value of r was > 0.487, a negative correlation was statistically significant when the value of r was < -0.487, and no statistically significant relationship was assumed between two considered factors when r was between -0.487 and 0.487, given the chosen error probability of $p < 0.01$ (1%). In Table 18, positive and negative correlations were distinguished by different colors.

Table 18. Pearson's coefficient r for correlations between gas production and material properties in PS layer. Bold = Pearson's coefficient r significant on a confidence level of 99.99%, two-sided test. Significant r = 0.487. Blue = positive correlation, red = negative correlation

		21-day- aerobic respiration		21-day-anaerobic respiration	
		/TOC	/DW	/TOC	/DW
In solids	TOC	0.71	0.87	0.85	0.93
	TN	0.72	0.87	0.85	0.92
	TOC/TN	-0.52	-0.50	-0.63	-0.56
	TOC/P	0.71	0.86	0.78	0.89
	TOC/S	0.69	0.90	0.81	0.95
	Water content	0.75	0.82	0.80	0.83
	Redox potential	-0.39	-0.25	-0.40	-0.24
	Dissolved gas	-0.12	0.11	0.21	0.31
	Dissolved organic matter_270 nm	0.64	0.66	0.59	0.61
	Share of mass in light density fraction	0.47	0.66	0.63	0.81
	Share of mass in heavy density fraction	-0.52	-0.54	-0.85	-0.76
	Ratio of light share to heavy share	0.55	0.72	0.75	0.88
	Share of dry matter	-0.50	-0.57	-0.63	-0.61
	Oxygen consumption in 3h	0.55	0.71	0.74	0.79
	Loss on ignition 550°C	0.69	0.82	0.80	0.83
	P	0.54	0.70	0.73	0.76
	S	0.35	0.40	0.50	0.44
	Fe	0.04	0.00	0.12	-0.01
	Ca	0.51	0.74	0.75	0.89
	Li	-0.10	-0.17	-0.03	-0.18
	Al	-0.09	-0.18	-0.05	-0.19
	Mn	0.62	0.72	0.74	0.73
	Cu	0.47	0.62	0.69	0.70
In pore water	pH-value	-0.36	-0.39	-0.44	-0.40
	Electric conductivity at 25°C	0.16	0.34	0.36	0.44
	Fe	0.01	0.16	0.16	0.21
	Mn	0.22	0.17	0.25	0.17
In the filtrate of pore water	DOC	0.57	0.61	0.58	0.62
	TN	0.58	0.80	0.72	0.87
	NO_2^-	0.05	0.02	-0.06	-0.04
	NO_3^-	-0.14	-0.20	-0.34	-0.28
	NH_4^+	0.60	0.81	0.72	0.86
	Fe^{2+}	0.52	0.53	0.48	0.51

	21-day- aerobic respiration		21-day-anaerobic respiration	
	/TOC	/DW	/TOC	/DW
Mn^{2+}	0.23	0.17	0.20	0.13
PO_4^{3-}	-0.12	-0.07	-0.13	-0.07
Na^{+}	-0.51	-0.43	-0.43	-0.37
Cl^{-}	-0.50	-0.39	-0.41	-0.33
Ca^{2+}	-0.37	-0.39	-0.34	-0.33
Mg^{2+}	0.17	0.06	0.10	0.00
SO_4^{2-}	-0.54	-0.55	-0.63	-0.58
SiO_2	0.31	0.42	0.51	0.51

The following trends are summarized according to the Pearson's coefficient r in the table:

(1) As expected, the total organic carbon (TOC) content and total nitrogen (TN) content are correlated on a high level to the 21-day-respiration, for both anaerobic and aerobic conditions and for both units. The strong correlation was also observed between TOC content and TOC-normalized gas production (r = 0.85), indicating that more proportion of readily degradable organic carbon is contained in a certain amount of sediment organic matter when the TOC content is higher.

(2) The inverse relationship between TOC/TN and 21-day-gas production was found for both anaerobic (r = -0.63 for TOC normalized and r = -0.56 for mass normalized) and aerobic (r = -0.52 for TOC normalized and r = -0.50 for mass normalized) conditions. This means that organic matter degradation increases when more TN per unit TOC is present. This can possibly be explained by the constant demand for nitrogen over the course of decomposition. The organic carbon is harder to consume by microbes when there is lack of nitrogen in the sediments. Decomposition rates for riverine sediments are thus positively linked to the TN/TOC ratio and negatively to the TOC/TN ratio. This also explains the relevance of total nitrogen for methane formation: TN serves as a substitute factor for the easily degradable organic matter pool (Gebert et al., 2006).

(3) No statistically significant relationship was found between the gas production and the pH value in the pore water. This might be because the pH value in the pore water is quite stable for the sediment samples in PS layer (ranges from 7.0 to 8.0), that the variance of pH can't influence gas production rate to a significant level. Dunfield et al. (1993) found that the optimum pH values at which maximum microbial activities were observed were up to about two units above the native pH; in some cases the activity declined very markedly both above and below the optimum pH. Therefore it is reasonable in this case that small variance in pH values does not reach a big effect on gas production.

(4) A positive correlation was observed between the proportion of light fraction and gas production, and negative one for proportion of heavy fraction and gas production. The bulk mass predominantly belongs to the heavy fraction, while the light fraction is strongly enriched in organic carbon and total nitrogen in percentage when compared to the heavy fraction (Gebert et al., 2019). Thus the mass-normalized gas production is strongly correlated to the proportion of light fraction mass (r = 0.81), as well as the light/heavy fraction mass ratio (r = 0.88).

(5) A positive correlation was also found between gas production and the ratios TOC/P and

TOC/S, water content, oxygen consumption ability, LOI at 550°C and P, Ca, Mn, Cu in the solids, as well as for NH_4^+ and Fe^{2+} in filtrate of pore water for the PS layer. A negative correlation was also found between gas production and dry matter percentage, SO_4^{2-} content in filtrate of pore water. No significant relationship was found between gas production and redox potential, dissolved gas in water, S, Fe, Li, Al in solids, NO_2^-, NO_3^-, Na^+, Ca^{2+} and some other elements in the filtrate of pore water. Among these factors, LOI reflects the content of organic carbon. High contents of Fe^{2+} and NH_4^+ in the pore water indicate that the sediment is under stable reduced conditions (with negative redox potentials); under positive redox potentials Fe^{2+} and NH_4^+ are oxidized in the pore water. They hence indicate persisting conditions for gas generation. SO_4^{2-} in the pore water is an oxidized component; in the redox chain, normally SO_4^{2-} is reduced before CH_4 generation begins.

The complete results of Pearson's coefficient r for correlations between gas production and material properties for all the layers are attached in Appendix E.

5.5 Time series analysis

The time series analysis was carried out for possibilities on estimation of gas generation. This kind of analysis helps to better understand the kinetics of gas production over time, so that a prediction of gas production in long-term can be made when only short-term measured data on gas production are available. In addition, the different pools of degradable organic matter in the sediments can be distinguished through the analysis.

The 'pool concept' used in the thesis is introduced briefly here. Labile pool and stable pool of degradable organic carbon are distinguished for the sediments. As summarized in literature study in the chapter 3.1.2, three successive phases are defined concerning CH_4 and CO_2 production. The share of organic carbon degraded in the first phase is regarded as pool of 'easily degradable' organic matter (pool 1). More phases with lower gas production rate exist for a long-term incubation corresponding to pools of medium or slow rate of degradation on organic matter (pool 2, pool 3).

Two questions are asked for the time series analysis:

- What is the relationship between magnitude of short-term and long-term gas production?
- What is the size of short-term and long-term degradable pools of organic carbon?

For answering the research questions and building the gas generation model, the analyses are separated in a measured data part and an estimation part. Note that the data used and analysis made in this chapter are all based on anaerobic incubation of samples.

5.5.1 Gas production 100-day versus 21-day

Based on the data of gas production under anaerobic incubation provided in previous chapter, the relationship between gas production after 21 days and after 100 days was analyzed. For most of the samples, '100 days' cannot be regarded as long-term, but still we are interested in how the relation looks like between short-term 21-days-value of gas production and relatively longer term

of 100-days-value of gas production, for different layers. Another important reason is that gas production data for these two time nodes (21 days and 100 days) provides the largest available data set so that the results of the statistical analysis have the highest possible certainty. The samples in first three campaigns are used in this part. As proved already the spatial variability can be large regarding to the depth, the analysis is separated for different layers (SPM, FM, PS, PS/CS, CS), as shown in Figure 13.

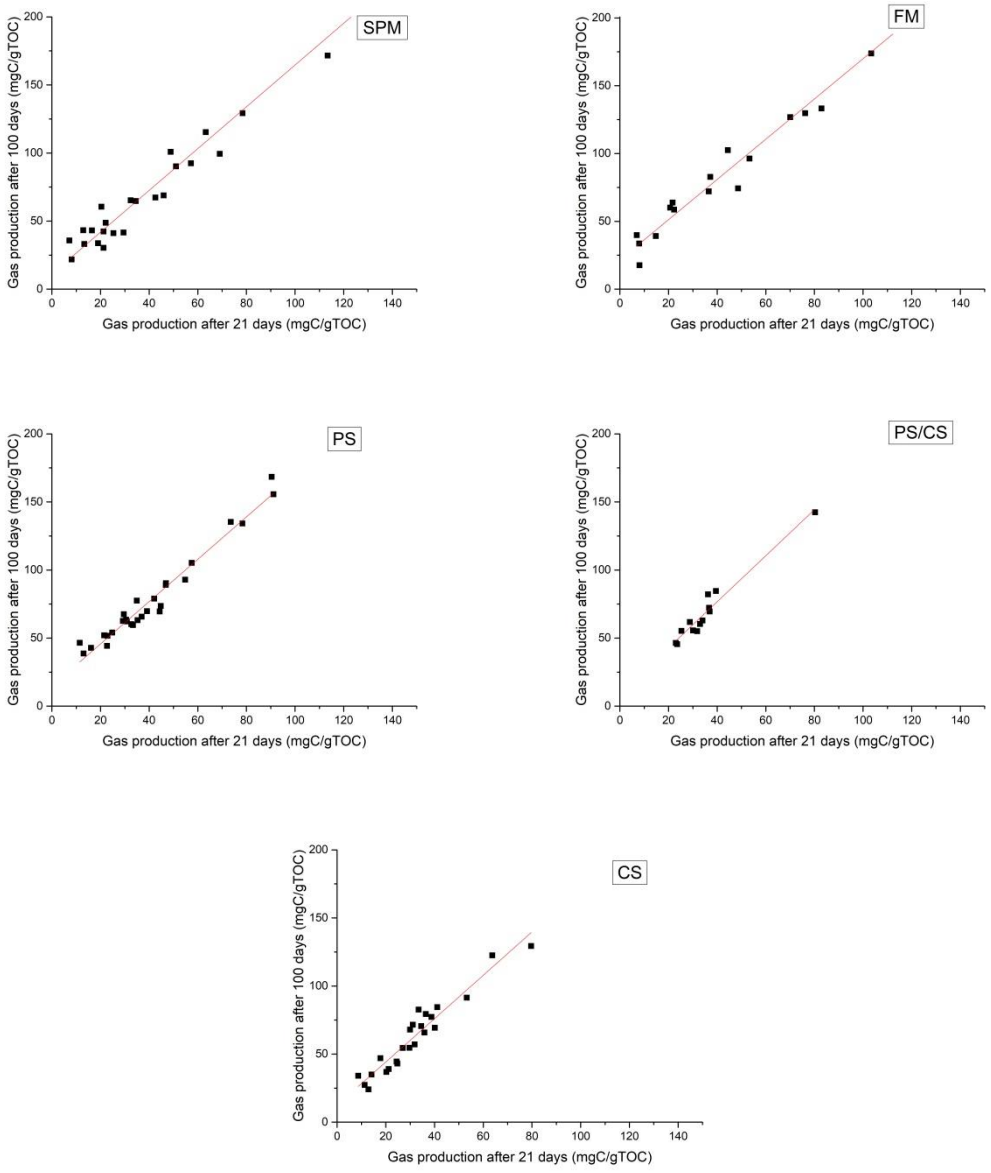

Figure 13. Relationship between gas production after 21 days and after 100 days, for each layer. Each data point represents the average of three parallels

From the above graph it is obvious that gas production after 100 days correlates very well to gas production after 21 days for sediment samples in all the layers. Individual regression functions for the relationship are simulated and presented in Table 19. The slopes of the functions range from 1.48 to 1.69, indicating some, but small, differences between the layers. The R squared value (R^2), which in statistics is called the coefficient of determination, describes the quality of a fit. An R^2 of

1 indicates that the regression predictions perfectly fit the data. Here in average the R^2 is about 0.95, which means that 95% of the variability of the gas production after 100 days can be explained by the gas production measured after 21 days. The general regression function is also given, when all the data point of different layers are put in one graph. As indicated by the magnitude of the slope, the gas production after 100 days is apparently higher than short-term gas production after 21 days, in this case by a factor of around 1.54. Gebert et al. (2019) found a slope of 1.69 between gas production after 21 days and after 91 days for dredged material, which is closed to the factor presented in this thesis. This factor is meaningful for further study on kinetics of gas production and can be used for the estimation of magnitude of gas production in a relatively long term when only short-term measured data are available.

Table 19. Regression function for relationship between gas production after 21 days and after 100 days (x represents data point of gas production after 21 days; y represents data point of gas production after 100 days)

Layer	Function 100d vs 21d	R^2
SPM	y = 1.53x + 11.14	0.946
FM	y = 1.48x + 21.56	0.963
PS	y = 1.55x + 14.62	0.962
PS/CS	y = 1.69x + 9.03	0.950
CS	y = 1.59x + 12.29	0.922
All layers together	y = 1.54x + 14.34	0.949

5.5.2 Estimation of total gas potential

Understanding the relationship between gas production after 21 days and after 100 days is not the ultimate purpose. As mentioned before, '100 days' cannot be regarded as a real long-term for most sediment samples. What we are most interested in for the gas production is the final amount of gas produced, here referred to 'total gas potential'. After a long-term incubation, the samples will finally stop to produce gas as the degradable part of carbon in the soil is consumed completely by microorganisms. The whole process can cost years as indicated in previous research (Gebert et al., 2019). As the experiment in this thesis hasn't taken for so long, the estimation of total gas potential is conducted through application of a mathematical model.

From the literature study in Chapter 3.3, the Afvalzorg multi-phase model has already been proved to be the most fitted model for describing and estimating gas production in this project. From the graph of gas production over time, different phases were observed during gas production process on the curve for most of the samples. Here gas production of sample No. 1073 and 1074 are plotted using measured data points as an example as shown in Figure 14. It is clear from the curve that at least two phases exist in the course of gas formation. In the first phase a strong increase of gas formation over time is observed. The relationship between amount of gas production and time in this phase is nearly linear. In the second phase, the rate of gas formation decreased asymptotically and reached a more long-term level. This pattern of the temporal change of gas production has also been described by Yao et al. (1999) and Conrad (2002) for paddy soil, but mainly for the methane part.

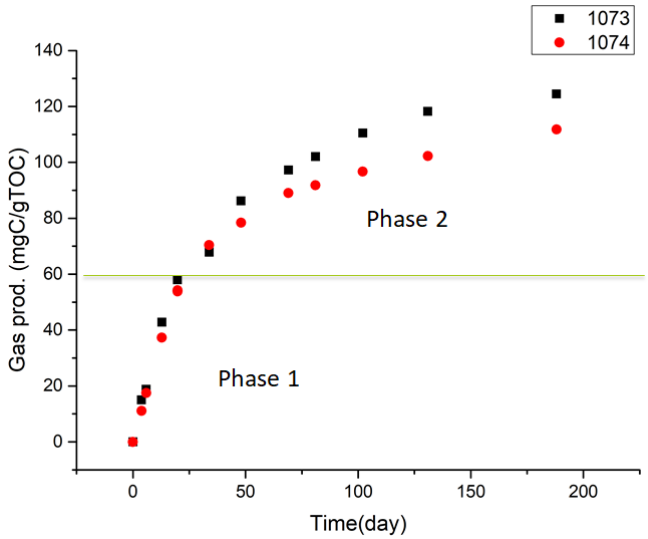

Figure 14. Gas production over time for sample 1073, 1074. Data points are based on pressure measurement

After determination of the model, measured gas production data points of different samples were input into the model for simulation, using the software of OriginPro (version 9.1). Here the samples of the first two campaigns from sites RV, RT, VH, KH, SW were used. The simulation results including all the parameters mentioned in the modified model are presented as below in Table 20.

Table 20. Estimation results of total gas potential (y_0) for selected samples

Sample No.	Loca-tion	Layer	Duration Phase1 (day)	Duration Phase2 (day)	21d-value measured (mgC/gTOC)	100d-value modeled (mgC/gTOC)	A_1 (-)	A_2 (-)	t_1 (day)	t_2 (day)	y_0 (mgC/gTOC)
1073	RT	SPM	20	188	63.3	115.3	-42.1	-90.9	11.3	70.5	129.4
1078	RV	FM	21	190	103.4	173.8	-125.1	-142.2	14.4	254.8	208.5
1079	RV	PS	25	162	90.4	168.5	-118.5	-105.6	18.8	135.6	195.9
1080	RV	CS	19	188	33.5	82.7	-49.5	-378.7	32.7	1185.9	121.2
1095	VH	PS/CS	17	188	36.9	69.6	-24.5	-80.0	6.0	117.6	102.6
1096	VH	FM	22	186	37.2	82.8	-51.6	-68.2	22.2	156.7	103.7
1097	VH	PS	21	187	36.9	65.8	-46.1	-49.3	17.6	155.0	79.3
1098	VH	PS/CS	18	188	39.5	84.6	-22.4	-101.2	5.7	101.7	120.6
1100	VH	SPM	16	187	13.3	33.2	-13.9	-86.8	3.5	91.9	100.7
1105	SW	PS	18	187	16.1	42.8	-5.2	-57.6	5.6	90.0	61.7
1106	SW	CS	17	187	17.8	47.0	-7.9	-85.3	5.1	166.9	92.8
1108	KH	FM	22	186	21.7	63.8	-15.0	-87.9	14.8	118.5	100.1
1109	KH	PS	19	187	29.2	62.6	-29.7	-67.3	14.9	154.2	83.7
1110	KH	CS	15	187	31.1	71.6	-13.9	-86.8	3.5	91.9	100.8
2207	RV	PS	22	160	91.2	155.6	-62.6	-127.5	8.4	81.9	187.2
2208	RV	CS	19	159	36.4	79.4	-12.7	-80.6	2.4	60.2	90.4
2217	RT	FM	20	158	70.0	126.8	-89.6	-101.8	17.2	206.7	149.0
2218	RT	PS	17	137	46.8	89.1	-30.6	-82.8	7.5	79.8	107.7
2219	RT	CS	13	153	38.8	77.2	-13.9	-71.9	3.4	49.7	85.2

Sample No.	Loca-tion	Layer	Duration Phase1 (day)	Duration Phase2 (day)	21d-value measured (mgC/gTOC)	100d-value modeled (mgC/gTOC)	A_1 (-)	A_2 (-)	t_1 (day)	t_2 (day)	y_0 (mgC/gTOC)
2222	VH	PS	16	160	30.5	63.5	-21.2	-67.6	9.2	101.7	81.4
2223	VH	PS/CS	19	155	25.3	55.3	-9.9	-66.0	4.1	82.6	74.6
2225	KH	PS	21	160	24.8	54.0	-14.8	-52.4	13.1	72.3	64.5
2226	KH	PS/CS	20	160	28.8	61.7	-13.0	-68.3	5.1	82.9	81.0
2235	SW	FM	20	158	7.9	33.6	-29.8	-29.9	134.5	134.5	52.0
2237	SW	CS	20	161	14.2	35.0	-6.0	-53.7	5.1	132.3	58.7

The values of total gas potential estimation for these samples are given in the last column marked with y_0. The turn point between phase 1 and phase 2 is mainly determined by hand, which might contain a certain amount of error of a few days. Generally, phase 1 takes around 20 days for a strong increase of gas formation. The measured data of gas production after 21 days and after 100 days are also listed in the table for comparison with total gas potential. Here the analysis of relationship between 21-day gas production and total gas potential was carried out for all the layers together, thereby increasing the size of the data set. The analysis results including fitted curve and regression function are shown in Figure 15.

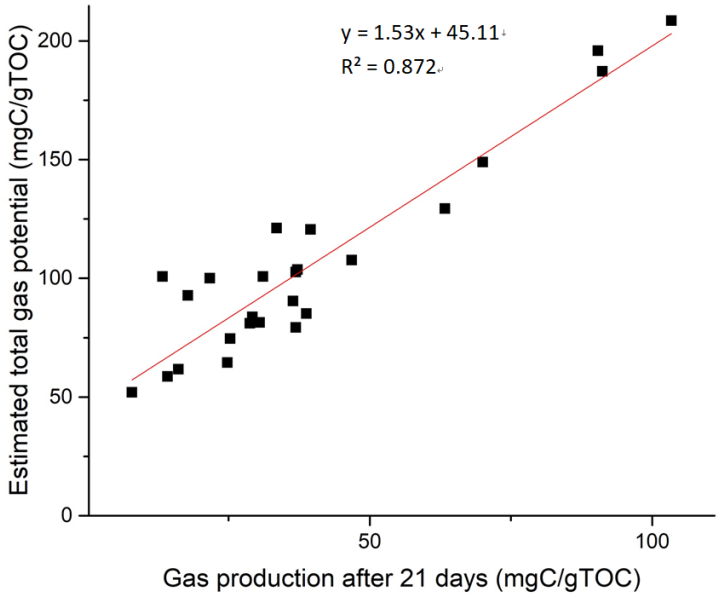

Figure 15. Relationship between gas production after 21 days and total gas potential, for all layers together

The regression function in this analysis is given as y = 1.53x + 45.11, with R^2 = 0.872. The slope of 1.53 is quite close to the slope of the regression function in analysis of gas production 100-day vs 21-day (1.54), while the intercept here (45.11) is significantly larger than the one (14.34) before. It makes sense as the total gas potential should always be higher than gas production after certain days. The fit in this analysis is not perfect, with a relatively lower value of R^2 = 0.872, but it is still acceptable for estimations. Improvements should be applied to the model once longer term data have been acquired.

Furthermore, the simulation results of the model provide feasibility for analyzing the different pool sizes of degradable organic matter in the sediments. The share of organic carbon

corresponding to the first phase is regarded as pool of 'easily degradable' organic matter. In other words, this part of 'easily degradable' organic matter is consumed by microorganisms in priority in phase 1. It also explains the fast increase of gas formation in phase 1. Then in phase 2 the residual part of the degradable organic carbon is gradually consumed, leading to an asymptotically decreased rate of gas formation. More phases (e.g. phase 3) with lower gas production rate can exist for a long-term incubation. The organic matter consumed in each phase consists of the total share of degradable organic matter with the same half-life in the sediments. Based on the analysis results of the model given in Table 20, sizes of different pools and share of degradable organic matter are calculated, as shown in Table 21.

Table 21. Calculated pool sizes and total share of degradable organic matter for selected samples

Sample No.	Location	Layer	Pool sizes (% of total degradable organic matter)			y_0 (mgC/gTOC)	Total share (% TOC)
			Pool 1	Pool 2	Pool 3		
1073	RT	SPM	26.1	64.2	9.6	121.2	12.1
1078	RV	FM	17.5	51.0	31.4	92.8	9.3
1079	RV	PS	27.1	61.6	11.3	100.8	10.1
1080	RV	CS	38.4	57.0	4.6	90.4	9.0
1095	VH	PS/CS	35.8	61.4	2.9	85.2	8.5
1096	VH	FM	23.7	50.0	26.3	58.7	5.9
1097	VH	PS	53.5	42.5	4.0	208.5	20.8
1098	VH	PS/CS	41.6	52.7	5.7	103.7	10.4
1100	VH	SPM	27.6	54.5	17.9	100.1	10.0
1105	SW	PS	50.9	44.1	5.1	149.0	14.9
1106	SW	CS	14.8	63.6	21.6	52.0	5.2
1108	KH	FM	53.2	42.6	4.2	195.9	19.6
1109	KH	PS	46.5	52.4	1.0	79.3	7.9
1110	KH	CS	24.6	64.5	10.9	61.7	6.2
2207	RV	PS	33.6	54.5	11.9	83.7	8.4
2208	RV	CS	49.3	43.7	7.0	187.2	18.7
2217	RT	FM	38.8	54.2	7.0	107.7	10.8
2218	RT	PS	32.4	58.8	8.9	81.4	8.1
2219	RT	CS	38.5	57.0	4.5	64.5	6.4
2222	VH	PS	33.2	54.3	12.5	102.6	10.3
2223	VH	PS/CS	30.7	55.3	14.0	120.6	12.1
2225	KH	PS	32.2	55.3	12.5	74.6	7.5
2226	KH	PS/CS	35.0	54.0	11.0	81.0	8.1
2235	SW	FM	44.8	51.4	3.8	129.4	12.9
2237	SW	CS	27.9	60.9	11.2	100.7	10.1
Average	-	-	35.1	54.5	10.4	105.3	10.5
Medium	-	-	33.6	54.5	9.6	100.1	10.0
Max.	-	-	53.5	64.5	31.4	208.5	20.8
Min.	-	-	14.8	42.5	1.0	52.0	5.2
S.D.	-	-	10.6	6.5	7.4	41.5	4.1

The calculation results are based on the assumption that the second phase of gas formation ends at the last data point of measurement. The estimated total gas potential y_0 and the modeled gas formation in phase 1 and phase 2 were acquired directly from the output of the model or the measured data set. As the estimated total gas potential y_0 is larger than the sum of gas production in phase 1 and phase 2, here pool 3 is defined for the residual part of gas production by subtracting the sum of gas formation in pool 1 and pool 2 from y_0. According to the calculation results in Table 21, in average 35.1% of total gas is produced in the phase 1, and 54.4% is produced in the phase 2. The rest part of gas production takes around 10.4%, which is included in phase 3. The percentage in each pool also indicates that about 35.1% of degradable organic carbon is the easily degradable part which is consumed in the very first stage of incubation; while 10.4% of degradable carbon is considered hard to be degraded by microbes but it is still degradable. From the calculation in the last column, it is found that in average 10.5% of the total organic carbon can be degraded in selected samples, indicating a high share of non-degradable organic carbon (89.5%). Gebert et al. (2015) found the share of degradable organic carbon in the dredged material to be 12%, which is closed to the result analyzed in this thesis. By multiplication of 35.1% and 10.5%, around 3.7% of total organic carbon can be easily degraded in our sediment samples.

5.6 Temperature effects analysis

The controlled experiment in which sediment samples were incubated at different temperatures was carried out for investigating the temperature effects on gas production. Sample 4401 (location: PK, layer: PS/CS) was used for the whole temperature experiment.

A research question is asked for the temperature effects analysis:

- How does temperature affect the rate and magnitude of gas generation and how sensitive is it?

Based on data provided in Table 22 and Table 25, analysis work was conducted mainly including comparison of gas production under different temperature conditions, Q_{10} value calculation and gas composition changes within the vessel. The temperature effects analysis gives knowledge to help explaining temporal variability of anaerobic gas production at Port of Hamburg, as well as the kinetics of gas generation development in the long term.

The raw data of the recorded pressure of all samples is given in Appendix C and the calculated gas production with time is listed here in Table 22. Average values of gas production in parallels were also calculated for convenience of analysis later.

Table 22. Calculated gas production of sample 4401 at different temperature with time

Gas production (mg C/g TOC), sample 4401										
	5°C						10°C			
Days	A	B	C	Average		Days	A	B	C	Average
0	0	0	0	0		0	0	0	0	0
8	0.50	0.66	0.67	0.61		8	0.65	0.79	0.38	0.61

18	1.12	1.22	1.28	1.20
32	1.84	1.88	1.94	1.89
45	1.90	1.71	1.83	1.82
57	2.01	1.99	2.11	2.04
71	2.29	2.16	2.33	2.26
95	3.07	2.93	3.16	3.05
121	3.47	3.26	3.72	3.48

	20°C			
Days	**A**	**B**	**C**	**Average**
0	0	0	0	0
2	2.76	2.63	2.66	2.68
5	4.08	4.15	4.05	4.09
9	5.78	5.42	6.10	5.76
16	8.22	7.44	8.65	8.10
24	10.02	9.41	10.31	9.92
33	13.28	12.53	13.17	13.00
46	15.64	15.14	15.63	15.47
58	18.16	17.44	18.15	17.92
72	20.90	20.42	20.97	20.76
93	24.13	23.85	24.29	24.09
122	28.15	28.04	28.27	28.15

	36°C			
Days	**A**	**B**	**C**	**Average**
0	0	0	0	0
3	8.13	9.18	8.77	8.69
6	16.35	16.55	16.79	16.56
9	19.46	20.08	20.56	20.03
13	23.22	23.48	24.53	23.74
17	26.57	26.68	27.52	26.92
22	29.07	29.72	30.57	29.79
26	33.26	33.63	34.95	33.94
31	35.27	35.60	36.19	35.69
36	37.60	37.58	38.13	37.77
41	39.77	39.20	39.67	39.55
48	44.71	43.98	43.96	44.21
55	47.63	46.82	46.30	46.92
62	50.35	49.48	48.85	49.56
70	52.39	51.74	51.03	51.72
91	58.59	58.50	56.65	57.91
101	58.75	59.95	57.01	58.57
119	62.94	64.94	60.21	62.70

18	1.47	1.64	1.24	1.45
32	2.39	2.60	2.10	2.36
45	3.26	3.50	2.96	3.24
57	3.91	4.07	3.56	3.85
71	4.73	4.86	4.25	4.61
92	5.97	6.10	5.49	5.85
121	7.76	7.67	6.99	7.48

	28°C			
Days	**A**	**B**	**C**	**Average**
0	0	0	0	0
4	3.32	3.51	3.66	3.49
9	6.57	6.62	6.49	6.56
11	7.32	7.23	7.26	7.27
15	11.37	11.32	10.91	11.20
18	12.88	13.40	13.24	13.17
25	16.69	17.40	17.08	17.06
32	20.69	21.92	21.69	21.43
45	25.88	27.40	26.82	26.70
57	31.37	33.02	31.94	32.11
72	36.57	38.28	37.03	37.30
92	42.95	44.60	42.89	43.48
121	50.70	53.77	51.93	52.13

	42°C			
Days	**A**	**B**	**C**	**Average**
0	0	0	0	0
3	7.01	7.49	7.42	7.31
4	8.50	8.93	8.68	8.70
6	12.28	12.67	12.07	12.34
10	18.76	19.00	18.85	18.87
14	24.01	24.42	24.03	24.15
19	34.48	34.79	34.63	34.63
23	40.30	40.28	40.59	40.39
28	42.11	42.01	42.36	42.16
33	44.67	44.56	45.04	44.76
38	49.66	49.48	50.22	49.79
45	52.78	52.39	53.36	52.84
50	55.15	54.59	55.05	54.93
57	58.62	58.11	58.50	58.41
65	60.70	60.12	59.95	60.26
86	65.84	65.48	65.52	65.61
96	68.10	67.63	67.60	67.78
114	71.12	70.84	70.85	70.94

Firstly, a comparison between gas production of samples incubated at different temperatures with time is made, as shown in Figure 16. A single phase first-order model was applied here to describe such a relationship, as it had already provided a nice fit based on the measured data. Apparently, cumulative gas production increases with temperature in this experiment. The result is in accordance with the theory that within a certain range microbial activity increases with temperature (Hofle, 1979). The accumulated gas production amount reached about 71 mg C/g TOC after 120 days of anaerobic incubation at 42°C, much higher than the gas production of sample incubated at 5°C (3.5 mg C/g TOC). The low gas production rate at 5°C proves that fresh sediment materials can be stored at low temperature for a long period for further experiments. What's more, gas production of samples incubated at high temperatures including 36°C and 42°C have already entered the second phase in which the rate of gas formation decreased and reached a low level. While for the samples incubated at relatively low temperatures such as 5°C, 10°C and 20°C, the gas production is still in phase one where the relationship between amount of gas production and time is nearly linear. This phenomenon indicates that high temperature might accelerate the whole process of gas generation, as well as the consumption of degradable organic carbon by microbes.

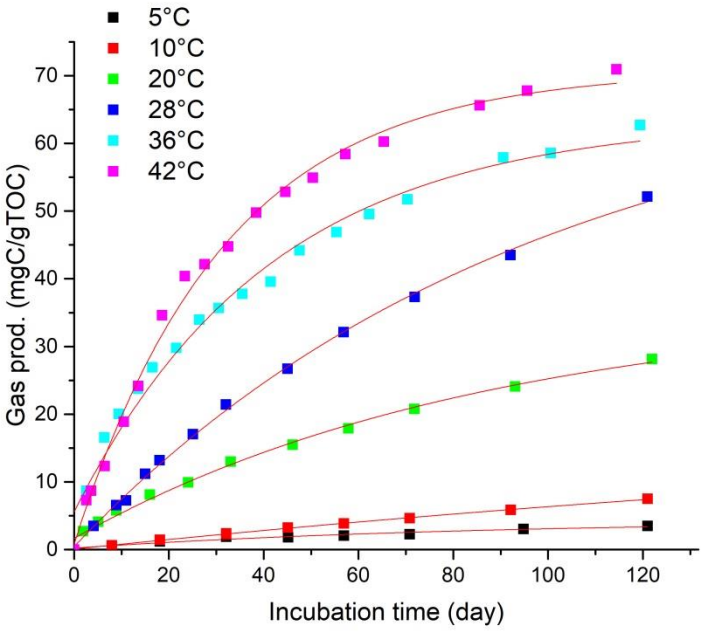

Figure 16. Gas production with time at different temperatures. Each data point represents the average of three parallels

From the difference of gas production rates at different temperature conditions, the Q_{10} value was calculated in order to assess the temperature sensitivity of gas generation, according to equation (1). Here 20°C and 36°C were chosen as T_1 and T_2 in the equation for calculation as they have relatively nicer fitted curves and a sufficient temperature range between two. At 5°C and 10°C too few gas production data points are available after 120 days' incubation thus the Q_{10} calculation results might be uncertain if these two temperatures were used. At 42°C some measured data points are not perfectly fitted on the curve so it was not used, either. A series of Q_{10} values were calculated from 20°C and 36°C at different time nodes, as listed in Table 23.

Table 23. Calculated Q_{10} values at different time nodes, for 20°C - 36°C

Sample No.	Location, layer	Duration of incubation (day)	Q_{10} (20°C - 36°C)
4401	PK, PS/CS	20	2.06
		40	1.94
		60	1.84
		80	1.76
		100	1.69
		120	1.64

Q_{10} value for a determined system is regarded to be a certain constant but here it was found that Q_{10} (20°C - 36°C) decreases with incubation time, from 2.06 at 20 days to 1.64 at 120 days. This can be explained by the fact that at high temperature (36°C) the easily degradable part of organic matter is consumed fast, and the reaction rate has already dropped from around 30 days, which means the gas production at 36°C has entered a second phase after a short term. While at 20°C the process is much slower that the gas production is still in phase one, the linear increasing phase, even at the end of the experiment. This leads to a drop in Q_{10} value with incubation time. Therefore, by evaluating gas production under both temperature conditions while in the same phase (phase one), the Q_{10} value at 20 days, 2.06, was determined to be the final Q_{10} of the system. For comparison with Q_{10} values in previous researches, a list of Q_{10} values are presented in Table 24 as below.

Table 24. Q_{10} values of gas production in other researches

Place	Soil type	Measures at (°C)	Q_{10}	Source
Sedge site at Stordalen, Sweden	Peat, Aug.	4-24	2.4-3.5	Lupascu et al., 2012
	Peat, Sept.	4-24	1.9-2.8	
Sphagnum site at Stordalen, Sweden	Peat, Aug.	4-24	3.2-5.8	
	Peat, Sept.	4-24	4.2-5.4	
Rice paddy field near Vercelli, Italy	Rice paddy soil	20-35	3.1-12.3	Schütz et al., 1990
California, USA	-	12-20	1.6-2.6	Westermann et al., 1989
		20-30	1.3-2.6	
Ombrotrophic bog, Scotland	Peat	2-30	20	Nedwell et al., 1995
Michigan lakes, USA	Lake sediments	9-29	1.2-5.7	Kelly et al., 1981
		4-9	0.8-4.7	
Northern Wetlands, Minnesota, USA	Peat	15-30	1.4-1.5	Updegraff et al., 1995
	Sedge peat	15-30	1.0-1.4	
	Surface bog	15-30	16.2	
	1m depth bog	15-30	28	
Waste water disposal pond, Russia	Silt	6-28	1.7-3.6	Kotsyurbenco,1993

The high Q_{10} values found in literature could possibly be explained by the fact that at different temperatures after a certain incubation time different phases have been compared. If the different phases distinguished here are not taken into account, the Q_{10} of gas production will

depend on the incubation length and the incubation temperatures (Hulzen, 1997). Compared to most of the Q_{10} values in previous researches, the Q_{10} in the thesis experiment (2.06) is at a low level which indicates a relatively low sensitivity of gas formation to temperature. The sample used in our experiment belongs to PS/CS layer with old sediment materials, which could possibly explain a relative low value of Q_{10}.

Table 25. Gas-chromatographic (GC) analysis results on 04.12.2018 and 06.02.2019, with dissolved CO_2 in the water considered

04.12.2018, mid-term of experiment

Sample No. (HPA)	Temperature °C	Parallels	Dissolved CO_2 mol	Gas composition (%)				
				N_2	CH_4	CO_2	O_2	CH_4/CO_2
4401	5	A	6.61E-05	92.13	2.77	4.05	1.05	0.69
		B	6.70E-05	92.13	2.75	3.98	1.14	0.69
		C	6.69E-05	92.48	2.55	3.87	1.10	0.66
	10	A	6.00E-05	90.15	4.07	4.93	0.85	0.83
		B	5.86E-05	90.21	4.10	4.94	0.76	0.83
		C	6.04E-05	90.12	4.07	4.94	0.87	0.82
	20	A	4.87E-05	75.97	12.81	10.73	0.49	1.19
		B	5.02E-05	76.16	12.96	10.54	0.35	1.23
		C	4.70E-05	76.49	12.32	10.35	0.83	1.19
	28	A	3.78E-05	59.06	24.13	16.78	0.02	1.44
		B	3.73E-05	57.21	25.10	17.66	0.02	1.42
		C	3.70E-05	57.75	24.92	17.31	0.02	1.44
	36	A	3.10E-05	42.67	33.68	23.63	0.02	1.43
		B	3.19E-05	40.81	35.05	24.12	0.02	1.45
		C	3.17E-05	39.98	35.43	24.56	0.02	1.44
	42	A	2.92E-05	32.62	40.02	27.34	0.02	1.46
		B	2.84E-05	32.42	40.37	27.19	0.02	1.49
		C	2.87E-05	33.07	39.75	27.16	0.02	1.46

06.02.2019, end of experiment

Sample No. (HPA)	Temperature °C	Parallels	Dissolved CO_2 mol	Gas composition (%)				
				N_2	CH_4	CO_2	O_2	CH_4/CO_2
4401	5	A	6.74E-05	92.04	3.32	3.78	0.87	0.88
		B	6.81E-05	92.23	3.48	3.75	0.54	0.93
		C	6.85E-05	92.40	3.67	3.90	0.03	0.94
	10	A	6.15E-05	87.12	7.47	5.38	0.03	1.39
		B	5.99E-05	87.21	7.38	5.38	0.03	1.37
		C	6.14E-05	86.93	7.57	5.47	0.03	1.38
	20	A	5.08E-05	65.55	22.28	12.15	0.02	1.83
		B	5.30E-05	64.33	23.17	12.48	0.03	1.86
		C	4.93E-05	65.50	22.31	12.17	0.02	1.83

Sample No. (HPA)	Temperature °C	Parallels	Dissolved CO_2 mol	Gas composition (%)				
				N_2	CH_4	CO_2	O_2	CH_4/CO_2
	28	A	4.29E-05	42.78	37.26	19.77	0.18	1.88
		B	4.30E-05	40.98	38.06	20.61	0.35	1.85
		C	4.27E-05	41.52	37.82	20.37	0.29	1.86
	36	A	3.24E-05	31.97	42.70	24.91	0.42	1.71
		B	3.47E-05	29.35	45.15	25.09	0.41	1.80
		C	3.29E-05	31.40	42.92	25.15	0.52	1.71
	42	A	2.86E-05	24.00	46.38	29.23	0.39	1.59
		B	2.82E-05	24.37	46.16	29.05	0.42	1.59
		C	2.86E-05	24.38	45.84	29.38	0.40	1.56

Furthermore, the change of gas composition inside the bottles over time in this experiment was analyzed. Measurements were carried out for gas composition at the middle and at the end of the four-month experiment. Based on measured data presented in Table 25, the percentages of gases content in bottles and the ratio of CH_4 to CO_2 at each temperature were plotted, as shown in Figure 17 and Figure 18. Dissolved CO_2 in the water was considered for correction. In both graphs, the percentages of CH_4 and CO_2 produced inside the bottles increase with temperature, indicating the increased gas production also registered by the pressure measurement. This leads to the relative decrease of N_2 which is present due to the flush at the beginning of the experiment for creating an anaerobic environment. The decrease is lowest at the lowest temperature due to low gas production and highest at the highest temperature. Nearly no O_2 was measured, confirming the anaerobic conditions. At the mid-term of the experiment (04.12.2018), more CO_2 content was observed than CH_4 at 5°C and 10°C which is in accordance with the theory that in anaerobic condition, at the very first stage only CO_2 is produced (Gebert et al., 2006). CH_4 production follows a lag phase thus CO_2 takes a higher percentage in this early stage. While at high temperatures the CH_4 and CO_2 were produced at a low rate already and the ratio between the two gases is close to 1.5. At the end of the experiment (04.12.2018), higher percentages of CH_4 and CO_2 inside the bottles as well as the higher ratio between the two gases were observed for all temperatures, when compared to the mid-term.

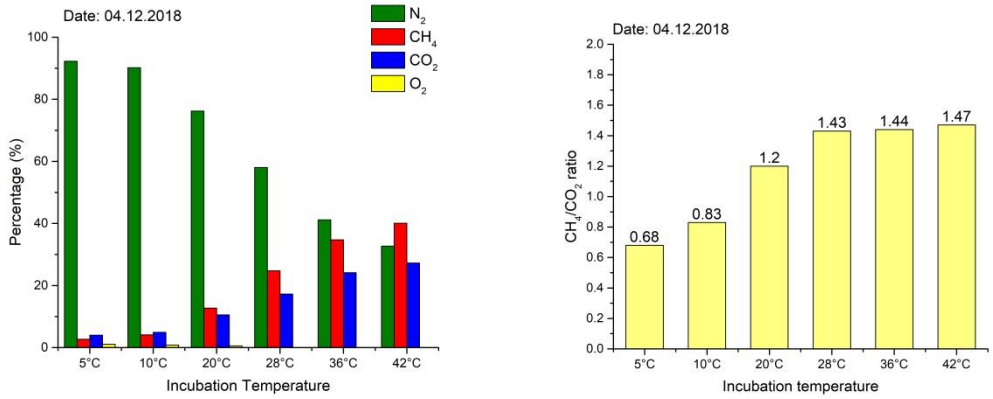

Figure 17. Gas composition and CH4/CO2 ratio at all temperatures, measured at mid-term of experiment (04.12.2018)

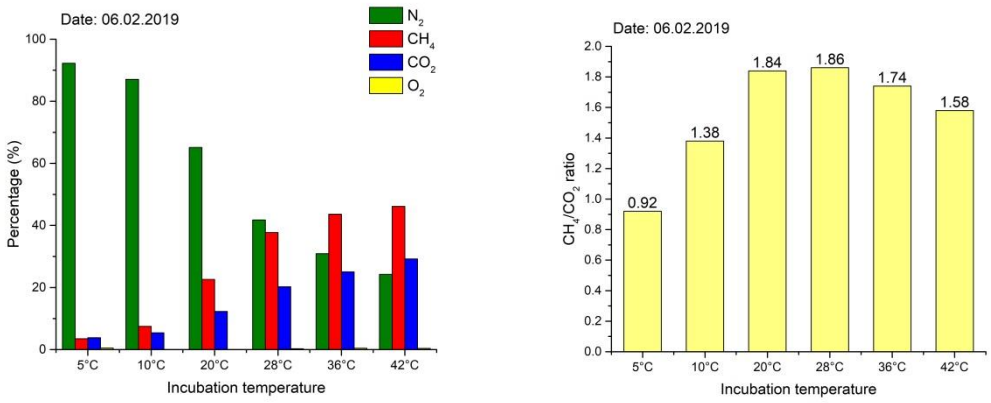

Figure 18. Gas composition and CH_4/CO_2 ratio at all temperatures, measured at end of experiment (06.02.2019)

According to the theory summarized in literature study in chapter 3.1.2 and 3.2, one pathway of methanogenesis at low temperature would be the degradation of acetate to CH_4 and CO_2. In this case the gas produced would be composed of 50% CH_4 and 50% CO_2 and the ratio between two gases would therefore be 1:1. With ongoing duration of the experiment, the degradable share of organic matter decreases and less and less acetate is available for consuming. Then CO_2 can be used as a substrate for CH_4 formation by reducing, especially at high temperatures. Therefore, amount of CO_2 reduces while production of CH_4 continues to increase so the ratio between the two gases increases in favor of CH_4.

6 Conclusions and recommendations

6.1 Conclusions

By answering the research questions, the main conclusions of this thesis are summarized as following:

(1) What is the spatial and temporal variability of gas generation within sediment profiles in the Port of Hamburg?

Generally speaking, variability of gas production exists in all aspects within sediment profiles in the Port of Hamburg. Spatially, gas production rate decreases from upstream to downstream in the Elbe River, according to the results analyzed from nine sampling locations aligned along the river approximately 20 kilometers. On the vertical dimension, gas production rate generally decreases with depth (FM > PS > CS). Older materials are settled in the deep layer which means the easily degradable share is already mostly depleted. The SPM layer shows a large variability of gas production due to the high flow-ability of the suspended particulate materials. The findings in spatial variability analyses suggest that more degradable organic matter are cumulated in the sediments of inland upstream areas and upper fresh layers at the Port of Hamburg, which is expected to occur in other ports and waterways as well. Temporarily, the variability of gas production is quite different depending much on locations and layers of the sediments. However, the gas production rate in the November campaign keeps at a low level in most cases, indicating a low readily degradable organic carbon content in the sediments in this last campaign.

(2) How do the mass-normalized and TOC-normalized gas generations correlate with the abiotic sediment properties?

When relating to the abiotic sediment properties, mass-normalized and TOC-normalized gas generation almost show the same results in various relationships. In the analysis, for all the layers strong correlations between gas generation and the content of TOC, TN, and an inversed correlation between gas generation and the ratio of TOC/TN were observed, suggesting that TN serves as a substitute factor for the easily degradable organic matter pool and may serve as a proxy to estimate total gas potential. For the PS layer, positive correlations were found between gas generation and TOC/P, TOC/S, water content, oxygen consumption ability, contents of P, Ca, Mn, Cu in the solids as well as NH_4^+, Fe^{2+} in filtrate of pore water; while negative correlation was found between gas production and the content of SO_4^{2-}. The contents of these elements and compounds reflect the extent of oxidation of the sediments and therefore reflect the ability of the sediments to produce gas. This indicates that part of the sediment basic properties can be applied to describe and predict gas production.

Furthermore, a strong positive correlation was observed between gas generation (especially mass-normalized gas generation) and the proportion of mass in the light density fraction, and a negative one for the proportion of mass in the heavy density fraction. It might indicate that the

light fraction is strongly enriched in degradable organic carbon and nitrogen in percentage when compared to the heavy fraction.

(3) How do the rate and magnitude of gas generation develop with time?

a. What is the size of short-term and long-term pools of degradable organic carbon?

The modified Afvalzorg multi-phase model was used for analyzing the rate and magnitude of gas generation on the timeline. For the long-term anaerobic incubation at 36°C, the total gas potential of the river sediments at Port of Hamburg was predicted as 105.3 mg C/g TOC on average, relating to 10.5% of the total organic carbon being degraded. In these 10.5% degradable parts of organic matter, around 35.1% belong to the easily degradable part which are consumed in priority; 54.5% of them are degraded subsequently; and the rest 10.4% is considered hard to be degraded but it is still degradable. By multiplication, around 3.7% of total organic carbon can be easily degraded as an average value over all layers and all times investigated in the five sampling campaigns considered in this thesis.

For the short-term (21 days) anaerobic incubation at 36°C, on average 35.7 mg C/g TOC gas was measured to be produced from the sediment samples, indicating the size of short-term pool of degradable organic carbon to be 3.6%. The value is also considered to be the proportion of easily degradable part in the total organic carbon, which is quite close to the calculated value (3.7%), determined by the pool 1 of the long-term anaerobic incubation. This proves that the determination of 'short-term' as 21 days in this thesis is reasonable; on average 21 days can reflect the duration of gas production phase corresponding to the pool 1.

b. What is the relationship between magnitude of short-term and long-term gas production?

It was found gas production after 100 days correlates very well with gas production after 21 days for sediment samples in all the layers. Individual regression functions for the relationships were written for each layer and the slopes of the functions range from 1.48 to 1.69. A general regression function over all layers was also given as $Gas_{100d} = 1.54*Gas_{21d} + 14.34$. The factor of 1.54 describes the relation between the magnitude of short-term and long-term gas production and is helpful in prediction work for the further study. This also validates that short-term tests can be suitable to predict long-term gas production.

Nevertheless, 100 days cannot be regarded as a real 'long-term'. The relationship between predicted total gas potential and measured short-term (21 days) gas production was also built for a try in the thesis. The regression function in this analysis was given as $Gas_{total} = 1.53Gas_{21d} + 45.11$. Note that the total gas potential is an estimated value which still needs to be verified, which might affect the accuracy of the function.

(4) How does temperature affect the rate and magnitude of gas generation and how sensitive is it?

By a controlled temperature experiment it was found that the gas production rate under anaerobic incubation increases with temperature. The results indicate that high temperature accelerates the whole process of gas generation, because gas production of samples incubated at high temperatures (36°C and 42°C) had already entered the 'stable' phase by the end of the experiment.

For assessing the sensitivity of gas production to temperature, a Q_{10} value of 2.06 was determined for the PS/CS layer sample used in the experiment. Compared to most of the Q_{10} values found in other researches, the Q_{10} in our experiment is at a low level which indicates a relatively lower sensitivity of gas formation to temperature.

6.2 Recommendations

Based on current results on gas generation in this thesis, some recommendations are also proposed for further researches and applications as following:

(1) During the analysis it was found some samples were missing for a certain layer, location or campaign. Especially in the Campaign #3 nearly all the samples for FM layer were missing which caused troubles in analysis on variability of gas generation at the Port of Hamburg. More complete sample sets are expected for the future sampling work.

(2) The distribution of organic matter over different density fraction is considered to be an important abiotic factor affecting gas generation as it can characterize the share of easily degradable organic matter. However, the data for this part were still missing. The analysis of carbon and nitrogen in the density fraction and their relationship to gas generation should be added after sufficient experimental data are acquired.

(3) The prediction model used data of gas production of samples incubated after around 200 days when predicting the total gas potential. By continuing the incubations further, validation and improvement of the model should be realized, especially regarding the fraction degradable in the long-term. Furthermore, the turn point between phase 1 and phase 2 was mainly determined by visual inspection in the analysis, which might lead an error of a few days on determining duration of each phase. A criterion should be set to better distinguish the turn point.

(4) The temperature experiment is expected to continue, so that whether temperature has an effect on the degradability of organic matter and therefore the calculated pool sizes can be verified.

(5) More information on river temperature in different seasons, human dredging activities should be recorded for better analyzing temporal variability of gas generation at the Port of

Hamburg in the future.

(6) During calculations for the magnitude of gas generation it was found that the automated low-flow measurement by gas endeavor (GE) provided more precise and detailed measured data than the pressure measurement, as the GE can always provide continuous data points while the pressure gauge can only measure data with time intervals. If conditions permit, the GE should be used for monitoring gas generation as more as possible.

Bibliography

Arndt, S., Jørgensen, B.B., LaRowe, D.E., Middelburg, J.J., Pancost, R.D., Regnier, P. (2013). Quantifying the degradation of organic matter in marine sediments: A review and synthesis. Earth-Science Reviews 123, 53-86.

Bastviken, D., Cole, J., Pace, M., Tranvik, L. (2004). Methane emissions from lakes: Dependence of lake characteristics, two regional assessments, and a global estimate. Global Biogeochemical Cycles, Volume 18, GB4009.

Blume, H.P., Brümmer, G.W., Fleige, H., Horn, R., Kandeler, E., Knabner, I.K., Kretzschmar, R., Stahr, K., Wilke, B.M. (2016). Scheffer/Schachtschabel – Soil Science. DOI 10.1007/978-3-642-30942.

Bot, A., Benites, J. (2005). The importance of soil organic matter. Food and agriculture organization of the United Nations. ISBN 92-5-105366-9.

Canfield, D.E. (1994). Factors influencing organic carbon preservation in marine sediments. Chemical Geology 114, 315-329.

Conrad, R., Bak, F., Seitz, H.J., Thebrath, B., Mayer, H.P., Schütz, H. (1989). Hydrogen turnover by psychrotrophic homoacetogenic and mesophilic methanogenic bacteria in anoxic paddy soil and lake sediment. FEMS Microbiol. Ecol. 62, 285-294.

Conrad, R. (2002). Control of microbial methane production in wetland rice fields. Nutrient Cycling in Agroecosystems, 64, 59-69.

Dan, J., Kumai, T., Sugimoto, A., Murase, J. (2004). Biotic and abiotic methane releases from Lake Biwa sediment slurry. Limnology, 5: 149-154.

de Leeuw, J.W., Largeau, C. (1993). A review of macromolecular organic compounds that comprise living organisms and their role in kerogen, coal and petroleum formation. In: Engel, M.H., Macko, S.A. (Eds.), Organic Geochemistry, Principles and Applications. Plenum Press, New York, pp. 23-72.

DepV – Deponieverordnung. (2009). Verordnung über Deponien und Langzeitlager. BGBl. I. Nr. 22.

Ding, W., Cai, Z. (2003) Effect of temperature on methane production and oxidation in soils. Chinese journal of applied ecology, 14(4): 604-608.

Dunfield, P., Knowles, R., Dumont, R., Moore, T.R. (1993). Methane production and consumption in temperate and subarctic peat soils: response to temperature and pH. Soil Biology & Biochemistry 25, 321-326.

Emerson, S., Fisher, K., Reimers, C., Heggie, D. (1985). Organic carbon dynamics and preservation in deep-sea sediments. Deep-Sea Research 32, 1-21.

Findlay, S., Tenore, K.R. (1982). Nitrogen source for the detritivore polychaete, Capitella capitata: detritus substrate or microbes? Science 218, 371-372.

Freeman, C., Ostle, N., Kang, H. (2001). An enzymatic 'latch' on a global carbon store. Nature 409, 149.

Gebert, J., Köthe, H., Gröngröft, A. (2006). Prognosis of methane formation by river sediments. J. Soils & Sediments 6, 75-83.

Gebert, J., Harms, C., Steinert, B. (2015). Full-scale implementation of methane oxidation windows on a mono-landfill: technical design and monitoring concept. In: Proceedings Sardinia 2015, Fifteenth International Waste Management and Landfill Symposium. CISA Publisher, Italy.

Gebert, J. (2018): Turnover of Suspended & Settled Organic Matter in Ports & Waterways (Project

BIOMUD). Internal document.

Gebert, J., Knoblauch, C., Gröngröft, A. (2019). Gas production from dredged sediment. Waste Management 85, 82-89.

Girkin, N.T., Turner, B.L., Ostle, N., Craigon, J., Sjögersten, S. (2018). Root exudate analogues accelerate CO_2 and CH_4 production in tropical peat. Soil Biology and Biochemistry 117, 48-55.

Glissmann, K., Chin, K.J., Casper, P., Conrad, R. (2004). Methanogenic pathway and archaeal community structure in the sediment of eutrophic lake Dagow: effect of temperature. Microbiol. Ecol. 48: 389-399.

Gregory, R.G., Attenborough, M.G., Hall, C.D., Deed, C. (2003). The validation and development of an integrated landfill gas risk assessment model GasSim. In Sardinia Proceedings 2003, Cagliari, Italy.

Grubbs, F.E. (1969). Procedures for detecting outlying observations in samples. Technometrics, Vol. 11, No. 1.

Henrichs, S.M. (1992). Early diagenesis of organic matter in marine sediments: progress and perplexity. Marine Chemistry 39, 119-149.

Henrichs, S.M. (2005). Organic matter in coastal marine sediments. The Global Coastal Ocean: Multiscale Interdisciplinary Processes. In: Robinson, A.R., Brink, K.H. (Eds.), The Sea, Volume 13. Harvard University Press, Boston, pp. 129-162.

Hofle, M.G. (1979). Effects of sudden temperature shifts on pure cultures of four strains of freshwater bacteria. Microb. Ecol. 5, 17-26.

Hogan, K. B. (1993). Current and Future Methane Emission from Natural Sources. Washington, D.C.: U.S. Environmental Protection Agency, Office of Air and Radiation.

Hulzen, H. (1997). Explaining the effect of temperature on methane production. Report of graduation course, Department Of Theoretical Production Ecology, Agricultural University of Wageningen.

Jones, W.J., Paynter, M.J.B. (1980). Populations of methane-producing bacteria and in vitro methanogenesis in salt marsh and estuarine sediments. Applied and Environmental Microbiology, Vol. 39, 864-871.

Kelly, C.A., Chynoweth, D.P. (1981). The contributions of temperature and of the input of organic matter in controlling rates of sediment methanogenesis. Limnology and Oceanography, 26(5), 891-897.

Kengen, S.W.M., Stams, A.J.M. (1995). Methane formation by anaerobic consortia on organic grassland soils: An analyses of the sequential processes that occur in grassland on peat soil under anaerobic conditions. NRP-I report, Department of Microbiology Wageningen.

Kotsyurbenko, O.R., Nozhevnikova, A.N., Zavarzin, G.A. (1993). Methanogenic degradation of organic matter by anaerobic bacteria at low temperature. Chemosphere 27: 1745-1761.

Kristensen, E., Holmer, M. (2001). Decomposition of plant materials in marine sediment exposed to different electron acceptors (O_2, NO_3^{2-}, and SO_4^{2-}), with emphasis on substrate origin, degradation kinetics, and the role of bioturbation. Geochimica et Cosmochimica Acta 65, 419-433.

Kuivila, K.M., Murraym, J.W., Devol, A.H., Novelli, P.C. (1989). Methane production, sulfite reduction and competition for substrates in the sediments of Lake Washington. Geochim Cosmochim Acta 53: 409-416.

Liu, Y., Conrad, R., Yao, T., Gleixner, G., Claus, P. (2017). Change of methane production pathway

with sediment depth in a lake on the Tibetan plateau. Palaeogeography, Palaeoclimatology, Palaeoecology 474, 279-286.

Lupascu, M., Wadham, J.L., Hornibrook, E.R.C., Pancost, R.D. (2012). Temperature sensitivity of methane production in the permafrost active layer at Stordalen, Sweden: A comparison with non-permafrost northern wetlands. Arctic, Antarctic, and Alpine Research, 44(4): 469-482.

Nedwell, D.B., Watson, A. (1995). CH_4 production, oxidation and emission in a UK ombrotrophic peat bog: influence of SO_4^{2-} from acid rain. Soil Biology and Biochemistry, Vol. 27, Issue 7, 893-903.

Nozhevnikova, A.N., Kotsyurbenko, O.R., Simankova, M.V. (1994). Acetogenesis at low temperature. In: Acetogenesis (Drake, H.L.m Ed.), pp. 416-431.

Nozhevnikova, A.N., Holliger, C., Ammann, A., Zehnder, A.J.B. (1997). Methanogenesis in sediments from deep lakes at different temperatures (2-70°C). Water Sci Technol 36: 57-64.

Nozhevnikova, A.N., Zepp, K., Vazquez, F., Zahnder, A.J.B., Holliger, C. (2003). Evidence for the existence of psychrophilic methanogenic communities in anoxic sediments of deep lakes. Appl Environ Microbiol 69: 1832-1835.

Nozhevnikova, A.N., Nekrasova, V., Ammann, A., Zehnder, A.J.B., Wehrli, B., Holliger, C. (2007). Influence of temperature and high acetate concentrations on methanogenensis in lake sediment slurries. FEMS Microbiol. Ecol. 62, 336-344.

Oonk, J., Boom, A. (1995). Landfill gas formation, recovery and emissions. NOVEM Programme Energy Generation from Waste and Biomass(EWAB), TNO report R95-203, Apeldoorn, Netherlands.

Prietzel, J., Thieme, J., Salome, M., Knicker, H. (2007). Sulfur K-edge XANES spectroscopy reveals differences in sulfur speciation of bulk soils, humic acid, fulvic acid, and particle size separates. Soil Biology and Biochemistry, Volume 39, Issue 4, Pages 877-890.

Sander, R. (2015). Compilation of Henry's law constants (version 4.0) for water as solvent. Atmospheric, Chemistry and Physics, 15, 4399-4981.

Scharff, H., Jacobs, J. (2006). Applying guidance for methane emission estimation for landfills. Waste Management 26, 417-429.

Schimel, J. P., Holland, E. A., and Valentine, D. (1993). Controls on methane flux from terrestrial ecosystems. Agricultural Ecosystems Effects on Trace Gases and Global Climate Change. Madison, Wisconsin: American Society of Agronomy, 167-182.

Schütz, H., Seiler, W., Conrad, R. (1990). Influence of soil temperature on methane emission from rice paddy fields. Biogeochemistry, Vol. 11, Issue 2, 77-95.

Updegraff, K., Pastor, J., Bridgham, S.D. (1995). Environmental and substrate controls over carbon and nitrogen mineralization in northern wetlands. Ecological Applications, Vol.5, Issue 1, 151-163.

Van Duyl, F.C., Kop, A.J., Kok, A.J., Sandee, A.J.J. (1992). The impact of organic matter and macrozoobenthos on bacterial and oxygen variables in marine sediment boxcosms. Netherlands Journal of Sea Research 29, 343-355.

Wagner, D., Pfeiffer, E.M. (1997). Two temperature optima of methane production in a typical soil of the Elbe river marshland. FEMS Microbiol. Ecol. 22, 145-153.

Westermann, P., Ahring, B.K., Mah, R.A. (1989). Temperature compensation in Methanosarcina barkeri by modulation of hydrogen and acetate affinity. Applied and environmental microbiology, Vol. 55, 1262-1266.

Westrich, J.T., Berner, R.A. (1984). The role of sedimentary organic matter in bacterial sulfate reduction - the G model tested. Limnology and Oceanography 29, 236-249.

Williams, R.T., Crawford, R.L. (1984). Methane Production in Minnesota Peatlands. Applied and environmental microbiology, Vol. 47, 1266-1271.

Yao, H., Conrad, R., Wassmann, R., Neue, H.U. (1999). Effect of soil characteristics on sequential reduction and methane production in sixteen rice paddy soils from China, The Philippines and Italy. Biogeochemistry 47, 269-295.

Zalman, C.A., Meade, N., Chanton, J., Kostka, J.E., Bridgham, S.D., Keller, J.K. (2018). Methylotrophic methanogenesis in Sphagnum-dominated peatland soils. Soil Biology and Biochemistry 118, 156-160.

Zeikus, J.G., Winfrey, M.R. (1976). Temperature limitation of methanogenesis in aquatic sediments. Appl Environ Microbiol 31: 9-107.

Appendix A

Basic information of samples

Table 26. Basic location and layer information of sampled sediments

Sample No. (HPA)	Location	River km	Layer	Layer thickness cm	Sampling Date
1073	RT	619	SPM	15	05.06.2018
1074			FM	10	
1075			PS	20	
1076			CS	40	
1077	RV	616	SPM	10	05.06.2018
1078			FM	15	
1079			PS	10	
1080			CS	50	
1081	SH	621	SPM	20	05.06.2018
1082			FM	5	
1083			PS	25	
1084			CS	50	
1085	SC	620	SPM	8	06.06.2018
1086			FM	15	
1087			PS	15	
1088			CS	50	
1090	KB	623	SPM	20	06.06.2018
1091			FM	10	
1092			PS	55	
1093			CS	15	
1095	VH	624	PS/CS	15	06.06.2018
1096			FM	10	
1097			PS	35	
1098			PS/CS	20	
1100			SPM	5	
1101	PK	627	SPM	20	07.06.2018
1102			PS	40	
1103			PS/CS	25	
1104	SW	643	SPM/FM	25	07.06.2018
1105			PS	15	
1106			CS	30	
1107	KH	629	SPM	25	07.06.2018
1108			FM	8	
1109			PS	17	
1110			CS	20	
2205	RV	616	SPM	30	26.06.2018
2206			FM	5	
2207			PS	20	
2208			CS	65	
2209	KB	623	SPM	45	26.06.2018
2210			PS	30	
2211			PS/CS	25	
2212	SH	621	SPM	20	26.06.2018
2213			FM	5	
2214			PS	25	
2215			CS	50	
2216	RT	619	SPM	30	26.06.2018
2217			FM	5	
2218			PS	30	
2219			CS	35	

Sample No. (HPA)	Location	River km	Layer	Layer thickness cm	Sampling Date
2220	VH	624	SPM	20	27.06.2018
2221			FM/PS	10	
2222			PS	20	
2223			PS/CS	50	
2224	KH	629	SPM	40	27.06.2018
2225			PS	20	
2226			PS/CS	40	
2227	SC	620	SPM	40	28.06.2018
2228			FM	5	
2229			PS	15	
2230			PS/CS	40	
2231	PK	627	SPM	30	28.06.2018
2232			PS	25	
2233			CS	45	
2234	SW	643	SPM	40	28.06.2018
2235			FM	10	
2236			PS	20	
2237			CS	30	
2238			SPM/FM	40	
3205	KH	629	PS	15	07.08.2018
3206			SPM	35	
3207			CS	15	
3208			CS	35	
3209	SW	643	SPM	45	07.08.2018
3210			SPM/FM	10	
3211			CS	25	
3212			CS	30	
3213	PK	627	SPM	15	07.08.2018
3214			PS	50	
3215			CS	30	
3216	RV	616	SPM	50	08.08.2018
3217			PS	25	
3218			CS	10	
3219			PS/CS	15	
3220	SH	621	SPM	50	08.08.2018
3221			PS/CS	30	
3222			CS	20	
3223	KB	623	CS	25	09.08.2018
3224	RT	619	SPM	30	08.08.2018
3225			PS	15	
3226			PS/CS	15	
3227			CS	40	
3228	KB	623	SPM	25	09.08.2018
3229			FM/PS	10	
3230			PS	15	
3231			PS/CS	20	
3232	VH	624	SPM	50	09.08.2018
3233			PS	20	
3234			PS/CS	15	
3235			CS	30	
3236	SC	620	SPM	30	09.08.2018
3237			PS	20	
3238			PS/CS	15	
3239			CS	35	
4201	SW	643	SPM	50	18.09.2018
4202			PS	10	
4203			FM	15	
4204			CS	25	

Sample No. (HPA)	Location	River km	Layer	Layer thickness cm	Sampling Date
4205	PK	627	SPM	40	18.09.2018
4206			PS	20	
4207			CS	40	
4209	KH	629	SPM	20	18.09.2018
4210			FM	10	
4211			PS	15	
4212			CS	55	
4213	RV	616	SPM	50	19.09.2018
4214			PS	15	
4215			CS	35	
4217	SH	621	SPM	50	19.09.2018
4218			PS	10	
4219			CS	40	
4221	RT	619	SPM	25	19.09.2018
4222			FM	25	
4223			PS	10	
4224			CS	40	
4225	SC	620	SPM	25	20.09.2018
4226			PS	35	
4227			CS	40	
4229	VH	624	SPM	25	20.09.2018
4230			PS	20	
4231			CS	25	
4232			CS	30	
4233	KB	623	SPM	30	20.09.2018
4234			PS	20	
4235			CS	50	
5201	RV	616	SPM	50	06.11.2018
5202			PS	20	
5203			CS	30	
5205	SH	621	SPM	20	06.11.2018
5206			FM/PS	30	
5207			PS	30	
5208			CS	20	
5209	RT	619	SPM	20	06.11.2018
5210			FM/PS	10	
5211			PS	30	
5212			PS/CS	40	
5213	SW	643	SPM	35	07.11.2018
5214			PS	20	
5215			CS	35	
5216			FM	10	
5217	VH	624	SPM	30	07.11.2018
5218			PS	30	
5219			CS	40	
5221	SC	620	SPM	25	07.11.2018
5222			PS	30	
5223			CS	45	
5225	KH	629	SPM	10	08.11.2018
5226			FM/PS	15	
5227			PS	35	
5228			PS/CS	40	
5229	KB	623	SPM	50	08.11.2018
5230			CS	50	
5232	PK	627	FM	15	08.11.2018
5234			FM/PS	30	
5235			PS	15	
5236			PS/CS	40	

Appendix B

Gas production results

Table 27. Aerobic and anaerobic release of carbon after 21 days and 100 days, incubation at 36°C. Each data represents the average of three parallels.

Sample No. (HPA)	Location	Layer	Aerobic respiration (36°C)		Anaerobic respiration (36°C)	
			21-day	100-day	21-day	100-day
			mg C/g TOC			
1073	RT	SPM	154.4	568.1	63.27	115.28
1074	RT	FM	174.3	637.6	53.33	96.30
1075	RT	PS	153.3	629.6	44.75	73.60
1076	RT	CS	147.1	727.7	53.26	91.44
1077	RV	SPM	248.2	1064.2	113.40	171.54
1078	RV	FM	268.4	778.9	103.39	173.76
1079	RV	PS	268.9	1157.0	90.37	168.46
1080	RV	CS	112.0	389.7	33.51	82.68
1081	SH	SPM	160.3	665.2	48.82	100.79
1082	SH	FM	163.3	700.2	48.60	74.31
1083	SH	PS	175.8	664.9	34.92	77.53
1084	SH	CS	173.1	621.9	41.13	84.46
1085	SC	SPM	177.4	705.9	16.47	43.18
1086	SC	FM	241.0	762.7	44.40	102.42
1087	SC	PS	174.7	750.8	54.80	92.92
1088	SC	CS	179.7	700.1	79.67	129.36
1090	KB	SPM	107.0	431.8	20.35	60.57
1091	KB	FM	124.7		20.68	60.10
1092	KB	PS	128.5	554.2	42.07	78.89
1093	KB	CS	67.2	311.7	29.99	67.92
1095	VH	PS/CS	104.6	526.4	36.94	69.54
1096	VH	FM	126.3	506.7	37.19	82.75
1097	VH	PS	147.6	601.8	36.91	65.76
1098	VH	PS/CS	117.0	547.1	39.48	84.56
1100	VH	SPM	194.4	602.9	13.32	33.20
1101	PK	SPM	60.1	229.4	12.94	43.20
1102	PK	PS	148.0	570.4	30.85	62.26
1103	PK	PS/CS	123.9	604.8	36.21	82.14
1104	SW	SPM/FM	82.2	403.2	7.17	35.72
1105	SW	PS	82.4	435.8	16.10	42.77
1106	SW	CS	59.6	344.0	17.79	46.94
1107	KH	SPM	71.7	278.5	8.16	21.86
1108	KH	FM	146.1	541.0	21.71	63.82
1109	KH	PS	136.9	593.4	29.20	62.58
1110	KH	CS	124.0	567.9	31.10	71.59
2205	RV	SPM			125.34	229.13
2206	RV	FM	306.0	982.8	112.29	200.78

Sample No. (HPA)	Location	Layer	Aerobic respiration (36°C)		Anaerobic respiration (36°C)	
			21-day	100-day	21-day	100-day
			mg C/g TOC			
2207	RV	PS	260.5	929.6	91.16	155.63
2208	RV	CS	142.2	402.9	36.40	79.42
2209	KB	SPM		2952.6		
2210	KB	PS	123.5	455.9	21.48	52.01
2211	KB	PS/CS	98.0	434.5	22.99	46.44
2212	SH	SPM			34.47	64.7
2213	SH	FM	264.3	507.6	76.22	129.77
2214	SH	PS	183.2	403.4	46.93	90.23
2215	SH	CS	127.1	623.6	34.52	70.50
2216	RT	SPM	182.1	719.9	45.96	68.88
2217	RT	FM	245.4	882.2	70.01	126.78
2218	RT	PS	201.9	418.5	46.82	89.06
2219	RT	CS	153.4	550.4	38.77	77.24
2220	VH	SPM	106.8		21.25	30.30
2221	VH	FM/PS	193.3	623.7	36.58	72.00
2222	VH	PS	127.1	564.4	30.54	63.45
2223	VH	PS/CS	94.9	458.2	25.31	55.31
2224	KH	SPM			21.26	42.4
2225	KH	PS	146.9	531.7	24.84	54.04
2226	KH	PS/CS	94.1	475.4	28.80	61.73
2227	SC	SPM	251.1	784.2	29.49	41.53
2228	SC	FM	255.3	473.3	82.93	133.25
2229	SC	PS	191.0	753.5	57.52	105.24
2230	SC	PS/CS	144.8	593.7	36.70	72.25
2231	PK	SPM	131.8	542.0	32.43	65.25
2232	PK	PS	122.6	514.7	22.88	51.64
2233	PK	CS	107.6	375.4	26.95	54.46
2234	SW	SPM	117.4	476.0	25.33	41.09
2235	SW	FM	76.6	293.0	7.95	33.62
2236	SW	PS	91.7	345.2	13.02	38.63
2237	SW	CS	63.2	309.7	14.18	34.99
2238	SW	SPM/FM	86.6	312.5	8.10	17.57
3205	KH	PS	142.8		44.31	69.51
3206	KH	SPM	76.5		57.20	92.39
3207	KH	CS	121.6		40.14	69.27
3208	KH	CS	89.9		24.47	44.51
3209	SW	SPM	80.6		18.98	33.66
3210	SW	SPM/FM	100.2	375.2	6.93	39.83
3211	SW	CS	99.2		11.34	27.27
3212	SW	CS	59.3		12.90	24.05
3213	PK	SPM	106.7	423.0	42.59	67.3
3214	PK	PS	104.6	403.2	22.71	44.25
3215	PK	CS	80.5	337.8	21.16	39.01
3216	RV	SPM	194.1	862.1	78.44	129.24

Sample No. (HPA)	Location	Layer	Aerobic respiration (36°C)		Anaerobic respiration (36°C)	
			21-day	100-day	21-day	100-day
			mg C/g TOC			
3217	RV	PS	289.1	953.7	73.58	135.34
3218	RV	CS			63.71	122.47
3219	RV	PS/CS	145.1		80.28	142.37
3220	SH	SPM				
3221	SH	PS/CS	130.7	515.1	30.12	55.64
3222	SH	CS	95.9	470.6	29.72	54.55
3223	KB	CS	71.7	327.2	20.22	36.84
3224	RT	SPM			69.04	99.39
3225	RT	PS	146.4	542.4	39.10	69.76
3226	RT	PS/CS	118.1	511.3	33.96	62.89
3227	RT	CS	117.2	464.0	35.85	65.76
3228	KB	SPM	79.3	352.1	28.25	
3229	KB	FM/PS	119.0	452.2	32.68	60.17
3230	KB	PS	106.5	432.1	35.22	63.08
3231	KB	PS/CS	97.2	427.1	23.56	45.46
3232	VH	SPM	96.8	395.9	22.13	48.73
3233	VH	PS	139.3	525.1	78.38	134.23
3234	VH	PS/CS	112.5	471.9	31.80	55.05
3235	VH	CS	90.9	401.3	24.73	43.06
3236	SC	SPM	130.1	554.3	51.04	90.15
3237	SC	PS	157.4	518.8	33.38	59.58
3238	SC	PS/CS	148.3	565.6	32.96	60.31
3239	SC	CS	119.7	490.4	31.87	57.07
4201	SW	SPM	84.2		11.82	
4202	SW	PS	64.8		6.46	
4203	SW	FM	124.7			
4204	SW	CS	56.9		13.15	
4205	PK	SPM	71.2		18.25	
4206	PK	PS	132.0		31.62	
4207	PK	CS	77.8		25.40	
4209	KH	SPM	93.3		27.25	
4210	KH	FM	115.3		18.05	
4211	KH	PS	124.5		7.79	
4212	KH	CS	74.7		21.72	
4213	RV	SPM	265.1		153.17	
4214	RV	PS	234.7		66.03	
4215	RV	CS	163.0		61.08	
4217	SH	SPM	351.2		137.15	
4218	SH	PS	132.1		31.03	
4219	SH	CS	101.7		28.02	
4221	RT	SPM	143.5		34.28	
4222	RT	FM	155.7		41.77	
4223	RT	PS	153.9		34.20	
4224	RT	CS	119.9		38.74	

Sample No. (HPA)	Location	Layer	Aerobic respiration (36°C)		Anaerobic respiration (36°C)	
			21-day	100-day	21-day	100-day
			mg C/g TOC			
4225	SC	SPM	200.6		63.63	
4226	SC	PS	156.8		30.94	
4227	SC	CS	111.3		32.27	
4229	VH	SPM	96.7		26.85	
4230	VH	PS	132.6		30.46	
4231	VH	CS	100.8		24.86	
4232	VH	CS	90.5		23.83	
4233	KB	SPM	113.2			
4234	KB	PS	108.9		19.50	
4235	KB	CS	86.8		20.71	
5201	RV	SPM	28.3		47.56	
5202	RV	PS	32.2		64.01	
5203	RV	CS	31.7		61.41	
5205	SH	SPM			25.87	
5206	SH	FM/PS	35.4		29.01	
5207	SH	PS	29.7		26.35	
5208	SH	CS	24.6		22.53	
5209	RT	SPM	25.5		21.6	
5210	RT	FM/PS	25.4		19.69	
5211	RT	PS	27.0		27.01	
5212	RT	PS/CS	26.0		30.01	
5213	SW	SPM	13.6		5.86	
5214	SW	PS	24.4		4.05	
5215	SW	CS	24.0		5.62	
5216	SW	FM	13.9		7.52	
5217	VH	SPM	22.5		21.03	
5218	VH	PS	28.8		15.10	
5219	VH	CS	24.5		25.25	
5221	SC	SPM	29.8		25.24	
5222	SC	PS	34.8		29.82	
5223	SC	CS	29.1		34.47	
5225	KH	SPM	19.0		12.62	
5226	KH	FM/PS	20.0		11.57	
5227	KH	PS	22.9		15.88	
5228	KH	PS/CS	27.1		22.93	
5229	KB	SPM	20.5			
5230	KB	CS	28.9		20.07	
5232	PK	FM	19.2		17.74	
5234	PK	FM/PS	28.4		18.25	
5235	PK	PS	29.0		23.48	
5236	PK	PS/CS	26.3		24.91	

Appendix C

Raw data of temperature experiment

P-atm = atmospheric pressure;
Red = decompression to P-atm after measurement.

Table 28. Raw pressure data recorded in temperature experiment.

Measured pressure (hPa), sample 4401									
	5°C					10°C			
Date	A	B	C	P-atm	Date	A	B	C	P-atm
2018/10/8	1030	1028	1032	1021	2018/10/8	1025	1024	1025	1021
2018/10/9	984	991	991	1021	2018/10/9	1000	998	1008	1021
2018/10/16	991	1001	1001	1017	2018/10/16	1010	1010	1013	1017
2018/10/26	1000	1009	1010	1004	2018/10/26	1023	1023	1027	1005
2018/11/9	1011	1019	1020	1008	2018/11/9	1038	1038	1041	1009
2018/11/22	1010	1014	1016	1018	2018/11/22	1052	1052	1055	1018
2018/12/4	1010	1017	1019	1024	2018/12/4	1062	1060	1064	1024
2018/12/18	1013	1018	1021	1019	2018/12/18	1037	1036	1035	1019
2019/1/11	1025	1030	1034	1025	2019/1/8	1058	1056	1056	1019
2019/2/6	1030	1034	1042	1019	2019/2/6	1089	1082	1082	1019
	20°C					28°C			
Date	A	B	C	P-atm	Date	A	B	C	P-atm
2018/10/8	1028	1028	1027	1021	2018/10/8	1024	1028	1023	1021
2018/10/9	1076	1076	1071	1021	2018/10/9	1096	1108	1097	1021
2018/10/12	1099	1104	1094	1016	2018/10/12	1158	1172	1164	1016
2018/10/16	1129	1127	1129	1017	2018/10/17	1217	1227	1214	1019
2018/10/23	1173	1165	1173	1024	2018/10/19	1230	1237	1227	1025
2018/10/31	1205	1202	1201	1011	2018/10/23	1101	1100	1092	1024
2018/11/9	1070	1070	1060	1008	2018/10/26	1128	1137	1134	1005
2018/11/22	1112	1119	1102	1018	2018/11/2	1200	1211	1205	1025
2018/12/4	1157	1162	1145	1024	2018/11/9	1100	1108	1110	1009
2018/12/18	1074	1081	1073	1019	2018/11/22	1198	1209	1205	1018
2019/1/8	1133	1147	1131	1019	2018/12/4	1121	1121	1112	1024
2019/2/6	1207	1228	1201	1019	2018/12/19	1122	1121	1118	1010
					2019/1/8	1129	1125	1117	1019
					2019/2/6	1274	1293	1283	1019
	36°C					42°C			
Date	A	B	C	P-atm	Date	A	B	C	P-atm
2018/10/8	1026	1026	1027	1021	2018/10/8	1022	1027	1028	1021
2018/10/9	1182	1188	1200	1021	2018/10/9	1258	1261	1273	1021
2018/10/12	1335	1369	1376	1016	2018/10/12	1160	1165	1166	1016

2018/10/16	1170	1160	1176	1017		2018/10/16	1186	1189	1187	1017
2018/10/19	1227	1228	1250	1025		2018/10/19	1260	1260	1252	1025
2018/10/23	1095	1091	1104	1024		2018/10/23	1154	1149	1159	1024
2018/10/26	1157	1153	1163	1005		2018/10/26	1258	1255	1261	1008
2018/10/31	1203	1212	1223	1011		2018/10/31	1214	1209	1215	1011
2018/11/5	1088	1086	1097	1007		2018/11/5	1125	1117	1127	1007
2018/11/9	1124	1123	1120	1009		2018/11/9	1159	1149	1160	1009
2018/11/14	1166	1160	1157	1025		2018/11/14	1208	1197	1211	1026
2018/11/20	1205	1190	1186	1009		2018/11/20	1125	1122	1128	1009
2018/11/26	1100	1101	1093	1013		2018/11/26	1186	1178	1189	1013
2018/12/4	1153	1155	1138	1024		2018/12/4	1232	1220	1221	1024
2018/12/11	1074	1074	1072	1024		2018/12/11	1092	1092	1091	1024
2018/12/19	1111	1116	1113	1010		2018/12/19	1132	1130	1118	1008
2019/1/8	1125	1138	1117	1019		2019/1/8	1108	1111	1116	1019
2019/1/18	1126	1164	1122	1019		2019/1/18	1151	1151	1155	1019
2019/2/6	1203	1258	1182	1019		2019/2/6	1209	1212	1217	1019

Appendix D

Henry's law constants for water as solvent

Table 29. Henry's law constants of CH_4, N_2, O_2 and CO_2, for water as solvent (Sander, 2015).

Substance Formula (Other name(s)) [CAS registry number]	H^{cp} (at $T^{\ominus}$) $\left[\frac{mol}{m^3\ Pa}\right]$	$\frac{d\ln H^{cp}}{d(1/T)}$ [K]	Reference	Type	Note
methane	1.4×10^{-5}	1900	Warneck and Williams (2012)	L	
CH_4	1.4×10^{-5}	1600	Sander et al. (2011)	L	
[74-82-8]	1.4×10^{-5}	1600	Sander et al. (2006)	L	
	1.4×10^{-5}	1500	Fernández-Prini et al. (2003)	L	1
	1.4×10^{-5}	1600	Abraham and Matteoli (1988)	L	
	1.5×10^{-5}		Mackay and Shiu (1981)	L	
	1.4×10^{-5}	1700	Wilhelm et al. (1977)	L	
	1.2×10^{-5}	2400	Lekvam and Bishnoi (1997)	M	
	1.3×10^{-5}	1400	Reichl (1995)	M	
	1.2×10^{-5}		Guitart et al. (1989)	M	19
	1.4×10^{-5}	1600	Crovetto et al. (1982)	M	
	1.4×10^{-5}	1600	Rettich et al. (1981)	M	
	1.3×10^{-5}	1900	Winkler (1901)	M	
	1.5×10^{-5}		HSDB (2015)	V	
	1.5×10^{-5}		Meylan and Howard (1991)	V	
	1.5×10^{-5}		Hine and Mookerjee (1975)	V	
	9.2×10^{-5}		Butler and Ramchandani (1935)	V	
	1.4×10^{-5}		Hine and Weimar Jr. (1965)	R	
	1.4×10^{-5}	1600	Clever and Young (1987)	X	3
	1.4×10^{-5}	1600	Clever and Young (1987)	X	5, 24
	9.6×10^{-6}		Liss and Slater (1974)	C	
	1.3×10^{-5}		Deno and Berkheimer (1960)	C	
	2.5×10^{-5}		Hilal et al. (2008)	Q	
		2300	Kühne et al. (2005)	Q	
	1.6×10^{-5}		Nirmalakhandan et al. (1997)	Q	
	2.4×10^{-5}		Meylan and Howard (1991)	Q	
		1700	Kühne et al. (2005)	?	
nitrogen	6.4×10^{-6}	1600	Warneck and Williams (2012)	L	
N_2	6.4×10^{-6}	1300	Sander et al. (2011)	L	
[7727-37-9]	6.4×10^{-6}	1300	Sander et al. (2006)	L	
	6.5×10^{-6}	1200	Fernández-Prini et al. (2003)	L	1
	6.5×10^{-6}	1200	Battino et al. (1984)	L	
	6.4×10^{-6}	1300	Wilhelm et al. (1977)	L	
	5.4×10^{-6}		Steward et al. (1973)	L	19
	6.6×10^{-6}	1200	Rettich et al. (1984)	M	
	6.5×10^{-6}	1400	Winkler (1891b)	M	2
	6.5×10^{-6}	1200	Battino (1982)	X	5
	6.3×10^{-6}	1600	Dean (1992)	?	6

oxygen	1.2×10^{-5}	1700	Warneck and Williams (2012)	L	
O_2	1.3×10^{-5}	1500	Sander et al. (2011)	L	
[7782-44-7]	1.3×10^{-5}	1500	Sander et al. (2006)	L	
	1.3×10^{-5}	1400	Fernández-Prini et al. (2003)	L	1
	1.3×10^{-5}	1500	Battino et al. (1983)	L	
	1.3×10^{-5}	1500	Wilhelm et al. (1977)	L	
	1.3×10^{-5}	1400	Rettich et al. (1981)	M	
	1.3×10^{-5}	1400	Benson et al. (1979)	M	
	1.2×10^{-5}	1800	Carpenter (1966)	M	
	1.3×10^{-5}	1200	Winkler (1891b)	M	2
	1.3×10^{-5}	1500	Battino (1981)	X	3, 4
	1.3×10^{-5}	1500	Battino (1981)	X	5
	1.2×10^{-5}	1700	Dean (1992)	?	6
	1.3×10^{-5}		Seinfeld (1986)	?	7
carbon dioxide	3.3×10^{-4}	2400	Sander et al. (2011)	L	
CO_2	3.3×10^{-4}	2400	Sander et al. (2006)	L	
[124-38-9]	3.3×10^{-4}	2300	Fernández-Prini et al. (2003)	L	1
	3.4×10^{-4}	2300	Carroll et al. (1991)	L	
	3.4×10^{-4}	2400	Crovetto (1991)	L	
	3.4×10^{-4}	2300	Yoo et al. (1986)	L	
	3.4×10^{-4}	2400	Edwards et al. (1978)	L	
	3.3×10^{-4}	2400	Wilhelm et al. (1977)	L	
	3.4×10^{-4}	2400	Weiss (1974)	L	
	3.6×10^{-4}	2200	Zheng et al. (1997)	M	
	3.5×10^{-4}	2400	Bohr (1899)	M	
	3.4×10^{-4}	2400	Chen et al. (1979)	R	
	3.1×10^{-4}	2400	Chameides (1984)	T	
	3.5×10^{-4}	2300	Scharlin (1996)	X	3
	3.4×10^{-4}		Perry and Chilton (1973)	X	10
	3.4×10^{-4}	2400	Lelieveld and Crutzen (1991)	C	
	3.4×10^{-4}	2400	Pandis and Seinfeld (1989)	C	
		2900	Kühne et al. (2005)	Q	
		2400	Kühne et al. (2005)	?	
	4.5×10^{-4}		Yaws (1999)	?	
	3.3×10^{-4}	2600	Dean (1992)	?	6
	4.5×10^{-4}		Yaws and Yang (1992)	?	92
	3.4×10^{-4}	2400	Seinfeld (1986)	?	7
	3.3×10^{-4}	2400	Hoffmann and Jacob (1984)	?	7

Appendix E

Correlation tables

Pearson's coefficient r for correlations between gas production and material properties in SPM, FM, PS, PS/CS, CS layer, respectively. Bold = Pearson's coefficient r significant on a confidence level of 99.99%, two-sided test.

DW = dry weight; FW = fresh weight; WC = water content; DOM = dissolved organic matter; DOC-cal. = dissolved organic carbon (calculated); LOI = loss on ignition; EC = Electric conductivity.

Blue = positive correlation, red = negative correlation.

Table 30. Pearson's coefficient r for correlations between gas production and material properties in the SPM layer, with significant r = 0.537

		Aerobic respiration			Anaerobic respiration					
		21 days			21 days			100 days		
		/TOC	/DW	/FW	/TOC	/DW	/FW	/TOC	/DW	/FW
In solids	TC-IfB	0.69	0.87	0.55	0.79	0.88	0.74	0.84	0.93	0.56
	TN-IfB	0.73	0.88	0.57	0.79	0.87	0.74	0.81	0.90	0.54
	TC/TN	-0.67	-0.64	-0.50	-0.44	-0.44	-0.41	-0.14	-0.17	-0.16
	TOC	0.53	0.73	0.45	0.67	0.80	0.65	0.67	0.82	0.49
	TN	0.73	0.88	0.59	0.77	0.85	0.73	0.77	0.86	0.54
	TOC/TN	-0.68	-0.65	-0.52	-0.55	-0.54	-0.53	-0.47	-0.46	-0.34
	TOC/P	0.20	0.34	0.11	0.05	0.18	0.14	0.26	0.41	0.11
	TOC/S	0.12	0.32	0.12	0.31	0.39	0.24	0.53	0.55	0.19
	WC	0.39	0.37	-0.03	0.08	0.10	-0.06	-0.13	-0.05	-0.24
	Redox potential	-0.20	-0.39	-0.46	-0.36	-0.51	-0.58	-0.46	-0.61	-0.56
	Dissolved Gas	0.06	0.01	-0.08	-0.27	-0.25	-0.29	-0.45	-0.37	-0.40
	DOM-270 nm	-0.11	-0.15	-0.03	-0.05	-0.10	-0.01	0.09	0.03	0.03
	DOM-350 nm	-0.07	-0.11	0.01	0.05	-0.01	0.11	0.30	0.25	0.26
	DOC-cal.-270nm	-0.11	-0.15	-0.03	-0.05	-0.10	-0.01	0.09	0.03	0.03
	TOC-IfB	0.71	0.89	0.37	0.76	0.85	0.59	0.75	0.86	0.51
	TIC-IfB	0.51	0.71	0.31	0.88	0.91	0.65	0.85	0.90	0.55
	Share of dry matter	-0.32	-0.38	-0.26	-0.33	-0.36	-0.33	-0.30	-0.36	-0.27
	> 2mm				0.84	0.88	0.65	0.88	0.91	0.65
	1000-2000µm	-0.13	-0.14	-0.05	-0.05	-0.07	-0.06			
	600-1000µm	-0.12	-0.15	-0.07	-0.01	-0.02	-0.01	0.61	0.60	0.66
	200-600µm	-0.19	-0.20	-0.15	0.20	0.20	0.10	0.91	0.93	0.62
	100-200µm	0.02	0.03	0.14	-0.14	-0.16	-0.24	-0.05	-0.07	-0.21
	63-100µm	0.67	0.62	0.63	-0.14	-0.14	-0.17	-0.24	-0.23	-0.27
	20-63µm	0.15	0.08	0.05	-0.08	-0.04	-0.07	0.03	0.03	-0.02
	< 20µm	-0.34	-0.28	-0.33	0.06	0.05	0.13	0.00	0.00	0.10
	< 100µm	0.13	0.14	0.06	-0.07	-0.07	0.01	-0.76	-0.75	-0.45

		Aerobic respiration			Anaerobic respiration					
		21 days			21 days			100 days		
		/TOC	/DW	/FW	/TOC	/DW	/FW	/TOC	/DW	/FW
	< 63µm	-0.37	-0.32	-0.39	0.04	0.05	0.13	0.02	0.01	0.12
	Oxygen-consume-3h	0.32	0.24	0.28	0.22	0.21	0.24	0.37	0.36	0.23
	LOI 550°C	0.52	0.54	0.35	0.46	0.44	0.46	0.54	0.58	0.40
	P	0.64	0.80	0.51	0.68	0.76	0.61	0.52	0.67	0.42
	S	0.30	0.22	0.20	-0.02	-0.02	0.02	-0.26	-0.19	-0.08
	Fe	-0.33	-0.43	-0.16	-0.17	-0.28	-0.17	-0.07	-0.19	0.03
	Ca	0.54	0.74	0.45	0.63	0.75	0.58	0.60	0.74	0.34
	Li	-0.41	-0.56	-0.26	-0.35	-0.48	-0.33	-0.30	-0.43	-0.10
	Al	-0.44	-0.57	-0.28	-0.28	-0.40	-0.30	-0.19	-0.33	-0.07
	Mn	0.59	0.69	0.34	0.62	0.65	0.43	0.49	0.58	0.17
	Vn	-0.40	-0.55	-0.27	-0.32	-0.39	-0.29	-0.34	-0.37	-0.08
	Cu	0.54	0.69	0.48	0.66	0.71	0.59	0.68	0.77	0.45
	Mg	-0.23	-0.43	-0.14	-0.36	-0.47	-0.29	-0.50	-0.57	-0.18
	Na	0.31	0.22	0.18	0.01	0.00	0.03	-0.25	-0.20	-0.09
	K	-0.23	-0.40	-0.18	-0.27	-0.40	-0.28	-0.30	-0.42	-0.14
In Fraction <20 µm	TOC in <20µm	0.63	0.83	0.44	0.79	0.88	0.63	0.59	0.80	0.33
	LOI 550°C	0.67	0.78	0.44	0.57	0.59	0.44	0.57	0.72	0.25
	As	-0.15	-0.25	-0.14	-0.19	-0.21	-0.11	-0.24	-0.31	-0.10
	Pb	-0.09	-0.21	-0.07	-0.44	-0.44	-0.29	-0.84	-0.86	-0.54
	Cd	0.46	0.68	0.39	0.69	0.80	0.65	0.73	0.85	0.46
	Cr	-0.49	-0.66	-0.43	-0.62	-0.70	-0.58	-0.73	-0.82	-0.40
	Cu	0.33	0.47	0.31	0.30	0.39	0.33	0.41	0.53	0.30
	Ni	-0.49	-0.69	-0.40	-0.71	-0.80	-0.63	-0.76	-0.85	-0.46
	Hg	0.24	0.40	0.22	0.43	0.53	0.44	0.25	0.30	0.16
	Zn	0.39	0.60	0.39	0.58	0.71	0.62	0.67	0.80	0.46
In pore water	pH-value	0.01	-0.07	-0.14	-0.05	-0.04	-0.07	-0.13	-0.14	-0.03
	EC at 25°C	-0.08	-0.06	-0.12	0.02	0.01	-0.08	0.11	0.09	0.03
	Fe	-0.08	-0.07	-0.11	-0.10	-0.07	-0.13	-0.08	-0.06	-0.16
	Mn	0.16	0.16	0.06	0.02	0.06	-0.03	0.13	0.15	-0.05
In the filtrate of pore water	DOC	0.12	0.10	0.10	-0.10	-0.06	-0.05	-0.01	0.00	-0.05
	TN	0.11	0.20	0.05	0.20	0.25	0.16	0.56	0.63	0.30
	NO_2^-	0.07	0.06	-0.13	0.04	0.05	0.20	0.14	0.15	0.21
	NO_3^-	-0.40	-0.34	-0.45	-0.12	-0.11	-0.21	-0.16	-0.16	-0.24
	NH_4^+	0.24	0.31	0.16	0.23	0.28	0.17	0.55	0.62	0.26
	Fe^{2+}	0.30	0.41	0.33	0.26	0.34	0.27	0.38	0.50	0.25
	Mn^{2+}	0.12	0.12	0.04	0.02	0.05	-0.03	0.13	0.15	-0.03
	PO_4^{3-}	-0.26	-0.32	-0.05	-0.51	-0.48	-0.30	-0.48	-0.51	-0.27
	Na^+	-0.22	-0.23	-0.26	-0.11	-0.13	-0.26	-0.14	-0.16	-0.21
	Cl^-	-0.18	-0.18	-0.22	-0.09	-0.11	-0.26	-0.11	-0.12	-0.21
	Ca^{2+}	-0.04	-0.02	-0.06	0.04	0.05	0.00	0.06	0.07	0.08

		Aerobic respiration			Anaerobic respiration					
		21 days			21 days			100 days		
		/TOC	/DW	/FW	/TOC	/DW	/FW	/TOC	/DW	/FW
	Mg^{2+}	-0.21	-0.27	-0.24	-0.27	-0.27	-0.34	-0.08	-0.13	-0.21
	SO_4^{2-}	-0.05	-0.12	0.06	-0.36	-0.35	-0.23	-0.38	-0.39	-0.22
	SiO_2	-0.18	-0.11	-0.14	-0.10	-0.03	-0.07	0.21	0.25	0.11

Table 31. Pearson's coefficient r for correlations between gas production and material properties in the FM layer, with significant r = 0.537

		Aerobic respiration			Anaerobic respiration					
		21 days			21 days			100 days		
		/TOC	/DW	/FW	/TOC	/DW	/FW	/TOC	/DW	/FW
In solids	TC-IfB	0.75	0.92	0.87	0.87	0.93	0.92	0.89	0.95	0.93
	TN-IfB	0.78	0.92	0.88	0.89	0.91	0.90	0.90	0.92	0.91
	TC/TN	-0.56	-0.53	-0.55	-0.56	-0.43	-0.46	-0.50	-0.37	-0.37
	TOC	0.73	0.91	0.86	0.88	0.93	0.92	0.90	0.94	0.92
	TN	0.81	0.93	0.88	0.92	0.93	0.92	0.92	0.93	0.90
	TOC/TN	-0.67	-0.59	-0.60	-0.61	-0.49	-0.52	-0.68	-0.56	-0.53
	TOC/P	0.79	0.85	0.80	0.88	0.90	0.91	0.91	0.90	0.93
	TOC/S	0.78	0.94	0.88	0.92	0.98	0.97	0.94	0.98	0.98
	WC	0.55	0.54	0.37	0.68	0.65	0.59	0.69	0.65	0.57
	Redox potential	-0.32	-0.42	-0.47	-0.61	-0.48	-0.55	-0.83	-0.68	-0.74
	Dissolved Gas	-0.31	-0.30	-0.35	-0.14	-0.15	-0.12	0.51	0.46	0.44
	DOM-270 nm	0.60	0.66	0.66	0.76	0.77	0.79	0.70	0.68	0.80
	DOM-350 nm	0.57	0.63	0.62	0.73	0.74	0.76	0.67	0.66	0.77
	DOC-cal.-270nm	0.60	0.66	0.66	0.76	0.77	0.79	0.70	0.68	0.80
	TOC-IfB	0.88	0.95	0.89	0.89	0.90	0.90	0.89	0.91	0.88
	TIC-IfB	0.69	0.88	0.86	0.82	0.93	0.93	0.82	0.93	0.92
	Share of dry matter	-0.30	-0.52	-0.50	-0.56	-0.62	-0.47	-0.60	-0.67	-0.42
	> 2mm	0.42	0.69	0.57	0.67	0.81	0.76	0.81	0.92	0.88
	1000-2000µm	-0.54	-0.40	-0.51	-0.35	-0.30	-0.35			
	600-1000µm	-0.18	-0.15	-0.21	-0.21	-0.17	-0.22	0.10	0.21	0.18
	200-600µm	-0.36	-0.33	-0.43	-0.38	-0.33	-0.40	-0.45	-0.37	-0.45
	100-200µm	-0.48	-0.52	-0.63	-0.60	-0.52	-0.59	-0.61	-0.51	-0.59
	63-100µm	-0.23	-0.34	-0.40	-0.49	-0.41	-0.45	-0.51	-0.44	-0.45
	20-63µm	-0.79	-0.77	-0.73	-0.75	-0.73	-0.72	-0.69	-0.68	-0.63
	< 20µm	0.60	0.63	0.70	0.67	0.61	0.66	0.73	0.66	0.67
	< 100µm	0.44	0.41	0.52	0.43	0.37	0.44	0.46	0.35	0.44
	< 63µm	0.41	0.45	0.55	0.51	0.43	0.50	0.53	0.43	0.48
	Oxygen-consume-3h	0.62	0.71	0.66	0.69	0.68	0.65	0.72	0.68	0.66
	LOI 550°C	0.66	0.80	0.75	0.79	0.80	0.79	0.84	0.83	0.79
	P	0.53	0.70	0.66	0.72	0.75	0.74	0.84	0.83	0.81

		Aerobic respiration			Anaerobic respiration					
		21 days			21 days			100 days		
		/TOC	/DW	/FW	/TOC	/DW	/FW	/TOC	/DW	/FW
	S	0.22	0.32	0.33	0.27	0.24	0.25	0.42	0.36	0.35
	Fe	-0.08	-0.05	-0.05	-0.18	-0.24	-0.24	-0.02	-0.11	-0.14
	Ca	0.53	0.80	0.70	0.72	0.88	0.84	0.83	0.94	0.92
	Li	-0.22	-0.22	-0.21	-0.35	-0.41	-0.42	-0.22	-0.32	-0.35
	Al	-0.22	-0.23	-0.22	-0.35	-0.42	-0.42	-0.23	-0.32	-0.35
	Mn	0.63	0.68	0.69	0.61	0.57	0.59	0.65	0.57	0.57
	Vn	-0.15	-0.15	-0.14	-0.27	-0.35	-0.34	-0.15	-0.25	-0.28
	Cu	0.51	0.68	0.64	0.68	0.71	0.71	0.83	0.82	0.81
	Mg	-0.28	-0.31	-0.30	-0.44	-0.52	-0.52	-0.34	-0.44	-0.46
	Na	0.30	0.25	0.22	0.10	0.05	0.03	0.10	0.05	-0.03
	K	-0.20	-0.24	-0.21	-0.36	-0.44	-0.44	-0.27	-0.37	-0.39
In Fraction <20 µm	TOC in <20µm	0.56	0.78	0.74	0.71	0.83	0.83	0.81	0.91	0.93
	LOI 550°C	0.76	0.87	0.88	0.77	0.83	0.82	0.84	0.93	0.93
	As	-0.45	-0.50	-0.49	-0.49	-0.51	-0.52	-0.38	-0.41	-0.40
	Pb	0.12	-0.05	0.10	-0.21	-0.30	-0.27	-0.69	-0.72	-0.70
	Cd	0.62	0.84	0.77	0.80	0.92	0.90	0.83	0.94	0.93
	Cr	-0.74	-0.84	-0.88	-0.81	-0.84	-0.87	-0.81	-0.86	-0.91
	Cu	0.50	0.67	0.66	0.69	0.72	0.75	0.80	0.80	0.85
	Ni	-0.69	-0.80	-0.80	-0.84	-0.85	-0.88	-0.82	-0.82	-0.85
	Hg	0.52	0.74	0.72	0.73	0.83	0.84	0.80	0.91	0.91
	Zn	0.59	0.82	0.75	0.75	0.88	0.86	0.82	0.93	0.93
In pore water	pH-value	-0.06	-0.13	-0.11	-0.08	-0.16	-0.16	-0.14	-0.25	-0.21
	EC at 25°C	0.03	0.11	0.03	0.18	0.19	0.19	0.44	0.43	0.40
	Fe	0.59	0.74	0.70	0.65	0.74	0.73	0.76	0.85	0.83
	Mn	0.64	0.58	0.65	0.54	0.42	0.46	0.43	0.31	0.35
In the filtrate of pore water	DOC	0.53	0.39	0.45	0.35	0.19	0.21	0.14	-0.02	-0.03
	TN	0.60	0.83	0.76	0.76	0.90	0.88	0.81	0.93	0.92
	NO_2^-	0.22	0.12	0.21	0.16	0.05	0.10	-0.04	-0.14	-0.08
	NO_3^-	0.14	0.13	0.05	0.30	0.24	0.21	0.31	0.21	0.16
	NH_4^+	0.57	0.80	0.73	0.73	0.88	0.86	0.79	0.92	0.91
	Fe^{2+}	0.64	0.74	0.65	0.73	0.76	0.71	0.70	0.71	0.66
	Mn^{2+}	0.52	0.48	0.54	0.40	0.31	0.34	0.29	0.21	0.24
	PO_4^{3-}	-0.70	-0.64	-0.68	-0.65	-0.56	-0.60	-0.62	-0.54	-0.53
	Na^+	-0.62	-0.68	-0.76	-0.58	-0.61	-0.64	-0.47	-0.55	-0.62
	Cl^-	-0.66	-0.73	-0.80	-0.68	-0.70	-0.72	-0.63	-0.68	-0.73
	Ca^{2+}	-0.07	-0.08	-0.06	-0.02	-0.11	-0.08	0.10	-0.02	0.01
	Mg^{2+}	0.48	0.36	0.42	0.40	0.23	0.28	0.24	0.07	0.09
	SO_4^{2-}	-0.82	-0.85	-0.82	-0.84	-0.78	-0.79	-0.81	-0.73	-0.71
	SiO_2	0.62	0.65	0.69	0.78	0.66	0.73	0.82	0.69	0.73

Table 32. Pearson's coefficient r for correlations between gas production and material properties in the PS layer, with significant r = 0.487

		Aerobic respiration			Anaerobic respiration					
		21 days			21 days			100 days		
		/TOC	/DW	/FW	/TOC	/DW	/FW	/TOC	/DW	/FW
In solids	TC-IfB	0.71	0.87	0.80	0.85	0.95	0.91	0.87	0.97	0.92
	TN-IfB	0.75	0.88	0.82	0.86	0.93	0.89	0.86	0.94	0.88
	TC/TN	-0.59	-0.54	-0.55	-0.62	-0.51	-0.54	-0.46	-0.39	-0.37
	TOC	0.71	0.87	0.80	0.85	0.93	0.90	0.85	0.95	0.89
	TN	0.72	0.87	0.80	0.85	0.92	0.88	0.85	0.94	0.88
	TOC/TN	-0.52	-0.50	-0.51	-0.63	-0.56	-0.58	-0.62	-0.60	-0.58
	TOC/P	0.71	0.86	0.81	0.78	0.89	0.85	0.84	0.93	0.89
	TOC/S	0.69	0.90	0.82	0.81	0.95	0.88	0.84	0.96	0.90
	WC	0.75	0.82	0.77	0.80	0.83	0.79	0.76	0.82	0.74
	Redox potential	-0.39	-0.25	-0.34	-0.40	-0.24	-0.33	-0.09	0.01	-0.04
	Dissolved Gas	-0.12	0.11	-0.04	0.21	0.31	0.26	0.60	0.70	0.61
	DOM-270 nm	0.64	0.66	0.69	0.59	0.61	0.61	0.51	0.53	0.54
	DOM-350 nm	0.56	0.57	0.61	0.50	0.51	0.52	0.45	0.46	0.49
	DOC-cal.-270nm	0.64	0.66	0.69	0.59	0.61	0.61	0.51	0.53	0.54
	Share of mass in light density fraction	0.47	0.66	0.57	0.63	0.81	0.72	0.42	0.87	0.62
	Share of mass in heavy density fraction	-0.52	-0.54	-0.55	-0.85	-0.76	-0.84	-0.93	-0.66	-0.89
	Share of mass in heavy density fraction	0.55	0.72	0.64	0.75	0.88	0.82	0.69	0.97	0.84
	TOC-IfB	0.94	0.92	0.93	0.84	0.90	0.86	0.82	0.89	0.83
	TIC-IfB	0.76	0.80	0.82	0.75	0.83	0.83	0.78	0.85	0.84
	Share of dry matter	-0.50	-0.57	-0.52	-0.63	-0.61	-0.61	-0.54	-0.62	-0.54
	> 2mm	-0.25	-0.21	-0.23	-0.02	-0.02	0.00	-0.16	-0.17	-0.16
	1000-2000µm	-0.49	-0.35	-0.45	-0.28	-0.21	-0.24			
	600-1000µm	-0.16	-0.20	-0.21	-0.25	-0.25	-0.27	0.01	-0.08	-0.05
	200-600µm	-0.31	-0.30	-0.34	-0.31	-0.30	-0.32	-0.23	-0.26	-0.26
	100-200µm	-0.39	-0.37	-0.39	-0.39	-0.36	-0.38	-0.04	-0.11	-0.06
	63-100µm	-0.42	-0.37	-0.38	-0.44	-0.36	-0.40	-0.23	-0.26	-0.22
	20-63µm	-0.44	-0.31	-0.37	-0.14	-0.16	-0.12	0.01	-0.08	-0.01
	< 20µm	0.57	0.49	0.53	0.47	0.43	0.44	0.16	0.24	0.17
	< 100µm	0.39	0.38	0.41	0.38	0.36	0.38	0.13	0.20	0.16
	< 63µm	0.48	0.44	0.47	0.49	0.43	0.46	0.23	0.28	0.22
	Oxygen-consume-3h	0.55	0.71	0.63	0.74	0.79	0.76	0.75	0.78	0.76
	LOI 550°C	0.69	0.82	0.74	0.80	0.83	0.80	0.74	0.81	0.74
	P	0.54	0.70	0.62	0.73	0.76	0.75	0.69	0.76	0.71
	S	0.35	0.40	0.37	0.50	0.44	0.47	0.31	0.29	0.28

		Aerobic respiration			Anaerobic respiration					
		21 days			21 days			100 days		
		/TOC	/DW	/FW	/TOC	/DW	/FW	/TOC	/DW	/FW
	Fe	0.04	0.00	0.00	0.12	-0.01	0.05	-0.09	-0.18	-0.16
	Ca	0.51	0.74	0.67	0.75	0.89	0.86	0.80	0.90	0.90
	Li	-0.10	-0.17	-0.16	-0.03	-0.18	-0.12	-0.21	-0.33	-0.30
	Al	-0.09	-0.18	-0.16	-0.05	-0.19	-0.13	-0.24	-0.35	-0.33
	Mn	0.62	0.72	0.66	0.74	0.73	0.71	0.66	0.67	0.63
	Vn	-0.01	-0.11	-0.09	0.02	-0.13	-0.07	-0.21	-0.33	-0.30
	Cu	0.47	0.62	0.54	0.69	0.70	0.69	0.66	0.70	0.67
	Mg	-0.19	-0.30	-0.27	-0.17	-0.33	-0.26	-0.36	-0.49	-0.45
	Na	0.35	0.31	0.30	0.31	0.25	0.25	0.27	0.21	0.20
	K	-0.10	-0.20	-0.17	-0.08	-0.23	-0.17	-0.28	-0.40	-0.37
In Fraction <20 µm	TOC in <20µm	0.56	0.78	0.68	0.73	0.85	0.79	0.82	0.91	0.88
	LOI 550°C	0.46	0.67	0.58	0.68	0.75	0.72	0.83	0.93	0.89
	As	-0.06	-0.03	-0.09	0.03	0.02	0.00	-0.08	-0.10	-0.12
	Pb	0.35	0.27	0.32	0.39	0.26	0.32	-0.03	-0.10	-0.08
	Cd	0.56	0.81	0.70	0.80	0.93	0.87	0.83	0.93	0.89
	Cr	-0.59	-0.67	-0.68	-0.48	-0.61	-0.56	-0.57	-0.71	-0.69
	Cu	0.41	0.63	0.51	0.69	0.75	0.72	0.70	0.79	0.72
	Ni	-0.25	-0.27	-0.30	-0.03	-0.19	-0.13	-0.20	-0.35	-0.34
	Hg	0.40	0.59	0.46	0.61	0.68	0.61	0.53	0.63	0.53
	Zn	0.54	0.77	0.67	0.81	0.91	0.87	0.84	0.94	0.90
In pore water	pH-value	-0.36	-0.39	-0.34	-0.44	-0.40	-0.39	-0.26	-0.26	-0.23
	EC at 25°C	0.16	0.34	0.23	0.36	0.44	0.39	0.67	0.75	0.69
	Fe	0.01	0.16	0.06	0.16	0.21	0.17	0.62	0.67	0.62
	Mn	0.22	0.17	0.16	0.25	0.17	0.19	0.04	-0.03	-0.03
In the filtrate of pore water	DOC	0.57	0.61	0.66	0.58	0.62	0.64	0.63	0.66	0.70
	TN	0.58	0.80	0.71	0.72	0.87	0.81	0.79	0.92	0.87
	NO_2^-	0.05	0.02	0.04	-0.06	-0.04	-0.05	-0.06	-0.05	-0.06
	NO_3^-	-0.14	-0.20	-0.19	-0.34	-0.28	-0.33	-0.42	-0.33	-0.39
	NH_4^+	0.60	0.81	0.73	0.72	0.86	0.80	0.78	0.91	0.86
	Fe^{2+}	0.52	0.53	0.57	0.48	0.51	0.52	0.51	0.51	0.55
	Mn^{2+}	0.23	0.17	0.17	0.20	0.13	0.14	-0.03	-0.08	-0.09
	PO_4^{3-}	-0.12	-0.07	-0.08	-0.13	-0.07	-0.09	-0.04	-0.03	-0.02
	Na^+	-0.51	-0.43	-0.51	-0.43	-0.37	-0.41	-0.15	-0.19	-0.23
	Cl^-	-0.50	-0.39	-0.49	-0.41	-0.33	-0.39	-0.11	-0.11	-0.16
	Ca^{2+}	-0.37	-0.39	-0.38	-0.34	-0.33	-0.32	-0.46	-0.42	-0.41
	Mg^{2+}	0.17	0.06	0.10	0.10	0.00	0.03	-0.09	-0.14	-0.14
	SO_4^{2-}	-0.54	-0.55	-0.58	-0.63	-0.58	-0.62	-0.50	-0.48	-0.52
	SiO_2	0.31	0.42	0.38	0.51	0.51	0.52	0.58	0.56	0.59

Table 33. Pearson's coefficient r for correlations between gas production and material properties in the PS/CS layer, with significant r = 0.708

		Aerobic respiration			Anaerobic respiration					
		21 days			21 days			100 days		
		/TOC	/DW	/FW	/TOC	/DW	/FW	/TOC	/DW	/FW
In solids	TC-IfB	0.43	0.80	0.57	0.93	0.95	0.94	0.90	0.96	0.92
	TN-IfB	0.55	0.85	0.65	0.85	0.85	0.83	0.78	0.84	0.78
	TC/TN	-0.46	-0.36	-0.36	-0.03	0.02	0.05	0.10	0.10	0.16
	TOC	0.42	0.80	0.57	0.92	0.95	0.93	0.88	0.95	0.89
	TN	0.42	0.80	0.58	0.93	0.96	0.95	0.90	0.96	0.92
	TOC/TN	-0.36	-0.65	-0.52	-0.76	-0.75	-0.78	-0.80	-0.78	-0.81
	TOC/P	0.45	0.45	0.38	0.22	0.22	0.16	0.10	0.15	0.06
	TOC/S	0.51	0.62	0.50	0.49	0.49	0.44	0.39	0.44	0.36
	WC	0.56	0.86	0.65	0.85	0.86	0.82	0.75	0.84	0.74
	Redox potential	-0.02	0.13	0.13	0.16	0.21	0.23	0.34	0.31	0.40
	Dissolved Gas	-0.10	0.32	0.03	0.75	0.76	0.76	0.89	0.90	0.86
	DOM-270 nm	0.30	0.23	0.38	0.00	0.01	0.05	-0.02	-0.05	0.05
	DOM-350 nm	0.28	0.21	0.36	-0.01	0.00	0.04	-0.02	-0.05	0.05
	DOC-cal.-270nm	0.30	0.23	0.38	0.00	0.01	0.05	-0.02	-0.05	0.05
	TOC-IfB	0.74	0.96	0.91	0.93	0.92	0.92	0.94	0.93	0.92
	TIC-IfB	0.48	0.84	0.74	0.97	0.99	0.98	0.98	0.99	0.98
	Share of dry matter	-0.28	-0.61	-0.39	-0.63	-0.67	-0.63	-0.53	-0.64	-0.54
	> 2mm	-0.50	-0.37	-0.46	-0.09	-0.07	-0.05			
	1000-2000µm	-0.65	-0.50	-0.62	-0.27	-0.21	-0.23			
	600-1000µm	-0.48	-0.39	-0.45	-0.14	-0.15	-0.12	0.06	-0.02	0.07
	200-600µm	-0.61	-0.44	-0.56	-0.13	-0.09	-0.08	0.33	0.29	0.35
	100-200µm	-0.36	-0.53	-0.41	-0.47	-0.42	-0.44	-0.46	-0.43	-0.42
	63-100µm	-0.16	-0.42	-0.23	-0.48	-0.47	-0.46	-0.52	-0.52	-0.48
	20-63µm	-0.70	-0.60	-0.72	-0.30	-0.23	-0.26	-0.16	-0.12	-0.16
	< 20µm	0.60	0.70	0.64	0.52	0.47	0.48	0.46	0.45	0.43
	< 100µm	0.63	0.61	0.63	0.37	0.32	0.33	0.31	0.30	0.27
	< 63µm	0.38	0.56	0.43	0.49	0.46	0.46	0.47	0.47	0.43
	Oxygen-consume-3h	0.20	0.35	0.28	0.45	0.42	0.45	0.37	0.38	0.39
	LOI 550°C	0.47	0.79	0.55	0.83	0.86	0.81	0.72	0.83	0.72
	P	-0.03	0.31	0.16	0.59	0.61	0.65	0.66	0.67	0.70
	S	-0.23	-0.01	-0.10	0.20	0.23	0.26	0.27	0.28	0.31
	Fe	-0.19	-0.18	-0.24	-0.32	-0.29	-0.33	-0.36	-0.29	-0.37
	Ca	0.26	0.66	0.43	0.93	0.96	0.95	0.91	0.97	0.93
	Li	-0.35	-0.37	-0.42	-0.48	-0.45	-0.48	-0.52	-0.46	-0.53
	Al	-0.30	-0.32	-0.37	-0.44	-0.41	-0.45	-0.50	-0.42	-0.51
	Mn	0.48	0.70	0.53	0.52	0.57	0.50	0.38	0.51	0.39
	Vn	-0.41	-0.36	-0.39	-0.31	-0.28	-0.28	-0.28	-0.24	-0.25

		Aerobic respiration			Anaerobic respiration					
		21 days			21 days			100 days		
		/TOC	/DW	/FW	/TOC	/DW	/FW	/TOC	/DW	/FW
	Cu	0.28	0.60	0.42	0.70	0.71	0.72	0.71	0.74	0.72
	Mg	-0.23	-0.30	-0.32	-0.40	-0.39	-0.42	-0.43	-0.39	-0.46
	Na	0.20	0.27	0.15	0.09	0.13	0.05	-0.06	0.07	-0.08
	K	-0.26	-0.31	-0.35	-0.46	-0.43	-0.47	-0.52	-0.45	-0.53
In Fraction <20 µm	TOC in <20µm	0.30	0.60	0.46	0.90	0.86	0.91	0.95	0.89	0.95
	LOI 550°C	0.49	0.71	0.61	0.83	0.82	0.83	0.86	0.86	0.86
	As	-0.42	-0.49	-0.41	-0.49	-0.48	-0.43	-0.39	-0.43	-0.35
	Pb	0.28	0.01	0.26	-0.27	-0.34	-0.28	-0.39	-0.47	-0.37
	Cd	0.37	0.66	0.52	0.87	0.86	0.88	0.88	0.86	0.89
	Cr	-0.51	-0.64	-0.59	-0.72	-0.68	-0.70	-0.78	-0.72	-0.76
	Cu	0.11	0.28	0.25	0.41	0.40	0.45	0.51	0.45	0.54
	Ni	-0.34	-0.57	-0.44	-0.77	-0.76	-0.77	-0.82	-0.79	-0.80
	Hg	0.11	0.50	0.29	0.81	0.83	0.84	0.87	0.89	0.89
	Zn	0.31	0.54	0.46	0.75	0.72	0.77	0.82	0.75	0.83
In pore water	pH-value	0.30	0.07	0.17	-0.18	-0.26	-0.27	-0.22	-0.30	-0.30
	EC at 25°C	-0.78	-0.73	-0.73	-0.46	-0.43	-0.39	-0.36	-0.40	-0.31
	Fe	-0.25	0.12	-0.09	0.53	0.58	0.59	0.61	0.67	0.66
	Mn	-0.47	-0.54	-0.52	-0.52	-0.45	-0.49	-0.54	-0.46	-0.50
In the filtrate of pore water	DOC	0.40	0.50	0.51	0.57	0.49	0.57	0.65	0.53	0.64
	TN	0.33	0.70	0.51	0.92	0.95	0.95	0.91	0.95	0.94
	NO_2^-	0.03	-0.14	0.06	-0.22	-0.23	-0.18	-0.19	-0.27	-0.15
	NO_3^-	0.21	-0.04	0.17	-0.25	-0.27	-0.25	-0.34	-0.38	-0.31
	NH_4^+	0.33	0.70	0.50	0.92	0.95	0.95	0.91	0.95	0.94
	Fe^{2+}	0.04	0.12	0.13	0.10	0.07	0.13	0.28	0.16	0.26
	Mn^{2+}	-0.45	-0.62	-0.54	-0.69	-0.65	-0.67	-0.72	-0.66	-0.69
	PO_4^{3-}	0.12	0.08	0.13	0.05	0.07	0.07	-0.02	0.01	0.01
	Na^+	-0.80	-0.66	-0.83	-0.44	-0.35	-0.41	-0.59	-0.42	-0.60
	Cl^-	-0.58	-0.52	-0.67	-0.39	-0.34	-0.40	-0.44	-0.33	-0.48
	Ca^{2+}	-0.70	-0.77	-0.70	-0.59	-0.57	-0.53	-0.48	-0.54	-0.45
	Mg^{2+}	-0.45	-0.40	-0.38	-0.30	-0.23	-0.22	-0.24	-0.18	-0.15
	SO_4^{2-}	0.01	-0.15	-0.10	-0.29	-0.28	-0.33	-0.35	-0.32	-0.38
	SiO_2	0.10	0.25	0.24	0.46	0.37	0.48	0.58	0.44	0.57

Table 34. Pearson's coefficient r for correlations between gas production and material properties in the CS layer, with significant r = 0.537

		Aerobic respiration			Anaerobic respiration					
		21 days			21 days			100 days		
		/TOC	/DW	/FW	/TOC	/DW	/FW	/TOC	/DW	/FW
In solids	TC-IfB	0.54	0.78	0.69	0.79	0.90	0.89	0.74	0.91	0.88
	TN-IfB	0.57	0.79	0.69	0.83	0.91	0.91	0.77	0.91	0.88
	TC/TN	-0.57	-0.64	-0.60	-0.71	-0.67	-0.69	-0.59	-0.63	-0.58
	TOC	0.51	0.77	0.67	0.78	0.89	0.88	0.71	0.87	0.85
	TN	0.73	0.91	0.84	0.78	0.88	0.86	0.74	0.88	0.85
	TOC/TN	-0.58	-0.66	-0.61	-0.66	-0.68	-0.68	-0.55	-0.67	-0.60
	TOC/P	0.50	0.63	0.56	0.72	0.73	0.72	0.59	0.62	0.58
	TOC/S	0.37	0.63	0.56	0.66	0.78	0.78	0.63	0.77	0.78
	WC	0.62	0.80	0.69	0.81	0.86	0.84	0.71	0.81	0.75
	Redox potential	-0.12	0.03	-0.04	-0.07	0.10	0.03	0.18	0.24	0.28
	Dissolved Gas	-0.05	0.20	0.05	0.66	0.71	0.68	0.37	0.39	0.36
	DOM-270 nm	0.56	0.58	0.60	0.38	0.34	0.34	0.42	0.38	0.37
	DOM-350 nm	0.51	0.50	0.52	0.24	0.20	0.20	0.34	0.30	0.29
	DOC-cal.-270nm	0.56	0.58	0.60	0.38	0.34	0.34	0.42	0.38	0.37
	Share of mass in light density fraction	0.31	0.52	0.45	0.84	0.79	0.82	0.73	0.71	0.71
	Share of mass in heavy density fraction	-0.54	-0.77	-0.66	-0.89	-0.86	-0.87	-0.91	-0.88	-0.88
	Share of mass in heavy density fraction	0.37	0.64	0.52	0.90	0.90	0.90	0.81	0.79	0.79
	TOC-IfB	0.78	0.92	0.88	0.76	0.85	0.85	0.83	0.91	0.89
	TIC-IfB	0.54	0.74	0.77	0.59	0.74	0.75	0.71	0.83	0.85
	Share of dry matter	-0.38	-0.59	-0.49	-0.70	-0.69	-0.71	-0.66	-0.67	-0.66
	> 2mm	-0.42	-0.28	-0.36	-0.07	-0.06	-0.03			
	1000-2000µm	-0.39	-0.13	-0.24	0.00	0.16	0.12	0.16	0.26	0.31
	600-1000µm	-0.15	-0.06	-0.08	-0.15	-0.05	-0.08	-0.27	-0.18	-0.13
	200-600µm	-0.19	-0.07	-0.05	-0.01	0.06	0.09	0.30	0.44	0.48
	100-200µm	-0.49	-0.57	-0.54	-0.62	-0.57	-0.59	-0.60	-0.56	-0.56
	63-100µm	-0.44	-0.61	-0.54	-0.67	-0.63	-0.66	-0.64	-0.67	-0.65
	20-63µm	-0.55	-0.52	-0.53	-0.48	-0.42	-0.43	-0.40	-0.44	-0.37
	< 20µm	0.56	0.65	0.61	0.68	0.62	0.64	0.60	0.61	0.56
	< 100µm	0.47	0.46	0.44	0.47	0.38	0.39	0.29	0.18	0.15
	< 63µm	0.50	0.63	0.57	0.69	0.62	0.65	0.62	0.62	0.59
	Oxygen-consume-3h	0.48	0.62	0.55	0.72	0.74	0.74	0.67	0.67	0.64
	LOI 550°C	0.53	0.72	0.62	0.81	0.83	0.83	0.73	0.78	0.75
	P	0.44	0.70	0.61	0.76	0.82	0.83	0.74	0.81	0.83
	S	0.43	0.58	0.50	0.65	0.61	0.63	0.53	0.48	0.48

		Aerobic respiration			Anaerobic respiration					
		21 days			21 days			100 days		
		/TOC	/DW	/FW	/TOC	/DW	/FW	/TOC	/DW	/FW
	Fe	0.44	0.51	0.46	0.50	0.40	0.44	0.46	0.45	0.40
	Ca	0.40	0.68	0.60	0.75	0.86	0.87	0.76	0.87	0.89
	Li	0.36	0.37	0.33	0.35	0.21	0.24	0.32	0.27	0.21
	Al	0.35	0.37	0.33	0.36	0.23	0.26	0.31	0.28	0.21
	Mn	0.42	0.63	0.49	0.75	0.77	0.75	0.60	0.61	0.56
	Vn	0.39	0.41	0.36	0.40	0.27	0.30	0.31	0.28	0.21
	Cu	0.47	0.71	0.65	0.73	0.78	0.80	0.72	0.82	0.83
	Mg	0.30	0.25	0.23	0.22	0.06	0.09	0.19	0.11	0.05
	Na	0.48	0.47	0.42	0.45	0.34	0.34	0.28	0.22	0.15
	K	0.41	0.38	0.36	0.34	0.18	0.22	0.29	0.22	0.17
In Fraction <20 µm	TOC in <20µm	0.26	0.56	0.45	0.67	0.79	0.78	0.75	0.81	0.86
	LOI 550°C	0.60	0.78	0.73	0.62	0.67	0.68	0.69	0.78	0.80
	As	-0.07	0.12	0.04	0.04	0.10	0.08	0.26	0.33	0.34
	Pb	0.39	0.45	0.48	0.27	0.26	0.31	0.35	0.41	0.45
	Cd	0.25	0.50	0.47	0.51	0.65	0.66	0.51	0.65	0.70
	Cr	-0.41	-0.45	-0.47	-0.49	-0.54	-0.54	-0.54	-0.52	-0.57
	Cu	0.19	0.47	0.43	0.49	0.61	0.64	0.54	0.67	0.72
	Ni	-0.19	-0.15	-0.17	-0.14	-0.16	-0.15	-0.14	-0.11	-0.12
	Hg	0.28	0.54	0.51	0.51	0.62	0.65	0.55	0.67	0.72
	Zn	0.24	0.51	0.47	0.51	0.64	0.66	0.54	0.68	0.72
In pore water	pH-value	-0.28	-0.45	-0.42	-0.52	-0.52	-0.57	-0.67	-0.72	-0.73
	EC at 25°C	-0.14	-0.15	-0.15	-0.13	-0.11	-0.12	0.71	0.77	0.75
	Fe	0.20	0.23	0.24	0.26	0.23	0.27	0.52	0.53	0.54
	Mn	0.15	0.12	0.09	0.09	-0.02	-0.01	0.08	0.00	-0.04
In the filtrate of pore water	DOC	0.48	0.45	0.48	0.49	0.39	0.45	0.57	0.50	0.51
	TN	0.08	0.23	0.24	0.39	0.47	0.51	0.62	0.75	0.78
	NO_2^-	0.08	0.05	0.08	-0.09	-0.08	-0.09	-0.12	-0.11	-0.11
	NO_3^-	0.02	-0.01	0.01	-0.17	-0.17	-0.18	-0.25	-0.23	-0.24
	NH_4^+	0.10	0.25	0.25	0.42	0.51	0.54	0.62	0.75	0.77
	Fe^{2+}	0.25	0.28	0.25	0.27	0.23	0.23	0.25	0.24	0.21
	Mn^{2+}	0.23	0.20	0.17	0.14	0.03	0.03	0.10	0.03	-0.01
	PO_4^{3-}	-0.16	-0.08	-0.10	-0.12	-0.08	-0.08	0.10	0.13	0.16
	Na^+	-0.33	-0.26	-0.37	-0.17	-0.17	-0.22	-0.17	-0.25	-0.33
	Cl^-	-0.10	-0.16	-0.19	-0.35	-0.41	-0.44	-0.16	-0.22	-0.29
	Ca^{2+}	-0.04	0.03	-0.02	0.09	0.05	0.06	0.37	0.30	0.30
	Mg^{2+}	0.14	0.12	0.08	0.08	-0.01	-0.01	0.17	0.09	0.04
	SO_4^{2-}	-0.17	-0.15	-0.13	-0.27	-0.15	-0.19	-0.31	-0.19	-0.18
	SiO_2	0.12	0.20	0.23	0.23	0.22	0.28	0.40	0.41	0.47

Appendix F

Table for checking the correlation coefficient for significance

Table 35. Checking the correlation coefficient for significance

	zweiseitige Fragestellung		einseitige Fragestellung	
α	.05	.01	.05	.01
1	0.9969	0.9999	0.9877	0.9995
2	0.9500	0.9900	0.9000	0.9800
3	0.8783	0.9587	0.805	0.934
4	0.811	0.917	0.729	0.882
5	0.754	0.875	0.669	0.833
6	0.707	0.834	0.621	0.789
7	0.666	0.798	0.582	0.750
8	0.632	0.765	0.549	0.715
9	0.602	0.735	0.521	0.685
10	0.576	0.708	0.497	0.658
11	0.553	0.684	0.476	0.634
12	0.532	0.661	0.457	0.612
13	0.514	0.641	0.441	0.592
14	0.497	0.623	0.426	0.574
15	0.482	0.606	0.412	0.558
16	0.468	0.590	0.400	0.543
17	0.456	0.575	0.389	0.529
18	0.444	0.561	0.378	0.516
19	0.433	0.549	0.369	0.503
20	0.423	0.537	0.360	0.492
21	0.413	0.526	0.352	0.482
22	0.404	0.515	0.344	0.472
23	0.396	0.505	0.337	0.462
24	0.388	0.496	0.330	0.453
25	0.381	0.487	0.323	0.445
26	0.374	0.478	0.317	0.437
27	0.367	0.470	0.311	0.430
28	0.361	0.463	0.306	0.423
29	0.355	0.456	0.301	0.416
30	0.349	0.449	0.296	0.409
35	0.325	0.418	0.275	0.381
40	0.304	0.393	0.257	0.358
50	0.273	0.354	0.231	0.322
60	0.250	0.325	0.211	0.295
70	0.232	0.302	0.195	0.274
80	0.217	0.283	0.183	0.257
90	0.205	0.267	0.173	0.242
100	0.195	0.254	0.164	0.230
120	0.178	0.232	0.150	0.210
200	0.138	0.181	0.116	0.164
500	0.0875	0.115	0.0735	0.104
1000	0.0619	0.0813	0.0520	0.0735
2000	0.0438	0.0575	0.0368	0.0519